



**HAL**  
open science

# Degradation modeling and degradation-aware control of wind turbine drive-trains

Elena Romero Fandiño

► **To cite this version:**

Elena Romero Fandiño. Degradation modeling and degradation-aware control of wind turbine drive-trains. Automatic Control Engineering. Université Grenoble Alpes [2020-..], 2023. English. NNT : 2023GRALT088 . tel-04531746

**HAL Id: tel-04531746**

**<https://theses.hal.science/tel-04531746v1>**

Submitted on 4 Apr 2024

**HAL** is a multi-disciplinary open access archive for the deposit and dissemination of scientific research documents, whether they are published or not. The documents may come from teaching and research institutions in France or abroad, or from public or private research centers.

L'archive ouverte pluridisciplinaire **HAL**, est destinée au dépôt et à la diffusion de documents scientifiques de niveau recherche, publiés ou non, émanant des établissements d'enseignement et de recherche français ou étrangers, des laboratoires publics ou privés.

THÈSE

Pour obtenir le grade de

**DOCTEUR DE L'UNIVERSITÉ GRENOBLE ALPES**

École doctorale : EEATS - Electronique, Electrotechnique, Automatique, Traitement du Signal (EEATS)

Spécialité : Automatique - Productique

Unité de recherche : Grenoble Images Parole Signal Automatique

**Modélisation et controle commande de la dégradation de la transmission d'une éolienne**

**Degradation modeling and degradation-aware control of wind turbine drive-trains**

Présentée par :

**Elena ROMERO FANDIÑO**

Direction de thèse :

**John Jairo MARTINEZ MOLINA**

PROFESSEUR DES UNIVERSITES, Université Grenoble Alpes

Directeur de thèse

**Christophe BERENQUER**

PROFESSEUR DES UNIVERSITES, Université Grenoble Alpes

Co-directeur de thèse

Rapporteurs :

**Antoine GRALL**

PROFESSEUR DES UNIVERSITES, Université de Technologie de Troyes

**Didier THEILLOL**

PROFESSEUR DES UNIVERSITES, Université de Lorraine

Thèse soutenue publiquement le **6 décembre 2023**, devant le jury composé de :

**John Jairo MARTINEZ MOLINA**

PROFESSEUR DES UNIVERSITES, Université Grenoble Alpes

Directeur de thèse

**Antoine GRALL**

PROFESSEUR DES UNIVERSITES, Université de Technologie de Troyes

Rapporteur

**Silvio SIMANI**

ASSOCIATE PROFESSOR, Universita degli Studi di Ferrara

Examineur

**Mitra FOULADIRAD**

PROFESSEURE DES UNIVERSITES, Centrale Marseille

Examinatrice

**Didier THEILLOL**

PROFESSEUR DES UNIVERSITES, Université de Lorraine

Rapporteur

**Christophe BERENQUER**

PROFESSEUR DES UNIVERSITES, Université Grenoble Alpes

Co-directeur de thèse

**Olivier SENAME**

PROFESSEUR DES UNIVERSITES, Université Grenoble Alpes

Président du jury





# Contents

<b>Abstract</b>	<b>1</b>
<b>Résumé</b>	<b>3</b>
<b>Acknowledgements</b>	<b>5</b>
<b>1 Introduction</b>	<b>7</b>
1.1 About this thesis . . . . .	7
1.2 Overview of wind energy generation . . . . .	7
1.3 Scope & Objectives . . . . .	15
1.4 Organization of the document . . . . .	16
1.5 Main Contributions . . . . .	17
<b>2 Literature Review &amp; Theoretical Background</b>	<b>21</b>
2.1 Fundamentals of Wind Turbines . . . . .	21
2.2 Deterioration in Wind Turbine . . . . .	29
2.3 Deterioration-Aware Control in Wind Turbines . . . . .	33
2.4 Conclusions . . . . .	37
<b>3 Modelling the Deterioration of a Drive Train in a Wind Turbine</b>	<b>41</b>
3.1 Dynamic of a Wind Turbine Drive-Train . . . . .	42
3.2 Dissipated Energy & Degradation Modelling . . . . .	43
3.3 Proposed Degradation Model for a Wind Turbine Drive-Train . . . . .	44
3.4 Case Study Analysis . . . . .	45
3.5 Experimental Validation in Prototype of Wind Turbine . . . . .	55
3.6 Conclusions . . . . .	63
<b>4 Gain Scheduling Control Strategy</b>	<b>65</b>
4.1 Introduction . . . . .	65
4.2 Problem Statement . . . . .	66
4.3 Proposed Gain-Scheduling Control Strategy . . . . .	67
4.4 Evaluation of performance of proposed strategy . . . . .	69
4.5 Conclusions . . . . .	75
<b>5 Long-Term Estimation of Deterioration</b>	<b>79</b>
5.1 Introduction . . . . .	79
5.2 Methodology for Long-Term Estimation of Deterioration . . . . .	80
5.3 Evaluation of Performance of the Proposed Methodology for Long-Term Esti- mation of Deterioration . . . . .	83
5.4 Conclusions . . . . .	91
<b>6 Control of the Rate of Deterioration</b>	<b>93</b>

---

6.1	Introduction . . . . .	93
6.2	Problem Statement . . . . .	94
6.3	Proposed Deterioration Control Strategy . . . . .	95
6.4	Performance Evaluation: Numerical Scenario & Results . . . . .	99
6.5	Conclusions . . . . .	108
	<b>Conclusions</b>	<b>111</b>
	<b>Bibliography</b>	<b>124</b>

# List of Figures

1.1	New installations of wind turbines outlook 2022-2026 (GW). <i>Images from [52]</i>	8
1.2	Major components of a wind turbine with the horizontal axis. <i>Image from: [56]</i>	9
1.3	Curve of power coefficient $C_p$ versus tip-speed ratio $\lambda$ .	10
1.4	Number of failure by major components in wind turbines	12
1.5	Power curve of a wind turbine	13
2.1	Speed control loop for variable speed operation	24
2.2	Torque control loop for variable speed operation	25
2.3	Characterization of curve $C_p$ vs $\lambda$ for Perturbation and Observation method	25
2.4	Scheme of wind speed generation model of two level Markov chain embedded with Stochastic differential equations proposed in [77].	29
3.1	Drive-train with a flexible shaft representation.	42
3.2	Considered wind speed scenarios: (a) laminar wind, (b) turbulent wind with low intensity, (c) turbulent wind with high intensity	48
3.3	Obtained torsion shaft angle for different wind speed scenarios: (a) laminar wind, (b) turbulent wind with low intensity, (c) turbulent wind with high intensity	50
3.4	Generated power with respect to rotor speed produced by optimal and sub-optimal torque controllers.	51
3.5	Comparison of the behavior of the Power Coefficient $C_p$ for different wind speed scenarios: (a) laminar wind, (b) turbulent wind with low intensity, (c) turbulent wind with high intensity	52
3.6	Dissipated energy at the flexible shaft versus time for different wind speed scenarios: (a) laminar wind, (b) turbulent wind with low intensity, (c) turbulent wind with high intensity	53
3.7	Generated energy at the flexible shaft versus time for different wind speed scenarios: (a) laminar wind, (b) turbulent wind with low intensity, (c) turbulent wind with high intensity	54
3.8	Prototype of wind turbine: a) Wind Turbine installation and b) Blades of wind turbine	55
3.9	Block diagram representing the functioning of the prototype of a wind turbine	56
3.10	Integration of a virtual drive-train on the fixed-shaft wind turbine prototype	57
3.11	Considered wind scenario a) Case I, b) Case II	60
3.12	Obtained torsion shaft angle for different wind a) Wind Case I, b) Wind Case II	60
3.13	Obtained generated power for a) Wind Case I, b) Wind Case II	61
3.14	Obtained dissipated power for a) Wind Case I, b) Wind Case II	61
3.15	Obtained generated energy for a) Wind Case I, b) Wind Case II	62
3.16	Obtained dissipated energy for a) Wind Case I, b) Wind Case II	62
4.1	Architecture of the proposed gain-scheduling control strategy.	68
4.2	Example of gain-scheduling depending on two wind conditions.	68
4.3	Scheme of the off-line optimization process for designing feedback control gains.	69

4.4	Considered wind speed conditions: (a) laminar and (b) turbulent . . . . .	71
4.5	Simulated scenario of wind speed with different wind conditions. . . . .	71
4.6	Comparison for different feedback gains: a) Relative torsion shaft angle $\theta_s$ , and b) Relative angular speed $\omega_r$ . . . . .	73
4.7	Comparison of the power coefficient $C_p$ with respect to the theoretical optimal case. . . . .	74
4.8	a) Generated energy for different feedback gains $K_c$ , and b) Dissipated energy for different feedback gains $K_c$ . . . . .	74
4.9	Comparison with respect to the optimal case from: a) Relative generated en- ergy, and b) Relative dissipated energy . . . . .	75
5.1	Dissipated Energy for different control feedback gains $K_c$ . . . . .	80
5.2	Diagram flow to represent the proposed methodology of long-term estimation of deterioration. . . . .	81
5.3	Considered wind speed conditions: (a) Laminar and (b) Turbulent . . . . .	83
5.4	Dissipated Energy with: (a)Laminar wind with $K_c^{nom}$ and (b) Turbulent wind with $K_c^{nom}$ . . . . .	85
5.5	Dissipated Energy in one year of simulation using a suitable control gain and theoretical control gain for a period of: 1 Year . . . . .	88
5.6	Density function of a Beta distribution using a data-set of slopes in a curve Dissipated Energy VS Time. Case: a) Using the suitable $K_c^{Laminar}$ , and b) Using the $K_c^{opt}$ . . . . .	89
5.7	Density function of a Gamma distribution using a data-set of slopes in a curve Dis- sipated Energy VS Time. Case: a) Using the suitable $K_c^{Turbulent}$ , and b) Using the nominal $K_c^{opt}$ . . . . .	89
5.8	Simulated Dissipated Energy using a suitable control gain and theoretical control gain for the periods of: a) 5 years, b) 10 years, c) 15 years, and d) 20 years . . . . .	90
6.1	Proposed control strategy for deterioration rate considering an intelligent mod- ification of the control gain $\Delta k_c$ . . . . .	96
6.2	Proposed Intelligent Robust Control Strategy implementing a $H_\infty$ method . . . . .	97
6.3	Standard scheme for $H_\infty$ control synthesis . . . . .	98
6.4	Estimated error of estimation of the controller . . . . .	101
6.5	Comparison in the deterioration rate between a case with $\beta$ and $\beta^{ref}$ . . . . .	103
6.6	Comparison of Dissipated Energy between a scenario with controller and refer- ence scenario for wind of: a) 6m/s, b) 8 m/s, and c) 12 m/s . . . . .	104
6.7	Comparison of Generated Energy between a scenario with controller and refer- ence scenario for wind of: a) 6m/s, b) 8 m/s, and c) 12 m/s . . . . .	105
6.8	Wind Speed Case considered for the evaluation of performance to disturbances. . . . .	106
6.9	Comparison of $\beta$ and $\beta^{ref}$ under disturbances . . . . .	106
6.10	Evaluation of performance of controller under disturbances in dissipated energy . . . . .	107
6.11	Evaluation of performance of controller under disturbances in dissipated power . . . . .	107
6.12	Evaluation of performance of controller under disturbances in: Generated Energy . . . . .	108

# List of Tables

3.1	Parameters of the simulated wind turbine . . . . .	49
3.2	Parameters of the prototype of wind turbine . . . . .	56
3.3	Parameters of the prototype of wind turbine . . . . .	59
4.1	Suitable control gains for laminar and turbulent wind conditions . . . . .	70
5.1	Comparison of dissipated energy in different periods . . . . .	88
6.1	Parameters for the estimation of system $G$ . . . . .	100
6.2	Parameters of the Sensitivity functions . . . . .	100





# Abstract

The interest in producing energy through renewable sources has been increasing in recent years, particularly in using wind energy conversion systems. Nevertheless, as wind turbines continue to advance, there is a growing demand to decrease the cost of wind energy. Wind turbine operation and maintenance (O&M) represent a high cost for wind power projects of the overall energy cost. One of the significant challenges associated with the cost of O&M is related to the high failure rates in the transmission system and the need to detect and address potential issues before they become serious problems that require costly repairs

The wind conditions can pose significant challenges to wind turbine transmission systems, leading to vibration and damage. Dynamic loads from wind can also cause fatigue damage and reduce reliability, increasing the need for maintenance. Therefore, implementing intelligent control strategies can mitigate the effects of wind-induced vibration and reduce overall stress on the transmission system, thereby reducing maintenance costs and improving operational efficiency.

Pitch control is widely used to decrease damage from changes in wind conditions. However, this strategy cannot be applied to variable speed-fixed pitch (VS-FP) wind turbines, where the pitch is ideally zero, and any control action is made through the tip-speed ratio. In the case of VS-FP wind turbines, a maximum power point tracking (MPPT) control law is commonly used. The generator torque is the control torque and is estimated based on the rotor speed and a control gain.

This thesis focuses on developing a control strategy to address the degradation of the drive-train of wind turbines caused by non-optimal functioning in response to changes in wind conditions, by using an indicator of degradation that can be estimated considering the torsional dynamics of a flexible drive-train.

This work first presents a deterioration model for the drive-train of a wind turbine. The model considers dissipated energy as an indicator of degradation caused by various physical phenomena, such as fatigue, vibration, and others. Additionally, a gain scheduling control strategy is presented to find a trade-off between generated and dissipated energy. The strategy uses optimization to find suitable control gains depending on wind conditions.

Furthermore, a long-term methodology is proposed to evaluate deterioration under a control strategy adapted to follow variations in wind conditions. The approach simulates degradation by learning an empirical relationship between Dissipated Energy and Time with random effects.

Finally, a novel intelligent control strategy is presented to minimize the degradation of a wind turbine drive-train when wind or set point changes occur. The proposed method enables the turbine to operate under different conditions while maintaining energy generation without accelerating the degradation process. To achieve this objective, a robust H-infinity control strategy is implemented to adapt the theoretical control gain to an intelligent control gain

that guarantees system stability in the presence of uncertainties and external disturbances, such as changes in wind conditions.

# Résumé

L'intérêt pour la production d'énergie à partir de sources renouvelables s'est accru ces dernières années, en particulier pour l'énergie éolienne. Néanmoins, alors que la technologie éolienne continue de progresser, il existe une demande croissante pour réduire son coût de production. L'exploitation et la maintenance représentent une grande partie de dépenses des projets éoliens par rapport au coût global de l'énergie.

L'un des principaux défis associés au coût de l'exploitation et de la maintenance est lié aux taux élevés de défaillance du système de transmission. Il est primordial de détecter et de traiter les problèmes potentiels avant qu'ils ne surviennent et ne nécessitent des réparations coûteuses. Les conditions de vent peuvent provoquer des problèmes importants aux systèmes de transmission, entraînant des vibrations et des dommages, ce qui a pour conséquence d'augmenter la fatigue et réduire la fiabilité.

Par conséquent, la mise en œuvre d'une stratégie de contrôle intelligente peut atténuer les effets des vibrations, et ainsi réduire les contraintes globales sur le système de transmission, ce qui aura pour effet de diminuer les coûts de maintenance et améliorer l'efficacité opérationnelle.

Le contrôle du tangage est largement utilisé pour réduire les dommages causés par les changements de conditions de vent. Cependant, cette stratégie ne peut pas être appliquée aux éoliennes à vitesse variable et à pas fixe (VS-FP), où le pas est idéalement nul et où toute action de contrôle se fait par le biais du rapport de vitesse en bout de pale. Dans le cas des éoliennes VS-FP, une loi de commande de suivi du point de puissance maximale (MPPT) est couramment utilisée. Le couple du générateur est le couple de commande et est estimé en fonction de la vitesse du rotor et d'un gain de commande.

Cette thèse se concentre sur le développement d'une stratégie de contrôle pour traiter la dégradation du groupe motopropulseur des éoliennes causée par un fonctionnement non optimal en réponse aux changements des conditions de vent, en utilisant un indicateur de dégradation qui peut être estimé en tenant compte de la dynamique de torsion d'un groupe motopropulseur flexible.

Ce travail présente un modèle de détérioration pour la chaîne cinématique d'une éolienne. Le modèle considère l'énergie dissipée comme un indicateur de la dégradation, causée par divers phénomènes physiques, tels que la fatigue, les vibrations et autres. En outre, une stratégie de contrôle de la planification des gains est présentée pour trouver un compromis entre l'énergie générée et l'énergie dissipée. La stratégie utilise l'optimisation pour trouver des gains de contrôle appropriés en fonction des conditions de vent.



# Acknowledgements

First of all, my deepest gratitude goes to my supervisors, Christophe BERENGUER and John-Jairo MARTINEZ-MOLINA, whose expertise, understanding, and patience, allow me to pursue this thesis. I appreciate the willingness to spend time guiding, advising, and supporting me throughout this journey.

I must express my very profound gratitude to Antoine, for providing me with unfailing support and continuous encouragement throughout my years of study and through the process of researching and writing this thesis. This accomplishment would not have been possible without you. Thank you.

My thanks also go to my parents Rocio and Ivan, my sister Liss for the support and belief that all is possible, and my mother-in-law, Myriam who taught me French and who I consider as my second mother in this country who welcomed me.

I am also thankful to my colleagues at Gipsa Lab, Maxime, Ariel, Mathias, Houssam, Esteban, Mariana, Maria, Bob, and Monica for the time that we shared, the parties, and numerous memories that we created together during the last three years.

Finally, I would like to say thank you to Ivan Portnoy for the time that we spent through video calls, friendship, expert advice, and valuable suggestions every time I needed a friend.



# Introduction

---

## Contents

<b>1.1</b>	<b>About this thesis . . . . .</b>	<b>7</b>
<b>1.2</b>	<b>Overview of wind energy generation . . . . .</b>	<b>7</b>
1.2.1	Wind turbine Generalities . . . . .	8
1.2.2	Aerodynamics . . . . .	10
1.2.3	Effect of the wind . . . . .	10
1.2.4	Deterioration in Wind turbines . . . . .	11
1.2.5	Control methods for Wind Turbine . . . . .	13
<b>1.3</b>	<b>Scope &amp; Objectives . . . . .</b>	<b>15</b>
<b>1.4</b>	<b>Organization of the document . . . . .</b>	<b>16</b>
<b>1.5</b>	<b>Main Contributions . . . . .</b>	<b>17</b>

---

## 1.1 About this thesis

This thesis was developed from October 2020 to September 2023 as part of the SAFE (Safe, controlled and monitored systems) research team at the Gipsa Laboratory, which is a unit of the École Doctorale Électronique, Électrotechnique, Automatique, Traitement du Signal (EEATS) within the Institut Polytechnique de Grenoble (Grenoble INP), Université Grenoble Alpes (UGA), and Centre National de la Recherche Scientifique (CNRS). The thesis was supported by a doctoral contract provided by the Grenoble INP - UGA.

The major of the thesis is Automatic Control and Production Systems, which belongs to the doctoral school EEATS of the Université Grenoble Alpes.

## 1.2 Overview of wind energy generation

The demand for sustainable energy sources has increased due to society's numerous environmental problems. As a consequence, new sources of energy are being developed to convert reusable resources such as solar, biomass, geothermal water, and wind into electricity and supply the global demand, positively impacting the current energy landscape.

The Energy Agency predicts that renewable energy sources will account for 98% of the new 2.518 TWh of electricity generation by 20255 [52]. Wind energy is among the most popular



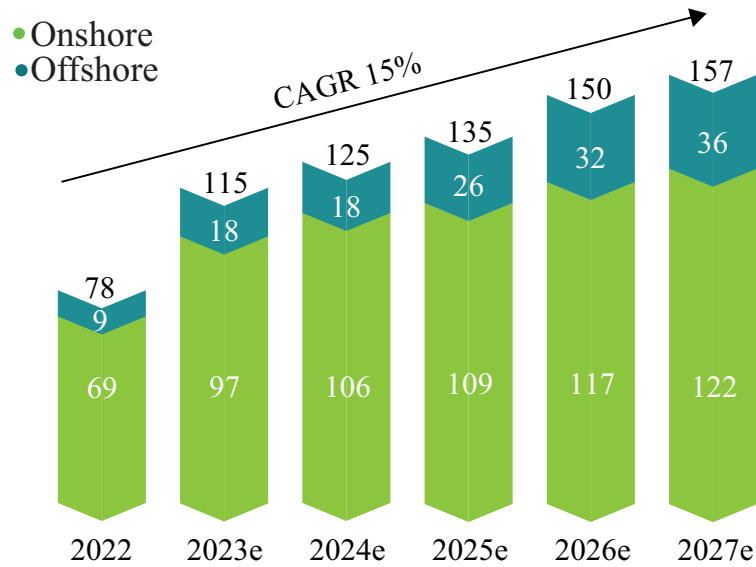


Figure 1.1: New installations of wind turbines outlook 2022-2026 (GW). Images from [52]

sources of renewable power due to its low water footprint compared to other forms of electricity generation.

Another advantage of wind energy is that wind turbine operations do not produce greenhouse gases. However, the construction of wind turbines is associated with  $CO_2$  emissions, typically eliminated after a year of operation. In terms of materials, wind turbines are made with concrete, steel, and composite materials for the blades. The cement used for turbine foundations is a material that does not contaminate the soil. Concerning the blades, the wind industry is working to create resource-efficient, sustainable materials, such as low-carbon steel and recyclable composites.

On the other hand, wind turbines onshore farms are a considerate, versatile energy source that can coexist with various agricultural activities or positively affect biodiversity by preserving habitats and ecosystems. Bottom trawling and dredging at offshore wind farms are prohibited, which helps conserve the seabed [128, 141].

As a result of the numerous advantages of implementing wind energy technologies, the global wind turbine capacity has been increased. According to the Global Wind Energy Council [52], during 2022, the new wind power capacity connected to the grid was in total 77.6 GW, resulting in an increment of 9% on the total installed wind capacity compared to the previous year, bringing it to 906 GW in 2022.

Furthermore, the wind energy sector is expected to add 136 GW per year until 2027, resulting in 680 GW of new capacity for the next five years with Compound Annual Growth Rate (CAGR) for the next five years of 15%, where 550 GW corresponds to the onshore wind sector installed capacity, resulting in a 12% growth between 2023 and 2027. On the other hand, for the offshore wind energy sector, the total new global installations are expected

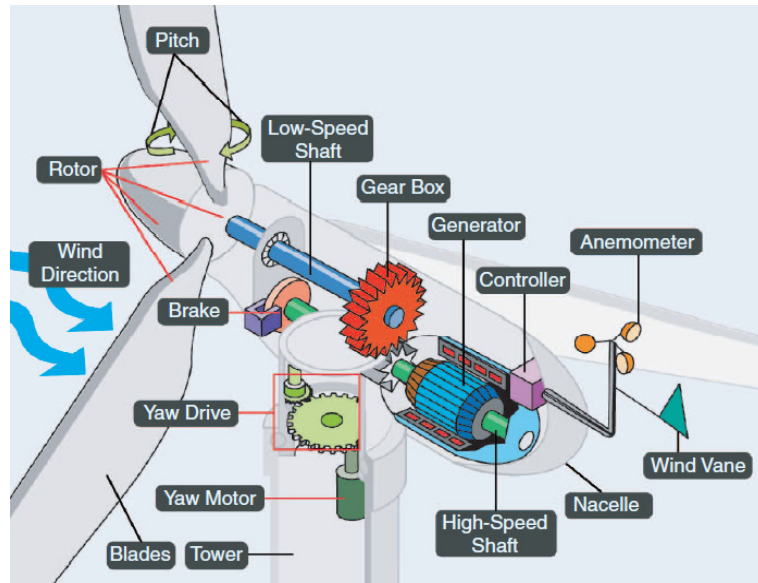


Figure 1.2: Major components of a wind turbine with the horizontal axis. *Image from:* [56]

to increase from 23% by 2027. In total, 130 GW of offshore wind is expected to be added worldwide from 2023 to 2027; see Figure 1.1.

### 1.2.1 Wind turbine Generalities

Wind turbines are mechanical devices that convert the wind's kinetic energy into mechanical energy to produce electricity. Typically, the blades are set in motion to rotate the rotor, which moves a drive-train connected to a generator to produce electricity [16].

Usually, the wind turbine has three key components: tower, blades, and transmission. The tower is the structural part of the wind turbine; the blades are in charge of capturing the wind energy, and the transmission is conformed by different parts such as the rotor, drive-train, and generator, which together are in charge of the process that converts kinetic energy into electricity [48].

The transmission of a wind turbine is a complex mechanical system with various configurations. Depending on the rotor's position, a wind turbine can be classified as either a vertical or horizontal axis.

Wind turbines with vertical axes have rotors located almost at ground level, allowing them to capture wind from any direction without additional devices. However, they are not often used due to their high maintenance costs, the need for a considerable amount of land to function, and their low energy production efficiency due to turbulent wind.

On the other hand, wind turbines with a horizontal axis are often used and connected to the grids; this type of turbine has a rotor at the top of a tower, where the wind is less turbulent and strong. Typically, the system includes a yaw that allows the turbine to rotate depending on the wind direction, which increases efficiency [15].

Most horizontal axis wind turbines use a transmission system illustrated in Figure 1.2. These systems typically have two or three blades, with the rotor acting as the low-speed shaft. Its rotation with an angular speed  $\omega_r$  creates the rotor torque  $\tau_r$  and connects to the generator through a gearbox. Also, the generator rotates with an angular speed of  $\omega_g$ , which creates the torque  $\tau_g$ . The shafts, gearbox, and generator are inside a nacelle cavity.

Moreover, the yaw drive can rotate the entire nacelle according to the wind direction. It relies on a motor and controller that receive signals from an anemometer and wind vane. In addition, the wind direction can be used to reduce the structural load on the rotor blades and maintain a steady speed and power output by adjusting the pitch angle. However, some wind turbines have a fixed pitch angle set to zero, so this feature would not be applicable.

### 1.2.2 Aerodynamics

According to different sources [16, 41, 48], wind turbines can be classified as fixed or variable speed. Some wind turbines, known as fixed-speed wind turbines, can operate at maximum efficiency for only one wind velocity. In contrast, variable-speed wind turbines can achieve maximum efficiency over a wide range of wind speed magnitudes, at least up to the rated power.

Variable-speed wind turbines are the most commonly used type, as they adjust the rotational speed proportionately to the external wind speed to maintain optimal operation through a parameter known as the tip-speed ratio ( $\lambda$ ), which is the ratio between the tip speed of the blade and the speed of the wind.

The efficiency of a wind turbine is commonly evaluated using the power coefficient,  $C_p$ , which represents the ratio between the extracted power and the wind power. The maximum possible value of  $C_p$ , known as the Maximum Power Coefficient,  $C_p^{max}$ , is limited by the Betz limit to 0.593 for all types of wind turbines.

Due to the wind variability, there is no static description between power and wind speed in dynamic conditions [56]. However, in the wind turbine industry, the value of  $C_p^{max}$  is provided by the turbine manufacturer; also,  $C_p$  can be estimated by various methods [8, 70, 93]. However, all these methods define  $C_p$  in terms of the pitch angle  $\psi$  and the tip-speed ratio  $\lambda$ .

For the fixed-pitch wind turbines,  $C_p$  only varies with respect to  $\lambda$ , and for variable-pitch, the  $C_p^{max}$  with a value of  $\psi$  is very small, ideally zero, which implies that any variation in the pitch angle results in a decrease in power capture [15]. Figure 1.3 shows a typical variation of  $C_p$  with respect to  $\lambda$  for a wind turbine with fixed-pitch; note that the  $C_p^{max}$  is located in the maximum point of the curve.

### 1.2.3 Effect of the wind

Wind is the primary source of power for wind turbines, and it has been harnessed for electricity generation for many years. However, the impact of wind on the functionality of this technology can affect its efficiency and potentially cause damage to certain turbine components. The

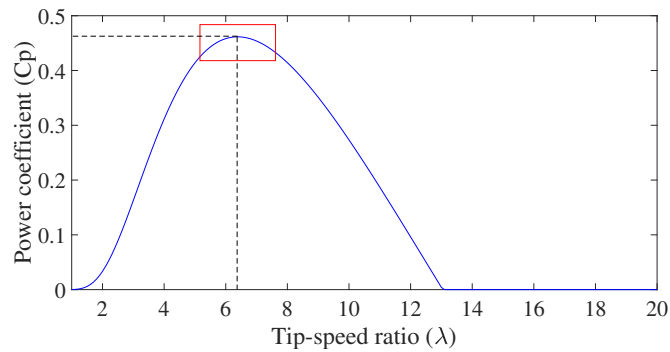


Figure 1.3: Curve of power coefficient  $C_p$  versus tip-speed ratio  $\lambda$ .

strength, variability, and direction of the wind play a significant role in this.

In situations where wind flows smoothly in a single direction and with organized layers, it is referred to as laminar wind. Otherwise, when the wind becomes unpredictable and moves in multiple directions, it is known as turbulent wind flow. Currently, the standards for designing wind power curves only take into account the average wind speed and air density. However, research has indicated that turbulence also affects the output of wind power [108].

Perturbations in the wind can be caused by changes in temperature, obstacles, or atmospheric parameters and affect the direction and velocity of the flow. Usually, the mechanical component of the blades or drive-train is designed considering data from laminar wind situations [53]. In general, turbulent wind does not affect the annual energy capture; however, it impacts aerodynamic load and power quality [16]. The changes in the direction, strength, or variability of the wind can negatively impact the regular operation of a wind turbine because the blades, tower, and drive-train are susceptible to excessive vibration and fatigue, creating structural damage and decreasing efficiency.

As demonstrated by various researchers, turbulent wind affects wind turbines' power performance and fatigue loading [6, 27, 148]. The level of turbulence is typically measured by its intensity which, although different ways to estimate wind variability have been developed, the most common definition is the ratio of the standard deviation to the mean wind speed [26, 77, 108].

The tower can also experience increased stress and fatigue, resulting in cracks or even collapse. On the other hand, the drive-train, which includes the gearbox and generator, can also be affected by turbulent wind, leading to increased wear and tear and reduced lifespan. The fluctuations in the wind conditions are important for the optimal function of the wind turbine, some studies have demonstrated a decrease in the rate of aging of the transmission when the wind is less turbulent [19], and others mentioned that loads increased at low wind speeds due to turbulence [79].

In addition to physical damage, turbulent wind can also impact the power quality of the wind turbine, leading to fluctuations in the electrical output, which can cause problems for the

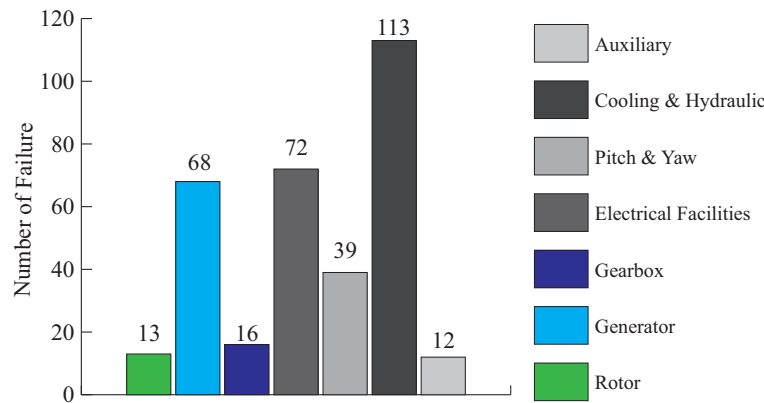


Figure 1.4: Number of failure by major components in wind turbines

electrical grid [131].

In conclusion, it is evident that turbulence in the wind plays a crucial role in the performance and reliability of wind turbines. While traditional standards for designing wind power curves primarily consider average wind speed and air density, it is increasingly clear that the effects of turbulence must also be taken into account. In light of these findings, this work, will prioritize the impact of turbulence to optimize the performance of wind turbines.

#### 1.2.4 Deterioration in Wind turbines

Wind turbines are complex mechanical systems that are affected by cyclic loads due to changes in atmospheric conditions such as dust, humidity, temperature, air pressure, and wind gusts. These loads can significantly damage the transmission system due to excessive vibration, particularly when high wind gusts strike the blades. Various sources indicate that wind turbine drive-train systems have a relatively high failure rate, with maintenance being the leading cause of downtime [10, 37, 63, 68, 101, 143], which generally increases with age: During the first 4 years, the unavailability remains relatively low at around 3.2%. However, between ages 14 and 19 years, the unavailability can increase, ranging from 5% to 9% [94].

Li et al. [64] utilized numerous databases from different countries to analyze the frequency of failures by components in wind turbines. They concluded that the parts related to the drive-train (rotor, generator, and gearbox) represent 27% of the failures present in wind turbines (see Figure 1.4). Additionally, 30% of shutdowns result from failures in one of the parts of the drive-train. Furthermore, 80% of critical and highly critical failures in the principal components of wind turbines occur in drive-train parts, of which 52.5% correspond to critical failures, meaning they reduce availability and require timely maintenance, and 47.5% are extremely critical, resulting in the stoppage of the wind turbine and requiring extended maintenance.

In wind turbines, the transmission can deteriorate and cause failures to occur within 2 to 11 years under poor working conditions; despite being designed to last for 20 years, it also can lead to a decreased efficiency in the operating time due to high vibrations [142]. Some studies evidenced that the drive-train contributes approximately a 30% share to the degradation [19].

The deterioration can lead to other types of failures, such as planetary gear, high-speed shaft bearing, planetary bearing, and intermediate shaft bearing failures. These failures can occur due to wear, scuffing, plastic deformation, contact fatigue, cracking, fracture, and bending fatigue [90].

The efforts to address these challenges have resulted in developing and implementing strategies for optimizing maintenance, such as advanced condition monitoring techniques. These techniques detect changes in vibration levels and other performance indicators that could indicate potential problems [22]. By taking preventive action before severe damage occurs, maintenance teams can reduce the overall cost of operation and maintenance (O&M) for the transmission system.

Mathematical models have recently been developed to predict wind turbine degradation and maintenance to understand the degradation process's behavior better [44]. These models include a probabilistic model that considers the stochastic nature of the failure and repair processes, as well as Markov Chain analysis [65, 93], to study the level of degradation. Additionally, a reliability-centered method has been implemented to demonstrate the effect of different maintenance strategies based on the system's reliability and the total maintenance cost [63].

On the other hand, to mitigate the effects of wind-induced vibration and reduce the overall stress on the transmission system, some wind power projects may implement intelligent control strategies. One such strategy is pitch control, which adjusts the pitch angle on the blades to maintain a stable output power when the wind speed exceeds the rated wind speed. However, implementing this type of strategy is difficult due to the non-linearities of the system and the uncertainty of the measurements [124]. However, this strategy does not apply to variable-speed fixed-pitch (VS-FP) wind turbines, where the pitch is ideally zero, and any control action is made through the tip-speed ratio [15, 56, 122].

Therefore, inappropriate control designs might accentuate the vibration modes, potentially destroying some mechanical devices such as gearboxes or blades. The controller must provide damping at the vibration modes whenever possible to mitigate high-frequency loads and reduce the risk of fatigue breakdown. On the other hand, the control strategy must avoid operation at points where those vibration modes that the controller cannot damp are likely to be excited [16]

### 1.2.5 Control methods for Wind Turbine

The purpose of wind turbine controls is to ensure the safe and automatic operation of the system, reduce operating costs, maximize energy capture, and prevent dynamic mechanical loads caused by the intermittent and variable nature of wind. The capacity of a wind turbine to produce energy, taking into consideration physical constraints, can be represented in a power curve. This curve illustrates generated power vs. wind speed, as shown in Figure 1.5. Under ideal conditions, a wind turbine will reach nominal power ( $P_{nom}$ ) when a nominal wind speed ( $V_{nom}$ ) occurs, following the behavior of the curve presented in Figure 1.5. At this point, the system is working at  $C_p^{max}$ , allowing for a compromise between available energy

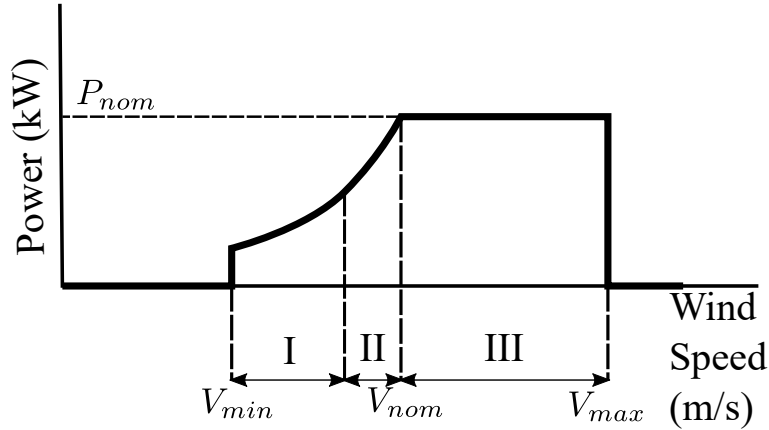


Figure 1.5: Power curve of a wind turbine

and operational cost.

The operational range of wind turbines is typically delimited by the cut-in wind speed ( $V_{min}$ ) and the cut-off wind speed ( $V_{max}$ ). Outside of these limits, the turbine remains stopped. The turbine will not operate when the wind is below  $V_{min}$  due to not compensating the cost of operations, and if the wind speed is higher than  $V_{max}$ , the system will shut down for structural safety [75].

The power curve is typically divided into three zones. Region I occurs at low wind speeds, where the available power is lower than the nominal power. In contrast, region III occurs at wind speeds higher than the nominal power. The control system limits power generation in this region by operating at a lower efficiency than  $C_p^{max}$  to avoid overloading. Besides, Region II is a zone of transition, where the control system will try to maintain the centrifugal forces below the values that the rotor can tolerate.

Wind turbines are subject to static and dynamic loads during normal functioning. Static loads result from wind speed and typically do not pose significant control problems. However, dynamic loads cause variations in the aerodynamic torque, affecting the integrity of the drive-train. These loads are usually caused by turbulence and wind gusts. Moreover, they are typically found in regions II. Commonly, the wind speed has a higher magnitude than  $V_{nom}$ . [16].

The design of a wind turbine's control system can vary depending on its modes of operation. Some configurations consider fixed speed or pitch, while others consider variable speed or pitch. It is also common to design wind turbines with combinations of these objectives. Depending on the desired objectives, the design can have either fixed or variable pitch for variable-speed wind turbines.

The variable speed-variable pitch (VS-VP) wind turbines are programmed to operate with a fixed pitch when the wind speed is lower than  $V_{nom}$  and with a variable pitch in region III. In contrast, VS-FP wind turbines always operate with a fixed pitch and can work with either passive or speed-assisted stall control strategies. The passive stall strategy aims to search for

---

$C_p^{max}$  until region II is reached. Then, the control switches work with a fixed speed to capture as much energy as possible without overloading or adding risk to the system. In contrast, the speed-assisted stall control strategy always operates with  $C_p^{max}$ ; the rotational speed increases proportionally to wind speed until it reaches the nominal point and will operate with this constant speed, creating some inevitable loads in region II [16].



### 1.3 Scope & Objectives

Wind turbines play a role in the renewable energy sector to address the global energy demand while mitigating environmental concerns. However, these complex systems are susceptible to degradation over time due to the dynamic and unpredictable nature of wind conditions. The degradation can affect the system in multiple ways, including reduced power quality and structural damage to the drive-train components, ultimately reducing the overall efficiency and lifespan of wind turbines.

Understanding and managing degradation is crucial for optimizing the performance and reliability of wind turbines. However, a significant challenge is to develop an accurate dynamic model of the drive-train that accounts for the deterioration process, especially when resonance modes are present. Additionally, implementing control strategies significantly impacts vibration modes and mechanical component damage, making it a critical aspect of turbine operation. It is important to note that traditional control strategies primarily rely on adjusting the pitch angle, which does not apply to fixed-pitch wind turbines. Therefore, there is a strong need for developing a sophisticated control system aware of degradation and capable of effectively optimizing wind turbine operation in variable-speed fixed-pitch configurations.

The primary objective of this research is to develop and evaluate a control strategy for variable-speed fixed-pitch wind turbines that takes into account the degradation caused by the variability in wind conditions. This control strategy aims to minimize the negative impact of degradation on the turbine's drive-train. The ultimate goal is to achieve a balance between energy dissipation and energy generation, maximizing turbine performance while reducing degradation.

To accomplish this central objective, the following specific tasks and objectives will be pursued:

1. **Deterioration Modeling:** Develop an accurate deterioration model that describes the influence of changes in the control, and system disturbances, on the degradation process. This model will provide a theoretical foundation for understanding degradation dynamics.
2. **Control Strategy Development:** Create a control strategy that integrates the degradation model's insights, effectively optimizing the trade-off between energy dissipation and energy generation. The control strategy will be adaptable to fluctuations in wind conditions, allowing for the mitigation of drive-train degradation.
3. **Long-term Degradation Simulation:** Establish an approach for simulating the long-term deterioration of the wind turbine. This simulation will incorporate the developed control strategy to ensure that it considers the trade-off between degradation and energy generation.
4. **Robust Control:** Propose a robust control strategy capable of managing the rate of degradation, ensuring that wind turbine performance remains consistent even when confronted with sudden changes in wind conditions or set-points.

## 1.4 Organization of the document

This thesis is organized into six chapters, organized as follows:

- **Chapter 2:** provides a literature review and background information on wind turbine degradation and deterioration-aware control, which is necessary for understanding the problem addressed in this thesis and the proposed solution. The chapter is divided into three main sections: The first part explains the fundamental principles and equations for modeling the dynamic of the drive-train in a wind turbine. On the other hand, the second section mentions the principles of degradation modeling methods. The third section covers different control strategies that utilize strategies such as prognostic or health management information to control degradation. The chapter concludes by summarizing the key findings of the literature review and highlighting the research gaps that the proposed solutions aim to address.
- **Chapter 3:** This chapter introduces the proposed degradation model for a wind turbine's drive-train. The model is based on contact mechanics and estimates the dissipated energy at the shaft for different wind conditions and control gains, both optimal and sub-optimal. The second section validates the proposed model by using simulation scenarios and implementing a wind turbine prototype. The results illustrate the impact of persistent variations in the shaft angle when the system is submitted to wind speed with high variances and sub-optimal conditions.
- In **Chapter 4** a gain-scheduling control strategy is proposed to optimize the efficiency of a wind turbine under varying weather conditions. The proposed strategy aims to find an optimal trade-off between generated energy and degradation due to dissipated energy in the drive-train. The chapter is divided into two sections: The first section explains the details of the proposed gain-scheduling control strategy, including the methodology of selecting suitable control gains and the optimization process. The Results section tests the proposed strategy using different wind speed scenarios to consider a wide range of possible wind conditions affecting the turbine. The results demonstrate that the gain-scheduling control strategy allows for maximizing generated energy and decreasing dissipated energy by switching the control gains depending on the wind flow conditions. This leads to a closer approximation to the theoretical optimal behavior.
- **Chapter 5** presents a proposed methodology for estimating the long-term degradation of a wind turbine's drive-train using a gain-scheduling control strategy and considering the variation in wind conditions. The chapter is divided into two main sections: implementation of the proposed methodology by steps, results, and discussions. The first section describes the detailed process of implementing the methodology, including acquiring wind speed data, simulating the dissipated energy in the drive-train, estimating the slope in the dissipated energy vs. time curve, and generating new slope data. The second section presents the analysis results, including graphs of dissipated energy for different periods and a comparison of the dissipated energy for the cases using the suitable control gain and the theoretical control gain.

- **Chapter 6** proposes a strategy for managing the degradation rate of a wind turbine's drive-train while maintaining energy generation under varying conditions. The chapter is divided into three main sections. The first section presents the definition of the problem that can be solved with the proposed strategy. In the second section, the design of the robust deterioration controller using  $H_\infty$  method. The third section presents the implementation of the degradation controller and evaluates its performance under different scenarios, including changes in the set point and variations in disturbances. The chapter concludes with suggestions for future research, including implementing the proposed control strategy in an experimental system and integration with a remaining useful lifetime control method.

The document finishes with a section where are presented the conclusions and perspectives of this thesis.

## 1.5 Main Contributions

In this thesis, a new degradation model was developed for the drive-train in wind turbines. This model considers the effects of wind turbulence that result from operation on sub-optimal points. The results led to the development of a gain-scheduling control strategy that balances degradation and energy generation. A methodology for estimating long-term energy dissipation considering suitable control gains depending on wind conditions was also developed.

Finally, the results obtained in the previous stages aided in developing a degradation-aware control strategy that adjusts the maximum power point tracking control gain using a robust H-infinity control strategy. This strategy ensures system stability in the presence of uncertainties and external disturbances, such as changes in the wind.

## Publications

As result of the work of this thesis, different articles and presentations were made:

- Romero, E.E., Martinez, J.J., and Berenguer, C. (2021) **Degradation of a wind-turbine drive-train under turbulent conditions: effect of the control law**, In Proc.5th International Conference on Control and Fault-Tolerant System - SYSTOL 2021 2, *Saint-Raphaël- France, September 29-October 1st 2021*.
- Romero, E.E., Martinez, J.J., and Berenguer, C. (2022) **Gain-scheduling wind-turbine control to mitigate the effects of weather conditions on the drive-train degradation.**, In Proc. 11th IFAC Symposium on Fault Detection, Supervision and Safety for Technical Processes - SAFEPROCESS 2022, *Pafos - Cyprus, 8-10 June 2022*.
- Romero, E.E., Martinez, J.J., and Berenguer, C. (2022) **Long-term degradation estimation of wind turbine drive-train under a gain-scheduling control strategy according to the weather conditions.**, In Proc. 5th IFAC

Workshop on Advanced Maintenance Engineering, Services and Technology - AMEST 2022, *Bogotá - Colombia, 26-29 July 2022.*

- *Submitted.* Romero, E.E., Martinez, J.J., and Berenguer, C. (2023) **Intelligent robust control for the degradation rate of a wind turbine drive-train**, In Journal: Engineering Applications of Artificial Intelligence

### Awards & recognition

As result of the work and presentations made at conferences, the following awards were obtained:

- 5th IFAC Workshop on Advanced Maintenance Engineering, Services and Technology - AMEST 2022. Long-term degradation estimation of wind turbine drive-train under a gain-scheduling control strategy according to the weather conditions. **Best Paper Award-** *Bogotá - Colombia, 26-29 July 2022.*
- 5th IFAC Workshop on Advanced Maintenance Engineering, Services and Technology - AMEST 2022. Long-term degradation estimation of wind turbine drive-train under a gain-scheduling control strategy according to the weather conditions. **Best Young Author Award** - *Bogotá - Colombia, 26-29 July 2022.*

### Additional Activities

- Presentation of Mini Variable-Speed Wind Turbine in 6èmes journées des Démonstrateurs en Automatique. *Angers - France, 21-22 June 2022..*
- Presentation of "Evaluation and controlling of the degradation in a drive-train wind-turbine considering the weather conditions" in the Universidad del Valle (Project ECOS NORD). *Cali - Colombia, 17-22 July 2022.*
- Presentation of "Gain-scheduling wind-turbine control to mitigate the effects of weather conditions on the drive-train degradation" in the Universidad del Valle (Project ECOS NORD). *Cali - Colombia, 17-22 July 2022.*



# Literature Review & Theoretical Background

---

## Contents

<b>2.1</b>	<b>Fundamentals of Wind Turbines</b>	<b>21</b>
2.1.1	Control in Wind Turbines	23
2.1.2	Wind Modelling	27
<b>2.2</b>	<b>Deterioration in Wind Turbine</b>	<b>29</b>
2.2.1	State of art on deterioration modeling in wind turbines	30
<b>2.3</b>	<b>Deterioration-Aware Control in Wind Turbines</b>	<b>33</b>
<b>2.4</b>	<b>Conclusions</b>	<b>37</b>

---

This chapter aims to provide the basis and fundamentals for identifying the existing research gap in the literature concerning the study of deterioration on the drive-train of a wind turbine considering the wind conditions and how operating the wind turbine under sub-optimal conditions can affect the system's health.

Chapter 2 presents the fundamental principles of aerodynamics and control in wind turbines, along with various models and methods for simulating wind behavior. Section III provides an overview of the advancements in studying the deterioration of wind turbines, with a specific focus on drive-train degradation. Furthermore, the chapter discusses state-of-the-art methods that can be implemented as degradation-aware control in wind turbines, and concludes with general remarks and the identified gaps.

## 2.1 Fundamentals of Wind Turbines

The primary objective of a wind turbine is to extract the maximum amount of power from the wind to generate electricity. The power that can be obtained from the wind when passing through the rotor area  $A$  can be determined using the general equation of kinetic energy:  $E_{kinetic} = \frac{1}{2}\rho AV^2$  [16, 23, 56]. Therefore, the power that can be obtained from the wind ( $P_w$ ) can be expressed as:

$$P_w = \frac{1}{2}\rho AV^3 \quad (2.1)$$

The efficiency of the wind turbine can be determined by  $C_p$ , which is the ratio between the mechanical power from the rotor  $P_r$  and the wind power  $P_w$ . Thus,  $C_p$  can be expressed as follows:

$$C_p = \frac{P_r}{P_w} \quad (2.2)$$

Thus, the theoretical power output ( $P_r$ ) that a wind turbine can extract from the wind is given by the expression:

$$P_r = C_p(\lambda, \psi) \frac{1}{2} \rho R^2 \pi V^3 \quad (2.3)$$

where  $\rho$  is air density,  $R$  is the radius of the rotor swept area,  $V$  is the wind speed and  $C_p(\lambda, \psi)$  is the power coefficient, which is dependent on  $\lambda$  and can also be dependent on the pitch angle  $\psi$  in some operational modes. In addition, the aerodynamic torque applied to the rotor by the wind  $\tau_r$  can be calculated as follows:

$$\tau_r = \frac{1}{2} \rho \pi R^3 \frac{C_p(\lambda, \psi)}{\lambda} V^2 \quad (2.4)$$

As Section 1.2.2 mentions,  $C_p^{max}$  represents the maximum achievable  $C_p$ . According to the Betz limit, the maximum power that can be extracted from the wind is 0.59 or 16/27 of the total power in the wind. The value of  $C_p$  depends on the tip-speed ratio  $\lambda$ , as illustrated in Figure 1.3. The optimal value of  $\lambda_0$  corresponds to the point where  $C_p^{max}$  is reached. For other operating points,  $\lambda$  can be computed as follows:

$$\lambda = \frac{\omega_r R}{V} \quad (2.5)$$

The turbine design determines the  $C_p^{max}$ , but  $\lambda$  is variable, making it difficult to estimate the actual  $C_p$  during operation. Since  $C_p$  is the most reliable indicator of the system's efficiency, various methods have been developed to estimate the power curves of the turbines with accuracy. These methods include the theory of aerodynamics, blade element momentum (BEM) theory, computational fluid dynamics (CFD), fuzzy logic, and the generalized dynamic wake (GDW) model [1, 93, 100, 106, 138, 150]. However, a simple option to estimate the aerodynamic power coefficients is using numerical approximations, as explored in [29, 59, 116]. Those type of models has the form:

$$C_p(\lambda, \psi) = c_1 \left( \frac{c_2}{\lambda_i} - \frac{c_3}{\psi} - c_4 \lambda_i \psi - c_5 \psi^x - c_6 \right) e^{-\frac{c_7}{\lambda_i}} + c_8 \lambda \quad (2.6)$$

The authors of the article presented in [116], proposed to optimize the equation (2.6), the parameter  $\lambda_i$  and the different constants as:

$$\lambda_i^{-1} = (\lambda + c_9\psi)^{-1} - c_{10}(\psi^3 + 1)^{-1} \quad (2.7)$$

with  $c_1 = 0.22$ ;  $c_2 = 120$ ;  $c_3 = 0.4$ ;  $c_4 = 0$ ;  $c_5 = 0$ ;  $c_6 = 5$ ;  $c_7 = 12.5$ ;  $c_8 = 0$ ;  $c_9 = 0.08$ ;  $c_{10} = 0.035$ ;  $x = 0$ .

Note, for the case of VS-FP wind turbines,  $\psi$  is considered ideally zero. Thus,  $C_p$  will just depend on  $\lambda$ .

### 2.1.1 Control in Wind Turbines

The VS-FP wind turbines require precise control strategies to achieve maximum performance. One such strategy is integrating the Maximum Power Point Tracking (MPPT) algorithm, which helps maintain the optimal point of operation by controlling the rotor speed in response to the wind.

As previously mentioned, wind turbines reach their Maximum Power Point (MPP) at a specific point denoted as  $C_p^{max}$ . In variable-speed wind turbines, this is achieved at an optimal tip-speed ratio, which can be maintained by the control algorithm that adjust the rotational speed proportionally to the wind speed. This is critical for fully utilizing the advantages of variable-speed operation [16].

To achieve this, an MPPT control algorithm for VS-FP wind turbines must consider torque control, represented by  $\tau_c$ , as a function of the rotor speed, as follows:

$$\tau_c = K_c^{opt}(\omega_r)^2 \quad (2.8)$$

here  $K_c^{opt}$  is the optimal feedback control gain, which is given by:

$$K_c^{opt} = \frac{1}{2}AR^3 \frac{C_p^{max}}{\lambda_0^3} \quad (2.9)$$

Thus, the generator power will be:

$$P_g = \tau_c \omega_r \quad (2.10)$$

and, as a consequence, the generated energy will be:

$$E_g = \int_0^t P_g dt \quad (2.11)$$

When operating VS-FP wind turbines, finding a balance between the wind speed, rotor speed, and power is essential. In addition, some control strategies aim to reduce energy extraction to avoid areas where mechanical loads may occur. To address this concern, a speed or torque control loop can help mitigate the cyclic loads that impact the drive-train.



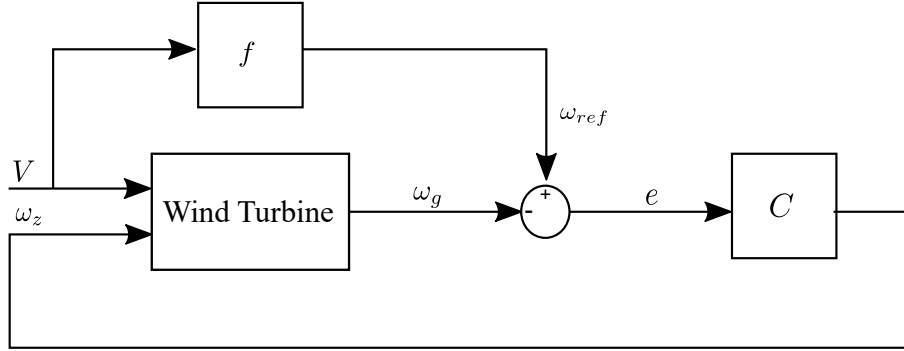


Figure 2.1: Speed control loop for variable speed operation

- **Speed Control Loop**

The speed control strategy is widely employed to ensure that a generator attains the desired angular speed and generates the maximum energy. Figure 2.1 illustrates a speed control loop architecture, similar to that presented in [16]. The wind turbine system receives the wind speed  $V$ , and  $\omega_z$  is used for controlling torque provided by the generator, whereas  $\omega_g$  is the actual angular speed of the generator. This output value is compared with an angular speed reference  $\omega_{ref}$  to estimate an error. The controller  $C$  receives the error signal to generate the signal  $\omega_z$ .

To estimate the reference, the MPPT control law for VS-FP wind turbines is considered for Regions I and II of operation, as follows:

$$f = \omega_{ref} = \begin{cases} \frac{\lambda_0 V}{R} & \text{for Region I} \\ \omega_{nom} & \text{for Region II} \end{cases}$$

To obtain the maximum value of  $C_p$ , the angular speed nominal ( $\omega_{nom}$ ) of the wind turbine is used. However, measuring the rotor speed to estimate the error ( $e$ ) can be challenging. In such cases,  $\omega_g$  is often used to estimate low frequencies, as pointed out in [16].

A simpler variation of this strategy is Tip Speed Ratio Control, where the principle is to keep the  $\lambda$  constant at its optimal value ( $\lambda_0$ ) to extract maximum energy. This strategy compares the actual tip speed ratio to the optimal one. It calculates an error ( $e = \lambda_0 - \lambda$ ), which a controller then uses to adjust the rotational speed and minimize the error [1].

- **Torque Control Loop**

Figure 2.2 illustrates a torque control loop, an alternative approach to controlling the speed tracking error [16]. It operates on two levels of control loops and relies on the generator speed to estimate the rotor speed. The wind turbine uses as

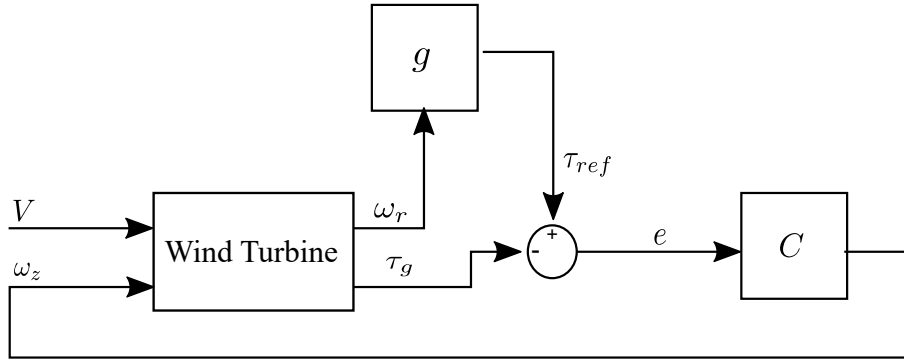


Figure 2.2: Torque control loop for variable speed operation

inputs the wind speed  $V$  and angular speed  $\omega_z$ ; this input is used for controlling the torque provided by the generator. The outputs are the real angular speed of the rotor  $\omega_r$  (using  $\omega_g$  for estimation) and the generator torque  $\tau_g$ .

The block  $g$  represents the MPPT control law presented in Equation 2.8. It estimates the reference torque and then compares it to the output  $\tau_g$  to compute an error. This error serves as the input to the controller  $C$ . The controller then adjusts the signal  $\omega_z$  that minimizes the error.

- **Perturbation & Observation Control (P&O)**

The Perturbation and Observation (P&O) method, or MPPT Peak Power Tracking or Hill-Climb Searching (HCS), is often used in VS-FP wind turbines to adjust the control variables during wind speed fluctuations [85]. It involves utilizing mathematical optimization to identify the local optimal point in a function. The method divides the graph  $C_p$  vs  $\lambda$  as shown in Figure 2.3 into three zones: These zones are categorized as the positive slope (to the left of  $C_p^{max}$ ), zero slopes (at  $C_p^{max}$ ), and negative slope (to the right of  $C_p^{max}$ ). When the operating point falls within the positive slope zone, the controller reduces the load current to increase the rotational speed. On the other hand, if the operating point falls within the negative slope zone, the controller takes the opposite action [85, 147].

The Perturbation and Observation method is commonly used because of its simple, sensorless, and flexible structure. However, in the P&O control method, the direction of the next perturbation is determined based on whether the power increased or decreased due to the previous perturbation. However, this control method does not consider wind changes, which can be misleading. The sign of the perturbation might be influenced by changes in wind rather than the applied perturbation. This incorrect decision leads to a failure in maintaining the maximum power point (MPP), causing the P&O control to move in the wrong direction [1, 61].

On the other hand, a more significant step size improves convergence speed but

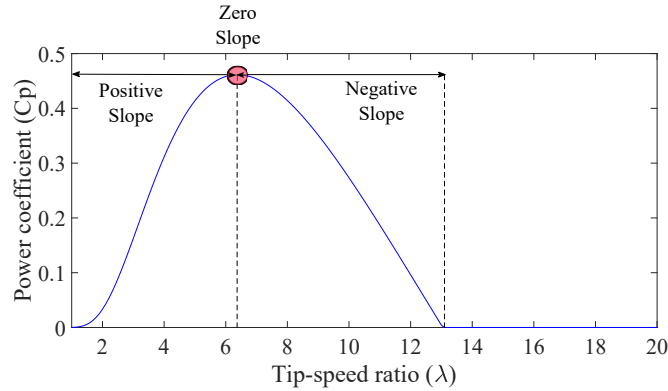


Figure 2.3: Characterization of curve  $C_p$  vs  $\lambda$  for Perturbation and Observation method

decreases the efficiency of MPPT by amplifying oscillations around the MPP. On the other hand, a smaller step size improves efficiency but slows the convergence speed, which may make the controller unable to track the MPP under rapidly changing conditions [1, 9, 61, 97].

Several wind turbine control strategies have been developed based on the earlier general architectures. Some methods are designed to maximize power output in Region II of operation, such as fuzzy logic-based MPPT algorithms.

Fuzzy logic control algorithms are applied to VS-FP wind turbine control with complex nonlinear models and parameter variations. These algorithms use rotational speed and an aerodynamic torque observer as inputs. This strategy uses a reference torque to limit the output power and speed fluctuations, as presented in [89]. Although this strategy has many advantages, it is only sometimes used due to its complicated implementation. [89]. Also, Simani in [126] presented an approach of fuzzy modeling and identification oriented to the design of a PI fuzzy controller for regulating both the pitch angle and the reference torque of a wind turbine model, and in [125] was presented a data-driven fuzzy wind turbine control method, where it is suggested to describe the system by a collection of local affine systems of the type of Takagi-Sugeno (TS) fuzzy prototypes.

On the other hand, Jargalsaikhan et al. [55], presented a new control algorithm for wind turbines in strong wind conditions and the proposition to create a new zone of operation called Region 4. The algorithm uses rotational speed and pitch angle control systems to regulate the generator's output power in different regions. The proposed control system reduces the active power and rotational speed in Region 4, whereas the conventional control method shuts down the wind turbine. Additionally, the proposed control system can reduce the pitch actuator action and high-aggressive aerodynamic behavior of wind turbines. The wind turbines using the proposed control method can generate power up to 35 m/s, beyond which they are automatically shut down.

Another method is the power signal feedback method, which uses the same loop architecture as the torque control method. However, instead of controlling the torque, it uses

power as the variable for control. This method can employ PI controllers to regulate the output power, and the control gains can be optimized using Particle Swarm Optimization. Nevertheless, the most effective solution is to use robust control strategies, such as  $H_\infty$  techniques for linear parameter varying (LPV) systems [82].

In recent years, the  $H_\infty$  method has been widely utilized in various areas of wind turbine control. Several studies have been conducted, including a control strategy presented in [81] to decrease wind turbine structural loads. Additionally, a pitch  $H_\infty$  control strategy was introduced in [129] for VS-VP wind turbines, improving the rotor standard deviation of the wind turbines under normal and extreme wind conditions. To maintain wind turbine performance in bad weather conditions, such as snow or rain droplets freezing on the turbine blades, a control technique using the  $H_\infty$  method was implemented [102]. Furthermore, Do et al. [34] developed a control strategy that accommodates disturbances, using the  $H_\infty$  approach and combining disturbance observers and rejection controllers to handle unknown disturbance effects.

Existing control strategies often focus on optimizing power output and improving efficiency without accounting for the impact of deterioration on turbine performance. Incorporating deterioration as a control variable could lead to more accurate and adaptive control strategies that can adjust turbine operation based on the health condition of the components.

Additionally, there exists a limited consideration of turbulence intensity variation as a factor to control in order to improve efficiency. By developing control algorithms that can dynamically respond to changes in turbulence intensity, it may be possible to optimize turbine operation and improve overall energy capture.

Exploring these research gaps and developing control strategies that consider deterioration and wind conditions as control variables could lead to more robust and efficient wind turbine systems.

### 2.1.2 Wind Modelling

Due to the geometry of the wind turbine, it is usual that the sensors do not accurately measure the wind speed; also, depending on the position of the anemometer, the wind speed gust will induce noise and error in the lecture of the sensor. In order to obtain a better measurement, sometimes an array of anemometers is utilized to estimate the wind speed field upstream of the turbine and then predict the wind speed at the turbine site; however, it is a complex alternative. Therefore, it is not uncommon to utilize other parameters that are easier to measure (such as temperature or pressure) to estimate the effective wind speed.[16].

The probability density and cumulative functions are some resources that often use recorded wind speed data to estimate effective wind speed. Due to the stochastic nature of the wind speed, it is not recommended to use these statistical methods for a

short time scale. However, for long-term time scales, wind shows patterns that allow probabilistic distribution to determine the statistical characteristics of wind [25, 73].

The Weibull distribution is frequently utilized in wind engineering to model wind speed distribution. In order to obtain acceptable prediction results, it is necessary to accurately estimate at least two parameters (shape and scale); otherwise, it can result in errors in wind power estimation, the power generation, and inaccurate wind load estimations that can affect the lifespan of the turbine. Although multiple studies have developed methods for parameter estimation, there is not a universally accepted formal method [58, 73].

To represent annual or seasonal periods, the Weibull distribution is typically used due to its favorable estimations for long-term scale. However, since it is not time-dependent but rather a static distribution, it is not recommended to represent the frequent short-term wind speed fluctuations essential for trading and storing wind energy [57]. Other distributions, such as the Gamma, Lognormal, Normal, Rayleigh, Joint-Gaussian, Burr, Nakagami, or Extended Generalized Lindley, have been implemented to achieve a better fit to data and predict wind speed with greater accuracy, and different research has conducted comparative analyses among these distributions in an attempt to identify the best one [3, 35, 67].

Another common way to reproduce wind speed is a time series model, often is implemented to simulate historical wind speed data for a specific location due to a simple structure and computational efficiency. However, their linear forms limit their usefulness, and the ability to predict accurately decreases as the time frame becomes longer [76]. Two of the most known methods of this type of model are: Autoregressive Moving average (ARMA) [38, 46] and Kalman Filter [2, 51, 149].

On the other hand, various models have been developed in the literature to reproduce or predict wind speed. In the prognosis or prediction of Remaining Useful Life (RUL) for wind turbines, short-term wind behavior forecasting is often employed to improve turbine efficiency [68, 78], the estimation of the expected RUL is quite helpful to reduce maintenance cost, safety hazards, and operational downtime [60].

Stochastic differential equations (SDE) are used to estimate the parameters of wind speed's underlying stochastic process. These models accurately represent the effect of turbulence in short time scales by introducing fluctuations in wind speed. Moreover, they enable the generation of long-term wind speed predictions that account for seasonal variations in wind behavior. The Ornstein–Uhlenbeck (OU) and the Brownian motion models are incorporated in SDE for reproducing wind speed and turbulence intensity on a scale of seconds [5]. Also, other authors have introduced Markov Chain methods to wind modeling, considering that the generation of wind does not need past information to generate new wind data and allowing the times between transitions to occur according to any distribution functions, which may depend on the current and the next visited state [36, 77, 136].

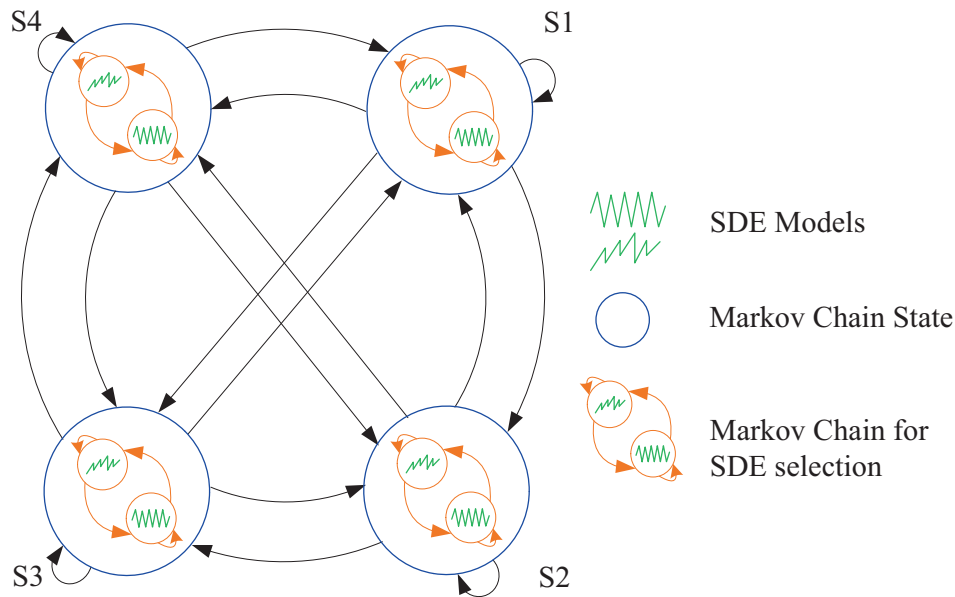


Figure 2.4: Scheme of wind speed generation model of two level Markov chain embedded with Stochastic differential equations proposed in [77].

A flexible wind speed generation model was presented by Ma et al. on [77], bringing an alternative method that allows generating continuous wind speed without time-length limitations due to generating short and long-term. This method is based on a 2-level Markov Chain with SDE, allowing the consideration of different levels of turbulence that can be adjusted depending on the indices on the SDE, see Figure 2.4: The external Markov Chain is used to model general wind speed trend such as average wind speed for a timescale, The embedded SDE is used for model continuous wind speed, and the inner Markov Chain randomly changes between the two classes of wind. Further information on [76, 77].

## 2.2 Deterioration in Wind Turbine

Deterioration or degradation refers to the process of decreasing the performance and reliability of assets. It is considered a health indicator of a system, as the maximum level of degradation often coincides with a specified failure threshold. Therefore, it is logical to conclude that degradation occurs earlier than failures, and valuable insights can be gained from this phenomenon [44]. It does not exist any general indicator or estimator of deterioration. However, various methods are available to assess the level of degradation of different mechanisms [111].

A large number of different research on the degradation of wind turbines have been developed during the last 15 years [119]. Some studies found that the wind turbines lose  $1.6 \pm 0.2\%$  of their output per year as a consequence of the degradation of the

systems [130]. Other studies found that the capacity factor can decrease around 6% during the lifetime of the system [42, 94], and the efficiency index of the turbine was found to decline by 0.64% every year of its operation [19, 80].

### 2.2.1 State of art on deterioration modeling in wind turbines

Modeling the deterioration is essential for predicting remaining useful life (RUL), planning for maintenance, and managing the overall health of the systems [121]. Various methods have been developed in the wind turbine industry, including some in discrete space-state and others in continuous states-spaces. These techniques help to predict and manage degradation accurately. The most common used for wind turbine degradation are: Markov Chain models, Data-driven or trend methods, Signal-based methods, Models with increments, Hybrid methods.

#### Markov Chain Models

Sometimes, it is considered that certain physical degradation phenomena have a discrete state-space, making Markov Chain a useful tool as a stochastic process with discrete states [107, 140]. Some of the studies that implemented the Markov Chain methodology to study the degradation of wind turbines are:

- A reliability assessment for the wind turbine bearing of 105 components was developed using a degradation model based on the Hidden Markov Chain in [65].
- A wind turbine component degradation maintenance model was developed using the Markov Chain methodology [95]. The study assumes that the components of a wind turbine degrade 90% of the lifetime in three stages: in maturity (50%), aging (30%), and terminal (10%). A Monte Carlo simulation also determined the transition probabilities between stages.

#### Data-driven or trend methods

A data-driven methodology was proposed in [86] to characterize the long-term and short-term performance degradation associated with wind turbine aging considering confounding factors, such as operative modes and environmental conditions.

Byrne et al. in [19] explored the performance degradation of a Vestas V52 wind turbine caused by drive-train aging through a multivariate Support Vector Regression with Gaussian Kernel. Another study was presented by Mathew et al. in [80] utilizing Deep Neural Networks and data from 10 years to estimate an efficiency index for measuring age-related performance degradation for a wind turbine.

A research conducted by Olauson et al. in [94] using regression analysis to examine the aging of wind turbines. The study utilized two data sets, with some overlap, consisting of 1,100 monthly and 1,300 hourly time series that spanned 5 to 25 years each.

In a study conducted by Astolfi et al. in [7], the focus was on the impact of aging on wind turbine performance. The study concluded that it is not accurate to assume that performance decline occurs at a consistent rate year after year based on cumulative data. Therefore, false expectations should not be made regarding wind turbine performance.

A data-driven methodology was proposed By Murgia et al. [86] to characterize the long-term and short-term performance degradation associated with wind turbine aging considering confounding factors, such as operative modes and environmental conditions.

To assess the age of wind turbines using SCADA data, various criteria for degradation in control and other systems were developed by Dai et al. in [28].

On the other hand, some studies have used efficiency variation to indicate the system's degradation level. He. et al. [47] used a linear Wiener process to estimate the system efficiency loss due to the degradation of some components.

### Signal-based methods

When analyzing signals, signal-based methods are often used to monitor wind turbines' structural health efficiently. This approach requires additional sensors for signal measurement, which can increase operational costs. In the research on the drive-train deterioration, different studies have been made:

The deterioration in the drive-train has been analyzed in [30] using vibration-based health-monitoring techniques, oil-debris analysis techniques, and wind turbine operational parameters combined to provide improved detection and decision-making capabilities compared to using only individual diagnostic tools.

Some researchers affirm that there are gaps in predicting degradation caused by vibrations in the drive-train. This is due to cross-term interference and the inability of conventional models to adapt to changes in probability distribution. Additionally, it is challenging to obtain accurate fault information using a single sensor because of attenuation and interference caused by complex signal transmission paths [74]. However, a multi-sensor learning strategy is proposed to solve the data distribution mismatch due to the change in sensor locations and operating conditions [98, 99].

### Models with increments

Models with increments are commonly used to represent degradation in a continuous state space over a specific time interval [107]. These models are typically utilized when it is feasible to monitor physical damages. Wind turbines have served as examples of where this method has been applied.

A study by Sun et al. [135] has developed a dynamic reliability model for wind turbine gear drives that considers stress deterioration and strength degradation. A Monte Carlo method was used to determine the probability distribution of gear contact stress.



Another method was presented in [103] to extract the degradation feature of a planetary gearbox based on the alpha-stable distribution (or Levy process). The study used the vibration signal at three different time points (0 h, 500 h, 1000 h) to estimate the working time of the system since it is considered that the vibration amplitude of the planetary gearbox is proportional to the working time.

### Mixed methods

Model methods construct physical models representing the degradation of a wind turbine or a specific system. However, building a precise physical model for the complex interaction between different components and the influence of circumstances is challenging. Therefore, it is common to mix different types of methods. Mixed methods are often implemented to study the degradation in wind turbines, as shown in the following studies:

- Su et al. proposed a stochastic differential equation model of gearbox state transition to maximize the utilization of gearboxes on wind turbines. The model used the Weibull distribution and polynomial approximation to construct the degradation model [133]. After a modification of the degradation model was developed to describe the state change process of wind turbines, the Brownian motion is used to describe the fluctuation process of wind turbine states affected by external disturbance [132]. Another degradation model was developed on [134] based on stochastic differential equations to describe the spatio-temporal evolution behavior of wind turbine generators. The model uses a Weibull proportional hazards function to represent the component's failure rate, simulates random disturbance with Brownian motion, and solves the stochastic differential equations model by constructing a function transformation.
- Ghamlouch et al. [43] consider the deterioration process to be modeled using a jump-diffusion process, which involves independent and time-dependent Gaussian distributed increments with possible random jumps. This article discusses the overall deterioration mechanism of a system, which is influenced by the health condition of its components and various internal and external working conditions. It is also important to consider that this process can be affected by several factors, both external and internal, as well as the instantaneous working conditions and stress. The influence of environmental conditions is modeled by covariates impacting the deterioration process parameters, as a Markov Chain model.
- Qin et al. [104] proposed to build a health indicator using a supervised multi-head self-attention autoencoder (SMSAE) neural network for monitoring the degradation of rotating machinery. The author evaluated the exactitude of the proposed method, implementing it in evaluating the degradation of a wind turbine gearbox bearing. Another method for predicting degradation on wind turbines using an artificial neural network was developed by Saidi et al., [115] to predict remaining useful life (RUL) in high-speed shaft bearings wind turbine systems.

- The energy dissipated by a system has been used as an indicator of degradation. The general idea of using the dissipated energy as a lifetime parameter was proposed on [137]. The same assumption was considered by Rodriguez et al., [112], where the dissipated energy could be considered an image of the heat and the material worn at the contact level during traction. On the other hand, Gosar et al. [45], use the dissipated energy to represent the energy that is released as a result of irreversible structural changes, such as dislocation movements and fatigue damage, and it is assumed that is proportional to the fatigue damage.

In conclusion, various methods have been developed to model the deterioration of wind turbines and to provide valuable insights into assessing their degradation. However, the dynamic behavior of a flexible shaft is an essential factor in understanding the degradation and performance of wind turbines. Further research is needed to develop models that can accurately capture the effects of flexible shaft dynamics on deterioration, which will improve the prediction and management of wind turbine health in the long-term, while taking into consideration external factors such as changes in control or environmental conditions, for example, the impact of the level of turbulence intensity.

## 2.3 Deterioration-Aware Control in Wind Turbines

To manage the behavior and health of a system using Prognostic and Health Management (PHM) information is necessary a closed-loop control system [91]. The objective of the control system should consider not only the system's dynamic behavior but also its state of health (SoH), which includes factors such as accumulated damage, reliability, and remaining useful life (RUL) [32]. In the context of health management requirements, deterioration-aware control refers to adjusting control responses to mitigate stress on a system based on known parameters. This approach considers the system's deterioration state as part of the control objectives [39].

As was mentioned previously, it does not exist as a universal indicator of deterioration. However, fatigue damage is one of the most widely used metrics to assess the degradation or health status of wind turbines [32]. Fatigue damage control strategies are the most common method of direct damage strategies. Several investigations have developed control strategies to manage the degradation of wind turbines based on fatigue damage; some of them are presented below:

- The article presented by Sanchez et al. in [118], describes the integration of MPC with fatigue-based prognosis to minimize the damage to wind turbine components. The proposed mechanism optimizes the trade-off between component life and energy production. A linear fatigue damage model is established by utilizing the slope of the accumulated damage vs. the time curve. This model establishes a relation between a control signal, the angular rotor speed, and a disturbance (wind speed) with the damage of the blade root moment.

- An adaptive fixed-time terminal sliding mode controller was proposed by Yang et al. in [145] to eliminate the chaotic oscillation in wind turbine drive-trains with combined harmonic excitation.
- An MPC formulation of Rain Flow Counting (RFC) has been presented in [72] in an application-focused manner, highlighting how it directly incorporates mechanical fatigue in predictive wind turbine control.
- A fatigue damage reduction data-based MPC strategy was designed and implemented on a non-linear model-based wind turbine in [13]. The main idea is to control a wind turbine, reducing output power fluctuation and the incurred fatigue. The MPC strategy utilizes a fatigue indicator based on the shaft torsion.
- Sanchez et al. [117] describes a method for controlling wind turbines to minimize component damage. The method involves integrating MPC with fatigue-based prognosis, which allows for predictions of blade degradation using a stiffness model embedded in a prognostics algorithm. The controller objective is modified to account for accumulated damage, which allows the turbine to operate safely while optimizing the trade-off between component life and energy production.
- Moghadam et al. in [84] proposed a data-driven model to estimate drive-train fatigue damage based on wind conditions adapted to the farm's active power control objective function. The model was developed through pre-analysis of single-turbine simulations and degradation calculations, considering the increased turbulence intensity due to the wind farm wake effect. Drive-train loads were calculated using a fully-coupled turbine-power train dynamic model, which allows for the reflection of fatigue damage of individual gears and bearings in the overall power train life function. Unlike high-fidelity models, this model can be easily adjusted for drive-train configurations.
- The study presented in [18] proposes a two-level control configuration. The upper level performs health management functions, while the lower level has a dual purpose: controlling the turbine below-rated wind speeds and preventing a complex optimization problem in the upper level due to bi-linearity resulting from polynomial fitting.

On the other hand, the reliability adaptive/supervisory control schemes are control strategies used in wind turbines to improve their reliability by using real-time information about the system's health. These strategies usually have two levels of control: a primary control loop and an adaptive control loop. The adaptive loop modifies the set-point of the primary loop based on feedback about the system's health status to improve the system's overall reliability. The reliability adaptive/supervisory control schemes can be classified as Fault tolerant control, Fault evasion control, or Lifetime control [32].

Fault-tolerant control (FTC) allows the system, in this case, a wind turbine, to withstand faults and maintain its performance at the desired level; as a consequence, the need for maintenance actions and downtime decreases, and improves the reliability of power generation [49]. Some examples of this type of strategy are:

- Palanimuthu et al. presented in [96] a fault-tolerant pitch control strategy for large-scale wind turbines to acquire reliable power extraction under simultaneous pitch actuator fault situations, using a non-singular terminal synergistic control manifold.
- Liu et al. proposed in [71] a strategy for designing fault-tolerant wind turbine systems using Bayesian optimization. The approach specifically aims to mitigate the impact of asymmetrical loads on the turbine's rotor system, which are caused by pitch actuator faults. The strategy involves using a Bayesian optimization algorithm to identify the optimal proportional-integral (PI) pitch controller coefficients. This improves the system's robustness without requiring complex modeling, which reduces rotor system fatigue and enhances sustainable operation.
- The study presented in [69] by Liu et al. describes a study in which a 4.8MW wind turbine system was modeled using a Takagi-Sugeno fuzzy model. An augmented unknown input observer was utilized to estimate actuator and sensor faults and signal compensation techniques were used to minimize the effects of these faults on the system dynamics and outputs. The study demonstrated that using existing controllers and compensation techniques, the wind turbine system can tolerate low-frequency actuator and sensor faults.
- Jain et al., describes an approach for designing a health-aware fault-tolerant control (HAFTC) system that generates the desired amount of power while taking care of the turbine's health according to the wind-power profile on [54]. Two interconnected modules were developed for fault diagnosis and receding horizon control to ensure the health of wind turbine systems. The HAFTC scheme is achieved through an unknown input-observer-based residual generation for fault detection and a specific estimation filter for extracting information about torque bias faults.

On the other side, fault-evasion control strategies are control schemes that initiate system reconfiguration before faults even appear. This approach relies on observing health indicators that represent the system's health status and provides RUL prognosis [32]. Some examples of this type of strategy are presented below:

- Barradas et al. proposed in [12] an active damage reduction control strategy for wind turbines based on the dissipation of a hysteresis operator through a model predictive control (MPC) based strategy that incorporates the dissipated energy as a proxy for damage in the cost functional.

- The study conducted by Frost et al. [40] explored the use of condition monitoring for wind turbine blades and contingency control to balance between maintaining the health of the system and maximizing energy capture. The contingency controller can modify the turbine's operation when environmental or fault conditions could lead to high cyclic or extreme loads on the turbine blades. The contingency controller adjusts the generator set-point whenever environmental factors or potential faults could result in excessive cyclic or extreme loads on the turbine blades.
- The article presented by Requate and Meyer on [109] describes the process for designing and implementing a reliability controller that uses a health index to express degradation. The control loop includes the MPC-reliability controller and the wind turbine model. A two-stage control setup is used to separate the turbine controllers from the reliability control loop. The turbine controllers operate on a fast time scale, while the reliability controller works on a slower time scale to handle degradation processes.

The lifetime controller is a system that utilizes a Structural Health Monitoring and Prognosis (SHMP) model to gather information about a structure's accumulated and predicted future damage. This information defines parameters and reference values for the primary controller, which controls the load mitigation level. By continuously controlling the load mitigation level, the lifetime controller can achieve an optimal balance between power generation and load mitigation, allowing maximum power generation while achieving the desired service lifetime for the structure. [32, 33]. Below are some examples of this type of control strategy:

- The article presented by Yin et al. [146] describes a control strategy for wind farms that aims to maximize power generation and reliability while minimizing thrust force, reducing the maintenance cost, and maximizing the lifetime. This strategy uses a high-fidelity wind farm model built using machine learning and heuristic optimizations, specifically a relevance vector machine (RVM) trained on data from the wind farm model.
- An adaptive lifetime controller is presented by Kipchirchir et al. in [62] to manage structural loading in the rotor blades to ensure a predefined damage level at the desired lifetime without compromising the speed regulation performance of the wind turbine. The goal is to ensure a desired lifetime while also considering the damage accumulation level in the tower. The proposed method uses an online structural health monitoring system to adjust the lifetime controller gains based on a state-of-health (SoH) measure, considering the desired lifetime at every time step.
- A deterioration-aware control strategy was presented by Boutrous et al. in [17], the strategy considers information about the system's deterioration in the control law. The objective is to extend the useful life of the wind turbine, especially

the blades. The controller uses MPC based on an LPV model of wind turbine dynamics. This study offers a solution to a multi-objective optimization problem, balancing system health and performance.

- The study presented by Do et al. in [33] proposes a new strategy to control the lifetime of wind turbines. The strategy integrates a system health monitoring and prognosis model into the control loop, which provides information about the current state of the system and its possible future lifetime. This information is used to adjust the parameters and references of the primary load reduction control loop. The trade-off between maximizing power production and reducing structural load is optimized by regulating the wind turbine lifetime to a predefined design value. The part-load region is considered to emphasize this trade-off. A robust observer-based controller (ROBC) is combined with the standard MPPT controller to reduce unwanted structural load. The ROBC is an optimal stable controller that minimizes the mixed-sensitivity  $H_\infty$ -norm of the transfer function from the exogenous inputs to the exogenous outputs with given weighting functions.

In conclusion, degradation-aware control strategies have become crucial for optimizing wind turbine performance. These strategies aim to balance power generation and structural damage minimization, thus extending the operational lifespan and reliability of wind turbines. Researchers have explored various control approaches, such as Model Predictive Control (MPC) and fuzzy models, which adapt to fluctuating wind conditions and incorporate real-time health monitoring data to enhance turbine performance. Integrating Structural Health Monitoring (SHM) and prognosis models into control loops has shown promise in making informed decisions about component health. Moreover, fault-tolerant control (FTC), fault evasion control, and lifetime control strategies have been developed to ensure continuous operation under fault conditions, predict and mitigate potential issues, and optimize power generation while maintaining structural integrity.

Despite significant progress in degradation-aware control for wind turbines, there are still research gaps that require attention. One such gap is the adaptation of these strategies considering the inherent variability of wind environments. Embracing intelligent control techniques and understanding the effects of changing wind conditions on degradation and control is an emerging but critical area.

## 2.4 Conclusions

This chapter comprehensively overviews wind turbine functioning, control strategies, and wind modeling. It emphasized the primary objective of wind turbines, which is to obtain maximum power from the wind to generate electricity, introducing aerodynamic power as a critical indicator of system efficiency. The chapter explored various control methods, including speed control, torque control, and Perturbation and Observation

techniques, underscoring the significance of precise control systems for optimizing wind turbine performance. The challenges of wind modeling were also discussed, highlighting the importance of accurate wind speed measurement and various statistical and hybrid models used for wind simulation.

Additionally, the chapter delved into the concept of deterioration or degradation of wind turbines, signifying a decline in asset performance and reliability. It noted the absence of a universal deterioration indicator and the potential insights offered by degradation monitoring. Several methods for assessing degradation were presented, including Markov Chain Models, data-driven trends, signal-based approaches, and mixed methods. Furthermore, the chapter highlighted the importance of effective control strategies in wind energy, emphasizing Prognostic and Health Management (PHM) information and deterioration-aware control to optimize objectives considering the system's health. It also acknowledged research efforts in developing control strategies to manage wind turbine degradation, focusing on fatigue damage and improving reliability through adaptive/supervisory control schemes using real-time health information.

However, within this comprehensive overview, several research gaps in wind turbine control and degradation management have been identified. Specifically, these gaps pertain to degradation modeling, degradation prediction, and control strategies considering the dynamic nature of wind conditions. This research aims to address some of these critical challenges. The contributions in this work will allow an accurate modeling and prediction of degradation in the presence of varying wind conditions. Hence, it will develop an exact dynamic deterioration model that considers various factors influencing the degradation process.

The second contribution of this research will be developing an advanced control strategy designed explicitly for variable-speed fixed-pitch wind turbines. This strategy will optimize energy generation while considering the negative impact of degradation on drive-train components. By adapting to variations in wind turbulence intensity, this control system will effectively decrease the degradation effect due to changes in the wind conditions. It will also introduce an approach for simulating long-term degradation that incorporates the developed control strategy. This simulation will ensure the careful management of the trade-off between degradation and energy generation over time. Furthermore, this research will focus on developing robust control strategies that can effectively manage the degradation rate, ensuring consistent turbine performance even in the face of abrupt changes in wind conditions or set-points.

This thesis will provide valuable insights and solutions to the challenges of degradation modeling, prediction, and control in wind turbines operating under variable wind conditions. By addressing these gaps, it will be possible to advance the field of wind energy and contribute to more efficient, reliable, and sustainable wind turbine operations in the renewable energy sector.





# Modelling the Deterioration of a Drive Train in a Wind Turbine

---

## Contents

<b>3.1</b>	<b>Dynamic of a Wind Turbine Drive-Train . . . . .</b>	<b>42</b>
<b>3.2</b>	<b>Dissipated Energy &amp; Degradation Modelling . . . . .</b>	<b>43</b>
<b>3.3</b>	<b>Proposed Degradation Model for a Wind Turbine Drive-Train . . . . .</b>	<b>44</b>
<b>3.4</b>	<b>Case Study Analysis . . . . .</b>	<b>45</b>
3.4.1	Evaluation of model under different control conditions . . . . .	46
3.4.2	Evaluation of model under different wind conditions . . . . .	46
3.4.3	Results and Discussion . . . . .	49
<b>3.5</b>	<b>Experimental Validation in Prototype of Wind Turbine . . . . .</b>	<b>55</b>
3.5.1	Presentation of the Prototype . . . . .	56
3.5.2	Validation of Deterioration Model . . . . .	58
<b>3.6</b>	<b>Conclusions . . . . .</b>	<b>63</b>

---

This chapter presents a degradation model for variable-speed fixed-pitch wind turbines to account for the drive-train deterioration produced by the system's operation at points below and above optimal feedback control, which corresponds to the first contribution of this thesis.

As established in Chapter I, one of the objectives of this thesis is to study the dynamic degradation caused by changes in control or wind conditions. Thus, the degradation model has been evaluated under different wind and control conditions in simulated scenarios and a real wind turbine prototype. The contributions presented in this chapter have been published in the article "Degradation of a wind-turbine drive-train under turbulent conditions: effect of the control law" and presented at the Control and Fault-Tolerant System - SYSTOL 2021 conference.

The degradation model uses a mechanical contact principle to simulate transmission damping. This approach estimates the power and energy dissipated at the shaft, which serves as an indicator of damage in the drive-train. Additionally, a simplified representation of the drive-train is employed to simulate the dynamic system of the transmission. This model consists of a two-mass model connected by a flexible shaft.

Different case studies were designed to evaluate the model under various control and wind conditions. Regarding the evaluation under different control conditions, it was analyzed the degradation of the system caused by operating below and above the optimal feedback control points. Additionally, different wind speeds and turbulence intensities were considered to illustrate the degradation resulting from the random effect of wind conditions. The proposed simulation is based on a wind speed model estimated from real data measurements of laminar wind speed and two classes of turbulent wind speed data obtained from stochastic differential equations.

Finally, an experimental validation was conducted to assess control variations' effect on the drive-train's degradation. The experiments were done using a prototype of a fixed-shaft wind turbine with a virtual flexible shaft. The purpose was to simulate the impact of fatigue, vibrations, friction, and other aerodynamic factors that can accelerate damage to the transmission.

### 3.1 Dynamic of a Wind Turbine Drive-Train

The drive-train of a horizontal axis wind turbine is a complex mechanical system consisting of numerous devices. It is vulnerable to vibrations, flexibility, and other phenomena that challenge modeling the dynamic behavior of the transmission. In order to analyze the stability, faults, and reactive powers compensation, various studies have designed simplified transmission models [88].

Among the simplified representations of devices, the six-mass drive-train model has emerged as one of the most complete models. This model considers three blades, the hub, the gearbox, and the generator connected by two shafts. Each body has its inertia, angular positions, and velocities, and the three blades, the shaft connecting the hub-gearbox, and the other shaft connecting the gearbox-generator are represented as springs to consider elasticity and damping. This model is the most precise for modeling the system's dynamics, particularly in Region II of the turbine's operation [87].

Although other models, such as the five or three-mass models, have been developed in a more simplified manner than a six-mass model, it has been demonstrated that the dynamics of the shaft can be accurately expressed using the two-mass model, as stated by Muyeen et al. in [88]. The simplified drive-train representation of two-mass bodies drive-train is shown in Figure 3.1, where two rigid bodies are linked by a flexible shaft that deforms with an angle  $\theta_s$  when the rotor speed  $\omega_r$  is slightly different from the generator speed  $\omega_g$ . The rigid bodies represent all mechanical devices on each side of the effective shaft. This representation of two rigid bodies allows us to include parts and mechanical devices on each side of the shaft, such as the rotor inertia  $I_r$ , generator inertia  $I_g$ , transmission damping  $B_s$ , and transmission stiffness  $K_s$ .

The dynamic behavior of in drive-train in a variable-speed wind turbine can be represented using the two-mass model with a nonlinear state-space format, allowing a

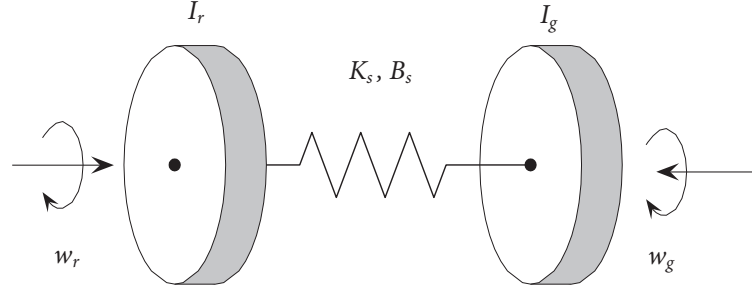


Figure 3.1: Drive-train with a flexible shaft representation.

description of the resonance mode while disregarding the high-frequency dynamics as model uncertainty [16, 123]. The system presented in Equation. 3.1 illustrates the behavior of the drive-train

$$\begin{pmatrix} \dot{\theta}_s \\ \dot{\omega}_r \\ \dot{\omega}_g \end{pmatrix} = \begin{pmatrix} 0 & 1 & -1 \\ -\frac{K_s}{I_r} & -\frac{B_s}{I_r} & \frac{B_s}{I_r} \\ \frac{K_s}{I_g} & \frac{B_s}{I_g} & -\frac{B_s}{I_g} \end{pmatrix} \begin{pmatrix} \theta_s \\ \omega_r \\ \omega_g \end{pmatrix} + \begin{pmatrix} 0 & 0 \\ \frac{1}{I_r} & 0 \\ 0 & -\frac{1}{I_g} \end{pmatrix} \begin{pmatrix} \tau_r \\ \tau_c \end{pmatrix} \quad (3.1)$$

### 3.2 Dissipated Energy & Degradation Modelling

As mentioned in Chapter 2.2, different methods for modeling deterioration in wind turbines have already been developed, which often are complex options for modeling degradation considering the dynamic of the torsional loads applied to the drive-train.

An approach presented by Rodriguez-Obando in [113] defines the friction force ( $F_c$ ) between two rotational devices as follows:

$$F_c = \Gamma(\Delta\omega) \quad (3.2)$$

Here,  $\Delta\omega$  represents the relative tangential speed that emerges from the contact between the rotational devices, and  $\Gamma$  is a parameter that defines the quality of contact between the devices.

In this context,  $\Gamma$  is a time-varying parameter used to analyze the degradation of a system throughout its lifetime. In traditional friction component modeling,  $\Gamma$  represents

the constant viscous friction coefficient. However, considering  $\Gamma$  as a time-varying parameter provides additional insights into studying deterioration over the system's lifetime.  $\Gamma$  is utilized to characterize the contact quality between rotational devices, considering factors such as inter-surface adhesion and surface roughness. Furthermore, it can be assumed that the parameter  $\Gamma$  will gradually decrease over time to represent the degradation of the friction drive, as presented in [113].

$F_c$  can be used to define the contact power ( $P_c$ ) produced by a rotational device at the contact level by considering the relative tangential speed between devices [112], as follows:

$$P_c = \Gamma(\Delta\omega)^2 \quad (3.3)$$

### Dissipated Energy-based model

Previous studies [83, 112] have utilized dissipated energy from contact between rotational systems to indicate deterioration. This is because the dissipated power represents the heat and frictional fatigue damage that occurs at the contact level during regular system operation.

As mentioned earlier, the parameter  $\Gamma$  defines the quality of contact between two rotational devices and decreases over time while the contact deterioration increases [92, 111, 112]. Rodriguez et al. citeRodriguez2018, proposed that deterioration can be quantified and calculated by estimating the dissipated energy. Thus, the degradation rate ( $\frac{dD}{dt}$ ) can be defined as a function that increases with the dissipated energy. Let us consider the case where  $\frac{dD}{dt} = P_c$  as follows:

$$\frac{dD}{dt} = P_c = \Gamma(\Delta\omega)^2 \quad (3.4)$$

Consequently, the energy dissipated in the contact  $E_c$  between the rotational systems can be defined as :

$$E_c = \int_0^t P_c dt \quad (3.5)$$

Wind turbines are subject to various phenomena that produce fatigue, such as vibration, friction, impacts, and cyclic torque fluctuations, which can potentially reduce the useful life of the drive-train [15, 24, 105]. In this thesis, the approach proposed in [112, 113] is extrapolated to the drive-train system of wind turbines, considering that it is common to model the flexible shaft as a spring and damper, as presented in the two rotational masses mentioned before (Figure 3.1).

### 3.3 Proposed Degradation Model for a Wind Turbine Drive-Train

The purpose of this section is to introduce a model for the deterioration of the drive-train of a wind turbine. This model considers the dissipated energy as an indicator of degradation caused by various physical phenomena, such as fatigue, vibration, and others.

This thesis considers a simplified representation of the two-mass model presented in Section 3.1 to model the dynamics of the drive-train in a wind turbine. The two-mass model consists of a low-speed mass of the turbine connected to the high-speed mass of the generator through a flexible shaft, which is modeled as a spring and damper. When the angular speed of the rotor  $\omega_r$  is slightly different from the angular speed of the generator  $\omega_g$ , the flexible shaft will be deformed with an angle  $\theta_s$ .

Since a flexible shaft is considered, a mass-spring model can be used, and the damping coefficient  $B_s$  could be considered to be constant, denoted here  $B_s^c$ . In particular, for control design, it will be used

$$B_s^c = \frac{3}{2}\alpha K_s \quad (3.6)$$

where  $K_s$  is the constant stiffness of the transmission, and  $\alpha$  is a constant parameter that depends on the material.

This thesis proposes to introduce the damping coefficient as a non-linear function of angular deformations in the drive-train, as it is often stated in contact mechanics, where the torsion angles affect the damping coefficient [50]. This point is intended for introducing a deterioration that depends of both: the amplitude of relative speed and the amplitude of torsion angles. This allows for the definition of a variable damping coefficient  $B_s$  as a function of the torsion angle  $\theta_s$ , as follows:

$$B_s = \frac{3}{2}\theta_s\alpha K_s \quad (3.7)$$

This variable damping coefficient is considered into the all simulations presented in this manuscript.

Additionally, considering the definition of the contact power  $P_c$  presented in Equation 3.3, the dissipated power  $P_d$  can be defined as follows:

$$P_d = B_s(\omega_g - \omega_r)^2 \quad (3.8)$$

Consequently, the amount of energy that is dissipated up to time  $t$  by the drive-train

will be:

$$E_d(t) = \int_0^t P_d(u) du \quad (3.9)$$

which is considered here as an index of the drive-train deterioration, Remark that this dissipated energy is a function of both the amplitude of the angular shaft torsion and the square of the relative velocity  $(\omega_g - \omega_r)$ .

### 3.4 Case Study Analysis

Wind turbines operate under variable conditions that can cause vibration and fatigue in the transmission system, leading to accelerated deterioration of the drive-train. Chapter 2 explains various control strategies commonly used in closed-loop systems. These strategies involve implementing controllers to manage the torque or speed of the system and maximize energy capture. However, they do not always consider system degradation.

This section demonstrates the performance of the deterioration model under different wind conditions and compares the levels of dissipated energy at the turbine shaft to the energy generated by optimal and sub-optimal control feedback gains. The objective is to establish a relationship that describes how degradation can be influenced by the selection of control gains and susceptibility to disturbances (wind conditions).

For the analysis and the evaluation of the degradation model, it will implement the simplified representation for the VS-FP turbines, as shown in Figure 3.1, where the whole transmission system is considered a system of two rigid bodies connected by a flexible shaft. The considered a VS-FP turbine of 2 MW with a 100 m rotor diameter, fixed gearbox, and horizontal axis.

First, the different scenarios considered for evaluating the model under different control and wind conditions will be explained, followed by the results and respective discussions:

#### 3.4.1 Evaluation of model under different control conditions

The normal operation of wind turbines is governed by a Maximum Power Point Tracking (MPPT) control law, presented in Section 2.1.1. This control law estimates a control torque (generator torque) by considering a constant optimal control gain  $K_c^{opt}$  and the rotor angular speed  $\omega_r$ .

For the turbine in consideration, the power coefficient curve,  $C_p$  versus  $\lambda$ , is presented in Figure 1.3, where the value of  $C_p^{max}$  that can be obtained is 0.4615 at  $\lambda_0$  of 6.4. Thus, the optimal feedback control gain can be estimated using Equation (2.9), and take the value of  $K_c = 9.5065e5$ .

Nevertheless, one part of this work aims to illustrate the performance of the wind tur-

bine sub-optimal control gains. For this reason, two additional scenarios were proposed to complete the analysis:

- System controlled at 10% below the optimal  $K_c$
- System controlled at 10% above the optimal  $K_c$ .

### 3.4.2 Evaluation of model under different wind conditions

To obtain a complete analysis of degradation in a wind turbine, it is necessary to consider variations in wind speeds over time. These variations can affect the efficiency and durability of the mechanical parts of the turbine. It is important to note that wind can be present under different regimes, such as laminar, transitional, or turbulent, and for each regime, it can be categorized according to the intensity of the variations. There are different ways to simulate each wind condition. However, for the purpose of this thesis, it is important to consider short-term dynamics that can impact the degradation of the drive-train system.

#### Wind Speed Generation

This thesis implemented the model proposed by Ma et al. in [77], for generating wind speed sequences of different intensities for the analysis of wind turbine degradation.

Considering the description of relative motion on fluids proposed by Reynolds [110], equation (3.10) allows modeling the wind speed  $V(t)$ , at any instant  $t$ , by taking into account its mean value  $\bar{V}(t)$  and its fluctuation  $v(t)$ :

$$V(t) = \bar{V}(t) + v(t) \quad (3.10)$$

The term  $\bar{V}(t)$  is often considered as an output of a simple low-pass filter corresponding to the daily, monthly, seasonal or annual mean behavior, and the fluctuation  $v(t)$  can be considered as an output of a high-pass filter, see for instance [20].

In [77], it is considered that the wind speed dynamics can be modeled as a diffusion process following a stochastic differential equation, defining a so-called Ornstein-Uhlenbeck (OU) process:

$$dV(t) = a(V(t), t)dt + b(V(t), t)dW \quad (3.11)$$

where  $a(V(t), t)$  and  $b(V(t), t)$  are the drift and diffusion terms, while  $dW$  is the standard Wiener process (or standard Brownian motion, a continuous process whose increments are normally distributed).

Turbulence can be classified into three different classes, where the first two include 99% of the wind speed sequences [20, 21]. The method presented in [77] allows generating different classes of wind speed, by using the stochastic equation (3.12) as a particular

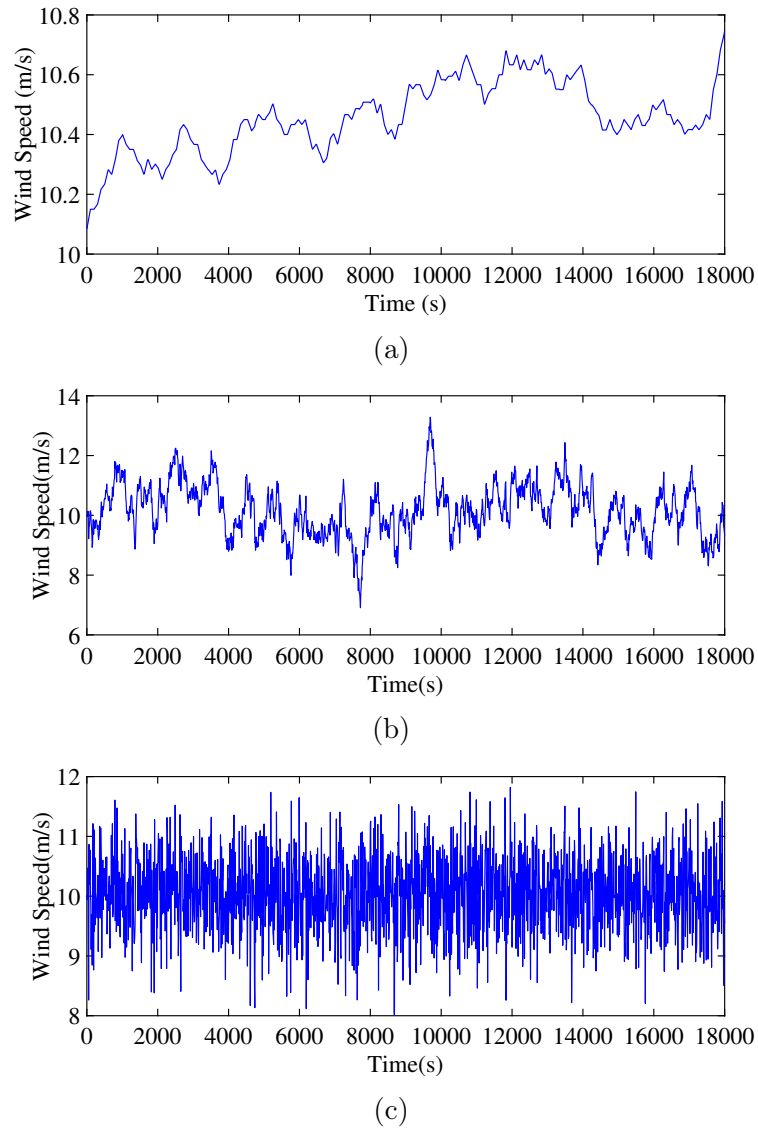


Figure 3.2: Considered wind speed scenarios: (a) laminar wind, (b) turbulent wind with low intensity, (c) turbulent wind with high intensity

case of model (3.11), by suitably choosing the model parameters  $\hat{a}$ ,  $\hat{b}$ , and  $\hat{u}$ .

$$dV(t) = -\hat{a}(V(t) - \hat{u})dt + \hat{b} dW(t) \quad (3.12)$$

The wind speed simulation has thus been performed using parameters presented in [77] providing the following models:

$$dV(t) = -0.0314(V(t) - 10.0245)dt + 0.2517 dW(t) \quad (3.13)$$

$$dV(t) = -(V(t) - 10.0245)dt + 0.6459 dW(t) \quad (3.14)$$



For the evaluation of performance of the degradation process, it was considered different wind speed scenarios with an air density of  $1.1 \text{ kg/m}^3$ :

- Scenario I: The first scenario corresponds to laminar wind flow where real measurements of wind speed were used to feed the model; see Figure 3.2a.

In addition, a turbulent regimen was also simulated, as it was mentioned before, with two classes of turbulent wind:

- Scenario II: Equation 3.13 was used to generate wind flow with a low intensity, see Figure 3.2b
- Scenario III: Equation 3.14 was used to generate wind flow with a high intensity, see Figure 3.2c.

Using these three types of wind conditions makes it possible to complete the different situations that a turbine may be subjected to in a more realistic environment.

### 3.4.3 Results and Discussion

The two-mass model with a non-linear state-space format presented in Equation 3.1 was utilized to simulate the dynamic behavior of the drive-train and describe the resonance mode of the transmission. This model allows for the estimation of variations around the torsion angle and the angular rotor and generator speed. Besides, was analyzed and compared the behavior of different parameters as the power coefficient  $C_p$ , generated power  $P_g$ , and generated energy  $E_g$ . Furthermore, the degradation of the system was estimated by calculating the dissipated energy ( $E_d$ ). The simulations were conducted for each previously presented scenario, providing a comprehensive analysis of the system's behavior. Three scenarios with different control gains were considered for three wind speed cases.

The simulation was conducted to analyze the degradation process in the drive-train over a short period of 5 hours ( $t = 18000s$ ). The value of  $K_s$  was set to  $1e8$ , and  $\alpha$  was chosen based on the suggested range in [50] with a value of 0.5. Table 3.1 provides a summary of the characteristics of the wind turbine and drive-train.

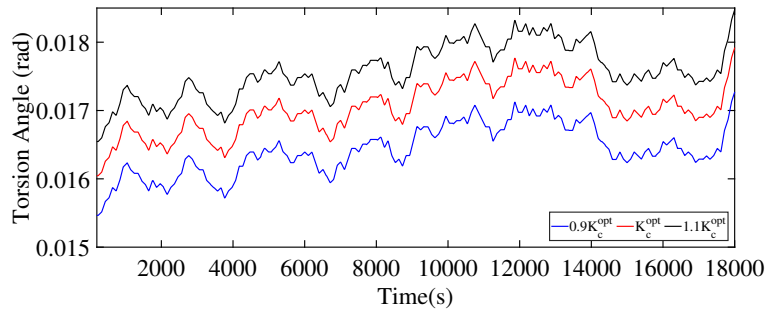
Table 3.1: Parameters of the simulated wind turbine

Symbol	$C_p^{max}$	$\lambda_0$	$K_c^{opt}$	$\alpha$	$R$	$K_s$
Value	0.4615	6.4	9.5065e5	0.5	50 m	1e8 $\text{kg/s}^2$

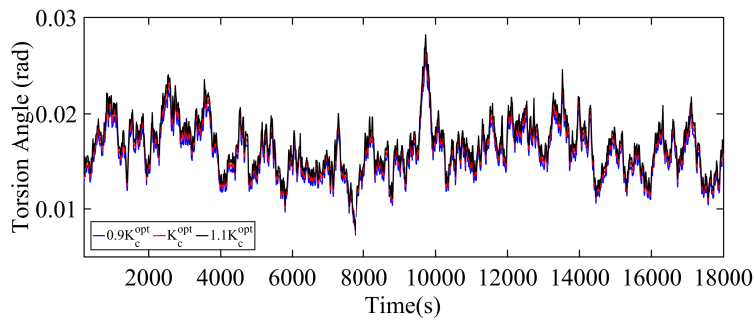
## Analysis of the Results

The obtained torsion angles are illustrated in Figure 3.3 for the different scenarios of interest. It is possible to observe that the angles have small magnitudes ( $< 0.03 \text{ rad}$ ) in all the scenarios, however, the frequency of fluctuations is more or less important depending on the wind conditions, which can lead to fatigue damage in the long term.

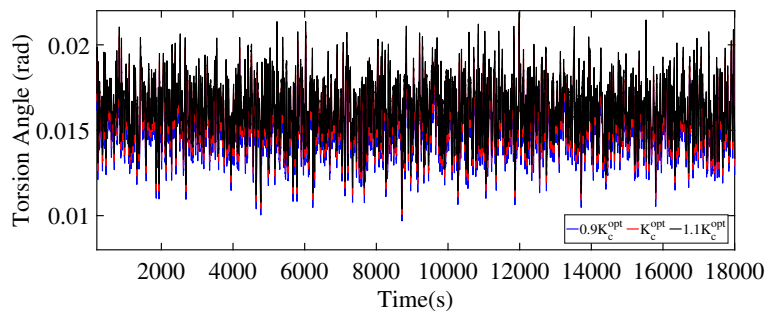
Concerning the effect of using different  $K_c$ , it is possible to observe that  $\theta_s$  always takes superior values in cases with a bigger control gain, which means that a bigger control gain leads to a bigger deformation.



(a) Laminar flow.



(b) Turbulent flow with low variance.



(c) Turbulent flow with high variance.

Figure 3.3: Obtained torsion shaft angle for different wind speed scenarios: (a) laminar wind, (b) turbulent wind with low intensity, (c) turbulent wind with high intensity

A common alternative for analyzing the performance of wind turbines is to examine the relationship between generated power and rotational speed. This analysis can be

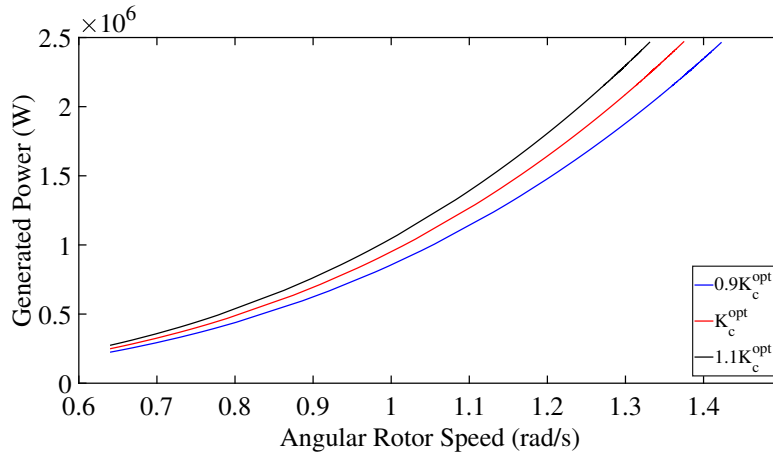
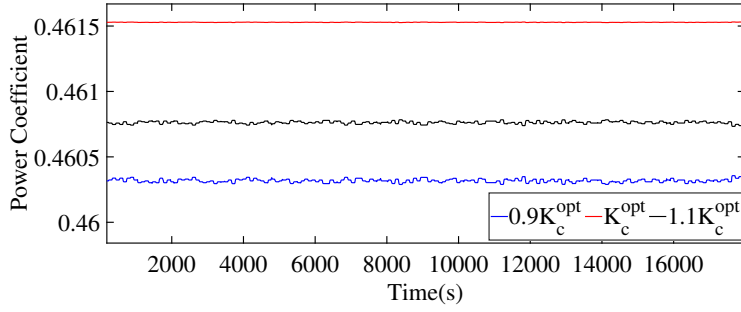


Figure 3.4: Generated power with respect to rotor speed produced by optimal and sub-optimal torque controllers.

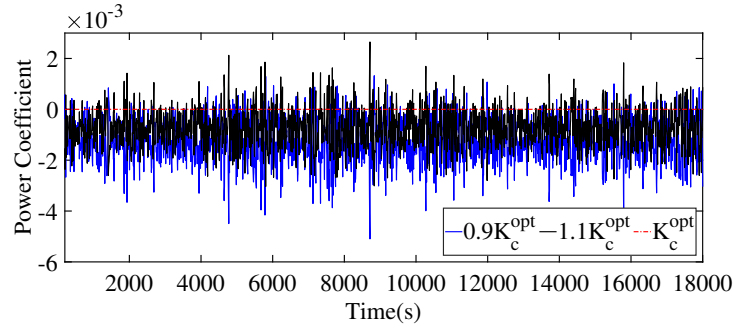
conducted using Figure 3.4, which displays the generated power for different angular rotor speeds under various control scenarios. As expected, the generated power exhibits a cubic relationship with the rotor speed. The graph indicates that, for a given rotor speed, the case with a control gain of  $1.1K_c$  yields higher power generation compared to the cases with  $0.9K_c$  and  $K_c^{opt}$  control gains.

The power coefficient  $C_p$  can be used as a parameter to analyze the effect of implementing sub-optimal control conditions that may affect the efficiency of the wind turbine. Figure 3.5 shows the  $C_p$  for the different wind scenarios, for the three cases of control gain:

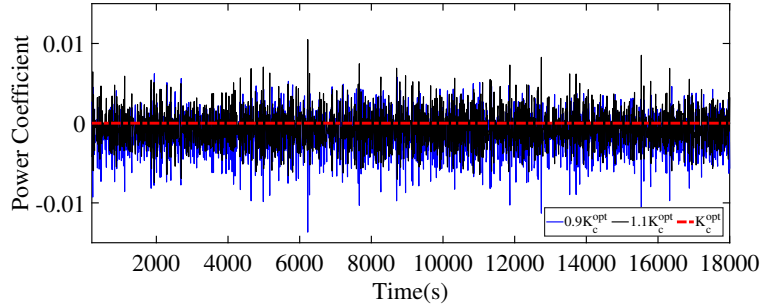
- In the cases of laminar wind, it can be observed in Figure 3.5a that  $K_c^{opt}$  leads to the optimal  $C_p^{max}$  value, as indicated by theory. However, it is interesting to note that the difference with respect to  $0.9K_c$  is higher than the case with  $1.1K_c$ , and in both cases, the difference with respect to the optimal value is extremely low (0.26% for the case with  $0.9K_c$  and 0.17% for the case with  $1.1K_c$ ).
- The performance of  $C_p$  in turbulent scenarios was analyzed by comparing sub-optimal cases with the one using  $K_c^{opt}$  in Figures 3.5b and 3.5c. One observation is that implementing a  $K_c$  lower than the optimal one leads to a lower  $C_p$  for the low turbulence case. However, the difference is less noticeable in the case with high variance. In the scenarios where  $0.9K_c$  was implemented, the mean difference of  $C_p$  is about 0.28% for both cases (low and high turbulence). On the other hand, in the case with  $1.1K_c$  the difference are 0.17% for low turbulence and 0.15% for high turbulence.



(a) Laminar



(b) Turbulent flow with low variance



(c) Turbulent flow with high variance.

Figure 3.5: Comparison of the behavior of the Power Coefficient  $C_p$  for different wind speed scenarios: (a) laminar wind, (b) turbulent wind with low intensity, (c) turbulent wind with high intensity

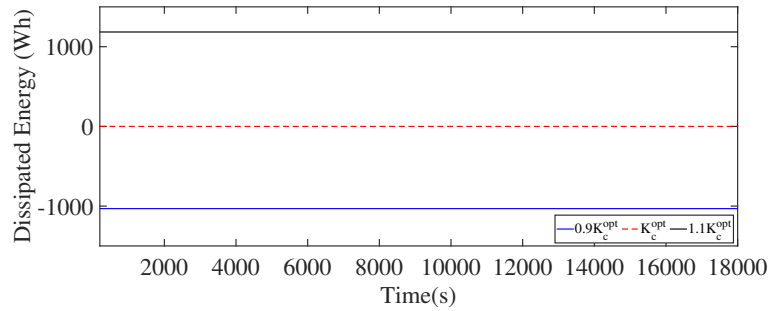
Furthermore, this chapter aims to propose a deterioration model for the drive-train of a wind turbine and evaluate it under optimal and sub-optimal control conditions. To obtain a complete analysis, it is necessary to evaluate the deterioration indicator, which in this thesis is the dissipated energy with respect to the optimal control scenario. Additionally, to evaluate the effect of sub-optimal conditions on the system's production efficiency, it is necessary to analyze the behavior of the generated energy, under the different wind scenarios:

- Concerning the dissipated energy, note that if the control gain is below the optimal point (e.g. in the case of  $0.9 K_c$ ), the total dissipated energy is less than in the

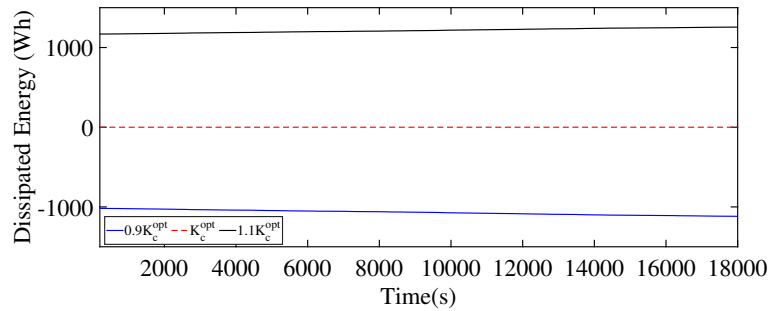
other two cases (e.g  $1.1 K_c$  and  $K_c^{opt}$ ). Nevertheless, when the wind flow has a more significant variance (turbulent), the dissipated energy increases notably for a higher gain. It decreases considerably for a smaller gain; see Figure 3.6.

- Regarding the generated energy, as expected, the amount of generated energy is lower than the optimal one in all cases of wind conditions. Nevertheless, a control gain higher than the optimal one always leads to an energy production higher than a control gain smaller than the optimal one. Note that the difference in the energy production between the tuning  $0.9K_c$  and  $1.1K_c$  is reduced when the flow is more turbulent; see Figure 3.7.

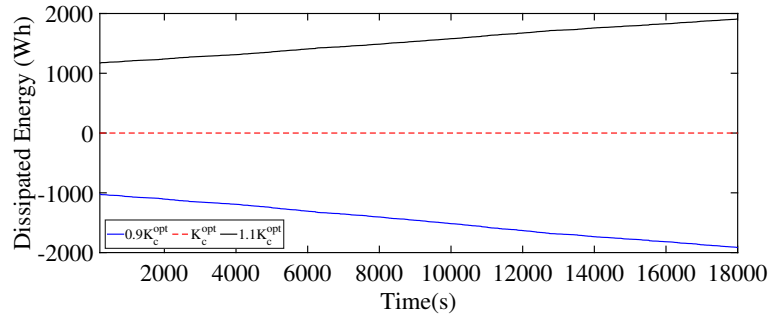
The simulation results demonstrate the impact of persistent variations in the shaft angle when the system is exposed to high-variance wind speeds. Furthermore, if the system operates under sub-optimal control conditions, the results indicate two possible scenarios: either more energy generation with increased degradation, or less dissipated energy (and thus less degradation) but with lower energy generation. In all cases, the optimal control gain consistently provides maximum power generation with a "nominal" level of degradation.



(a) Laminar flow

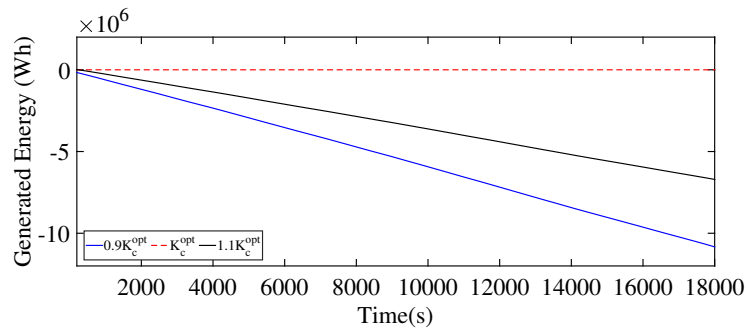


(b) Turbulent flow with low variance

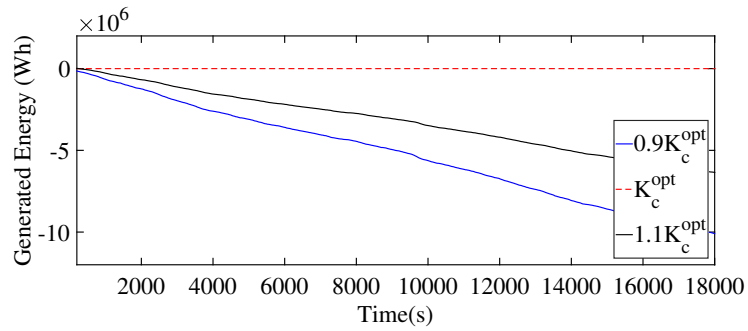


(c) Turbulent flow with high variance.

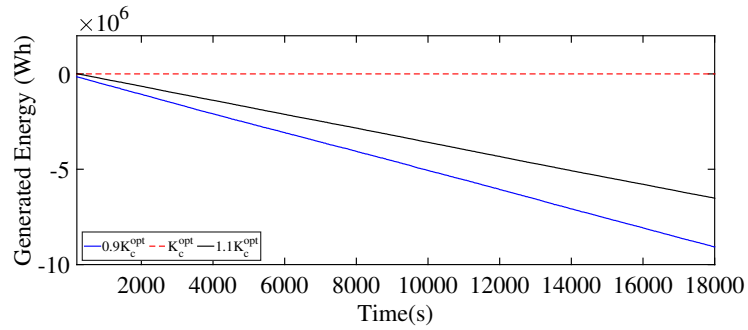
Figure 3.6: Dissipated energy at the flexible shaft versus time for different wind speed scenarios: (a) laminar wind, (b) turbulent wind with low intensity, (c) turbulent wind with high intensity



(a) Laminar flow.



(b) Turbulent flow with low variance.



(c) Turbulent flow with high variance.

Figure 3.7: Generated energy at the flexible shaft versus time for different wind speed scenarios: (a) laminar wind, (b) turbulent wind with low intensity, (c) turbulent wind with high intensity

### 3.5 Experimental Validation in Prototype of Wind Turbine

Based on the obtained results, the purpose of this section is to present an experimental analysis conducted on a real wind turbine prototype to observe how the deterioration model performs under various wind conditions and the effect of work in sub-optimal control conditions affect the deterioration. To achieve this, the proposed degradation model was implemented in a wind turbine prototype with a fixed drive-train. A modification to the dynamic model was made to add a virtual flexible shaft that allows for simulation of the dynamics of the torsional loads and damping effect.

The wind turbine prototype was designed and manufactured at Gipsa-Lab to test and validate control laws for variable-speed wind turbines.



(a)



(b)

Figure 3.8: Prototype of wind turbine: a) Wind Turbine installation and b) Blades of wind turbine



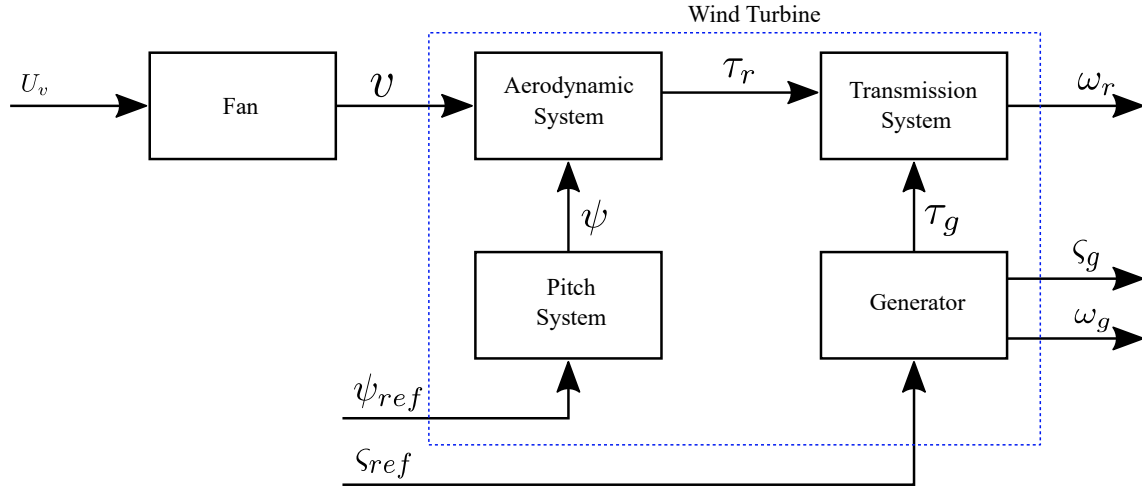


Figure 3.9: Block diagram representing the functioning of the prototype of a wind turbine

### 3.5.1 Presentation of the Prototype

The prototype is a 1000 *mW* wind turbine with two blades (see Figure 3.8a) that is driven by wind speed generated by a fan. A fan is attached to the back of the wind turbine, causing it to move through a suction phenomenon. These two components are located inside a cylindrical tube that promotes laminar flow with limited turbulence, acting as a wind tunnel. The wind turbine is connected to a DC generator that can be used to generate electrical energy. An electronic circuit allows for the control of the generated current. Table 3.2 presents other parameters characterizing the wind turbine model.

Table 3.2: Parameters of the prototype of wind turbine

Parameters	Symbol	Value	Unity
Air density at 25 degrees	$\rho$	1.184	$Kg/m^3$
Length of the blade	$R$	0.157	$m$
Electrical constant of the generator	$K_e$	$23.4e-3$	$NmA^{-2}$
Total inertia of the rotors	$I$	$8.08e-6$	$kgm^2$
Optimal blade angle	$\psi^{opt}$	5	$deg$

The wind turbine prototype can operate in two specific control modes:

- **Torque Control:** By adjusting the electric current, it can extract the maximum instantaneous power according to the wind speed.
- **Speed Control:** By adjusting the blade angle, it can maintain the generated power constant around an admissible maximum.

The normal operation of the prototype is illustrated in Figure 3.9:

A voltage  $U_v$  is supplied to the fan that will generate the wind speed  $v$ ,  $U_v$  can take

values from 0V to 24V, producing wind speeds between 0 and 5m/s. The wind speed  $v$  is the input of the aerodynamic system of the prototype, it will produce the movement of the rotor with torque  $\tau_r$ , and angular speed  $\omega_r$ .

The inputs of the system are the pitch angle ( $\psi$ ) of the wind turbine blades (ranging from 0 to 45 degrees), the desired electric current ( $\varsigma_{ref}$ ) of the DC generator (ranging from 0A to 1A), and the wind speed supplied by the fan ( $U_v^{ref}$ ) controlled by a voltage ranging from 0V to 24V, producing wind speeds between 0 and 5m/s.

To measure the speed of the wind passing through the turbine, a wire anemometer is fixed inside the cylinder, and an incremental encoder is used to determine the value of the angular speed of the wind turbine  $\omega$ . On the other hand, the prototype has a current sensor to provide the measure of the current generated  $\varsigma_g$ .

### 3.5.1.1 Model of transmission of the prototype

The wind turbine prototype used to validate the results presented earlier had a fixed drive-train, meaning there was no sliding mode between the angular rotor and generator speed. A modification to the system is necessary to implement the proposed deterioration model. This involves implementing a virtual flexible shaft as shown in Figure 3.10, where the real part of the system is shown in blue, the simulated flexible shaft is in green, and the connection between both systems is in red.

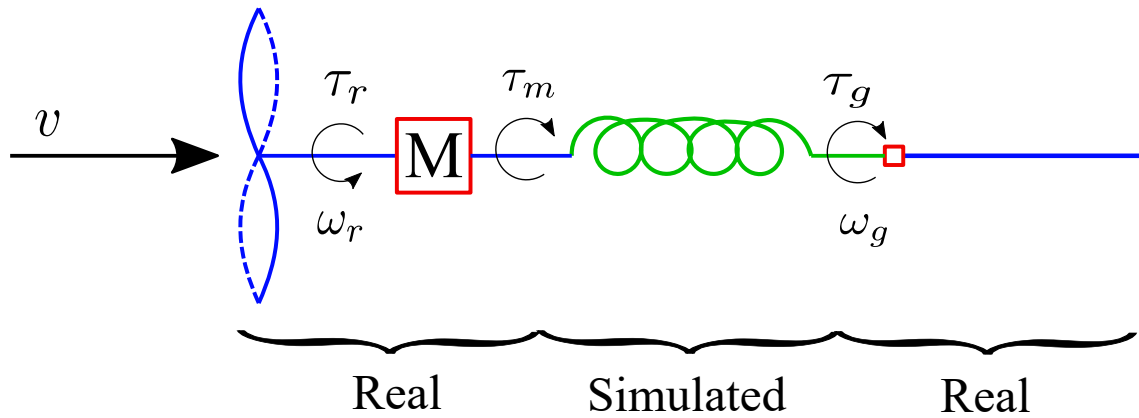


Figure 3.10: Integration of a virtual drive-train on the fixed-shaft wind turbine prototype

In Figure 3.10, the wind speed  $v$  causes the turbine rotor to move with angular speed  $\omega_r$  and torque  $\tau_r$ . The shaft is assumed to be connected to a flexible part, with a system M separating the real system from the simulated one with a torque  $\tau_m$ . Furthermore, it is assumed that there is a generator at the other end of the flexible shaft, with an angular speed of  $\omega_g$  and a torque of  $\tau_g$ .

The integration between the real and simulated systems can be described by Equation 3.15, where  $I_r$  represents the rotor inertia, and  $\omega_r$  and  $\tau_r$  are variables measured on the real system. The input used for simulating the flexible shaft is denoted by  $\tau_m$ .

$$I_r \dot{\omega}_r = \tau_r - \tau_m \quad (3.15)$$

Considering the dynamic system presented in Equation 3.1,  $\tau_m$  can be defined as:

$$\tau_m = -\frac{K_s}{I_r} \theta_s - \frac{B_s(\theta_s)}{I_r} \omega_r + \frac{B_s(\theta_s)}{I_r} \omega_g \quad (3.16)$$

Therefore, the dynamic behavior of the complete drive-train can be described using the following system of equations:

- Variation in the torsion angle is a simulated variable:

$$\dot{\theta}_s = \omega_r - \omega_g \quad (3.17)$$

with  $\omega_r$  been a real variable, and  $\omega_g$  been a simulated variable.

- Rotor Speed is a real variable:

$$I_r \dot{\omega}_r = -K_s \theta_s - B_s(\theta_s) \omega_r + B_s(\theta_s) \omega_g + \tau_r \quad (3.18)$$

where  $B_s$  depends on  $\theta_s$  and integrates real and simulated variables.

- Generator Speed is a simulated variable:

$$I_g \dot{\omega}_g = K_s \theta_s + B_s(\theta_s) \omega_r - B_s(\theta_s) \omega_g - \tau_g \quad (3.19)$$

where  $\tau_g$  is real feedback to the system considering the Equation 2.8.

Note that the values for variables such as  $K_s$  are assumed. As a result, the magnitude of the deterioration phenomenon will be more significant considering the size of the actual system. However, this approach allows for analyzing the effect of functioning under non-optimal conditions on deterioration.

### 3.5.2 Validation of Deterioration Model

The objective of the test is to validate the results obtained in the previous section using the wind turbine prototype concerning the effect of control gain in the degradation. This will be achieved by analyzing variables such as variation in torsion angle, generated power, dissipated power, dissipated energy, and generated energy.

To validate the results, the prototype wind turbine was tested in two different wind scenarios, where the wind speed can vary between 2.2 m/s and 3.2 m/s. Figure 3.11a and 3.11b illustrate the cases of interest. Note that in both cases, the variations are controller, and the wind is almost laminar; this is due to the large geometry of the wind tunnel not allowing the separation of the layers on the flow of the wind.

Additionally, the evaluation was conducted under different control conditions. The control gain was varied in this case, as shown in Table 3.3, with  $K_c^4$  being the optimal control gain.

Table 3.3: Parameters of the prototype of wind turbine

Control Gains	$K_c^1$	$K_c^2$	$K_c^3$	$K_c^4$	$K_c^5$
Value	$1.5e^{-8}$	$2.5e^{-8}$	$3.5e^{-8}$	$4.5e^{-8}$	$5.5e^{-8}$

As mentioned previously, the deformation in the drive-train will be simulated by modifying the system presented in Equation 3.1, as described in Section 3.5.1.1. Consequently, the simulation of torsion angle variation was performed using Equation 3.17.

The resulting  $\theta_s$  values are presented in Figures 3.12a and 3.12b for different control gains. It can be observed that, similar to the previous results, a larger control gain leads to a greater deformation in  $\theta_s$ , while  $K_c^1$  causes a smaller variation compared to the other cases due to its smaller control gain. Conversely,  $K_c^5$  continuously varies close to the optimal case,  $K_c^4$ .

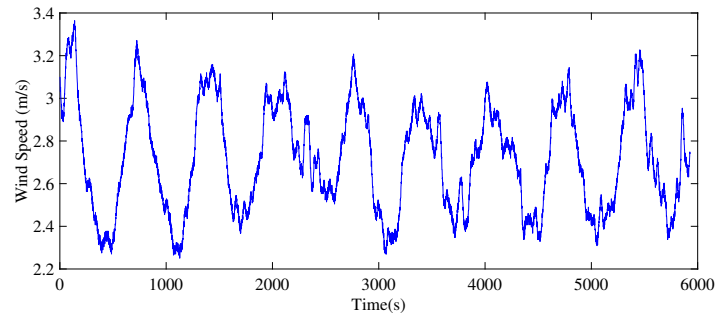
Moreover, the generated power is presented in Figures 3.13a and 3.13b for the cases of interest. The optimal control gain  $K_c^4$  leads to major production power, followed by the other cases in descending order of the control gains.

In contrast, the dissipated power is shown in Figures 3.14a and 3.14b. It is observable that a higher control gain does not lead to a more considerable dissipation of power. For instance, while  $K_c^5$  has the highest value, the dissipation level can sometimes be lower than that of  $K_c^1$ .

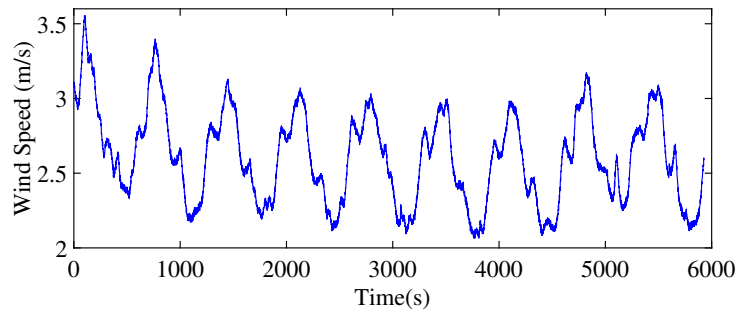
With respect to generated energy, consider Figures 3.15a and 3.15b, which show the generated during the simulation process. Is interested to note that  $K_c^5$  follows the behavior of the optimal control gain concerning generated energy, where the difference between the cases with  $K_c^4$  and  $K_c^5$  concerning generation is just around 3% in the first scenario and 1.8% in the second.

Concerning dissipated energy is presented in Figures 3.16a and 3.16b The optimal control gain  $K_c^4$  is not the most efficient in dissipating less energy.  $K_c^5$  produces less dissipated energy than other cases, with a difference of up to -10.46% and -8.19% concerning the optimal case.

It is possible to conclude that the results from the simulation are validated concerning the existence of an important effect when the control system of the wind turbine is operated without considering the wind conditions. Additionally, the proposed degradation model allows simulating the degradation of a drive-train wind turbine.

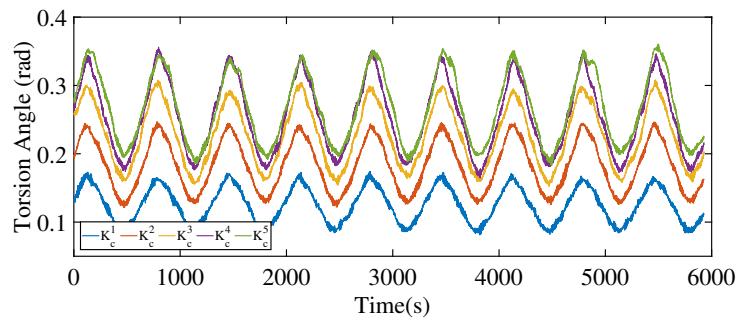


(a)

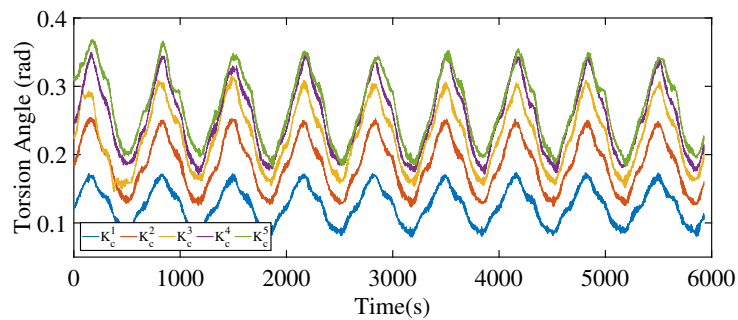


(b)

Figure 3.11: Considered wind scenario a) Case I, b) Case II

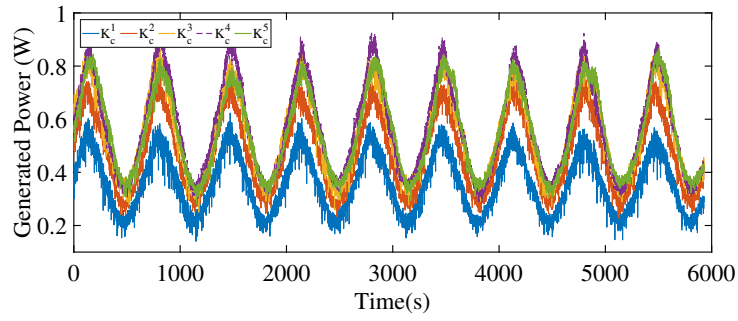


(a)

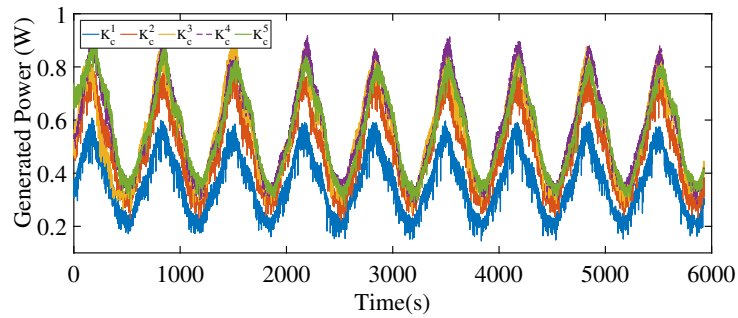


(b)

Figure 3.12: Obtained torsion shaft angle for different wind a) Wind Case I, b) Wind Case II

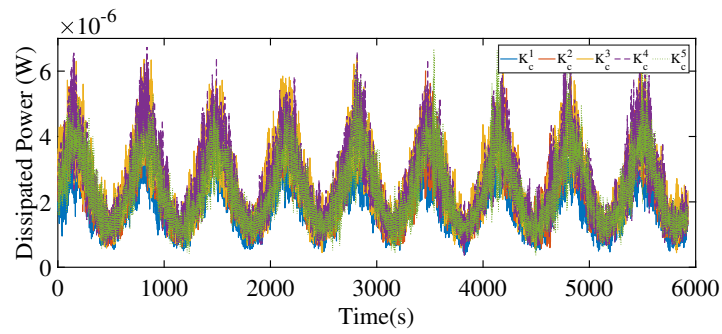


(a)

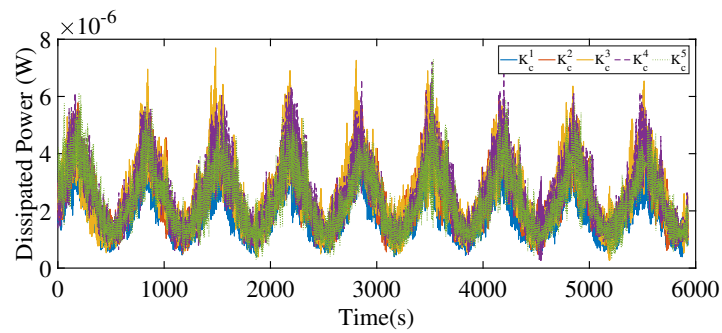


(b)

Figure 3.13: Obtained generated power for a) Wind Case I, b) Wind Case II

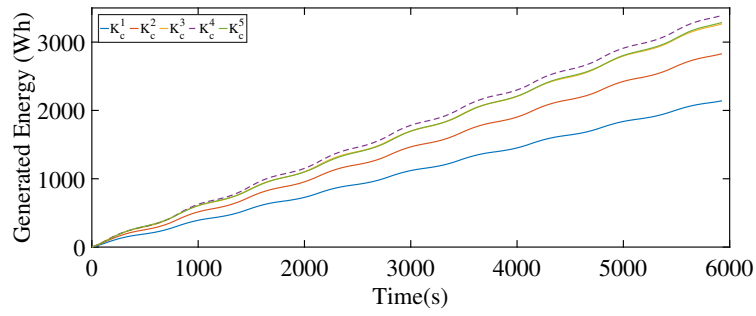


(a)

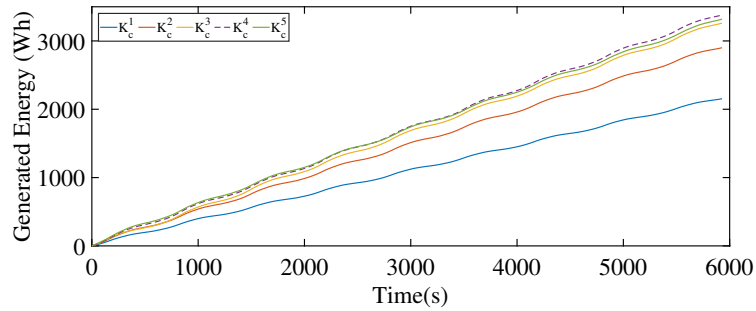


(b)

Figure 3.14: Obtained dissipated power for a) Wind Case I, b) Wind Case II

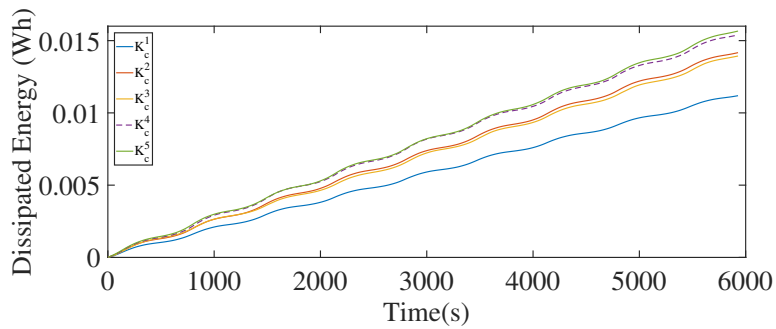


(a)

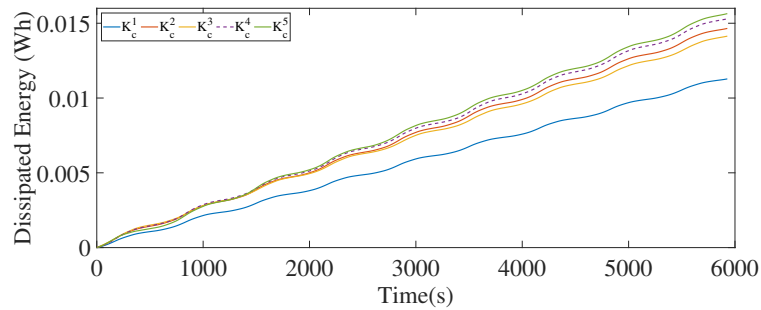


(b)

Figure 3.15: Obtained generated energy for a) Wind Case I, b) Wind Case II



(a)



(b)

Figure 3.16: Obtained dissipated energy for a) Wind Case I, b) Wind Case II

## 3.6 Conclusions

This chapter proposes a novel model of shaft degradation based on dissipated energy. The proposed model is based on contact mechanics and allows us to estimate through simulation the dissipated energy at the shaft for different wind conditions and different control gains (optimal and sub-optimal).

The proposed model was tested through simulations using real data of wind speed measurements concerning laminar flow, but also using simulated data of turbulent wind conditions obtained from stochastic differential wind models. The presented simulation provides a complete panoramic result about the possible situations affecting the turbine degradation.

The findings reveal that during periods of intense turbulence, a significant amount of energy can be rapidly dissipated, consequently accelerating system degradation and raising the risk of transmission failure. Additionally, the choice of control gain without due consideration of wind conditions can profoundly impact the rate of system degradation.

The simulation results illustrate the impact of persistent variations in the shaft angle when the system is submitted to wind speed with high variances. Additionally, when operating under sub-optimal control conditions, two scenarios emerge: one leads to greater energy generation but increases the degradation, while the other results in reduced energy dissipation but lower energy generation. Nevertheless, it is important to emphasize that the optimal control gain consistently delivers maximum power generation with minimal degradation across all scenarios.

Besides, the validation of the results was made using a real prototype of a wind turbine, where it was necessary to use a virtual flexible shaft to model the degradation in a real fixed shaft. As a result, it is validated that there exist an important effect on the degradation when the control system does not take into account the variations in the wind conditions.

This work is a first step towards a degradation-aware control approach that would allow to find dynamically the optimal trade-off between the generated energy and the turbine degradation (dissipated energy), taking into account the actual wind conditions.





# Gain Scheduling Control Strategy

---

## Contents

---

<b>4.1</b>	<b>Introduction</b>	<b>65</b>
<b>4.2</b>	<b>Problem Statement</b>	<b>66</b>
<b>4.3</b>	<b>Proposed Gain-Scheduling Control Strategy</b>	<b>67</b>
4.3.1	Gain-Scheduling Control Architecture	67
4.3.2	Optimization for gain-scheduling control design	69
<b>4.4</b>	<b>Evaluation of performance of proposed strategy</b>	<b>69</b>
4.4.1	Results & Discussions	70
<b>4.5</b>	<b>Conclusions</b>	<b>75</b>

---

This chapter aims to present a gain-scheduling wind-turbine control strategy that can mitigate the effects of adverse weather conditions by choosing a suitable feedback control gain depending on the wind turbulence conditions. The approach allows for establishing a trade-off between generated and dissipated energy to maximize the efficiency of a wind turbine by considering the actual wind conditions.

The contributions presented in this chapter, have been published in the article entitled "Gain-scheduling wind-turbine control to mitigate the effects of weather conditions on the drive-train degradation.", and presented in 11th IFAC Symposium on Fault Detection, Supervision and Safety for Technical Processes - SAFEPROCESS 2022.

## 4.1 Introduction

The deterioration model presented in Chapter 3 allows to use of the dissipated energy as an indicator of degradation on the drive-train of a wind turbine. Also, for the model, the drive-train dynamics are implemented in an MPPT control law where the control gain  $K_c^{opt}$  is estimated based on the theoretical maximum performance of the wind turbine for a specific optimal wind condition.

However, the random nature of wind speed conditions represents a challenge in optimizing the lifetime of wind turbines. In particular, if we consider that high wind speed variations are one of the principal factors of increasing degradation rate. Uncontrolled weather conditions (e.g., wind turbulence intensity) can deteriorate the mechanical

transmission in a wind turbine. This could be due to persistent variations in the radial and angular shaft deflections when the system is submitted to wind speed with high variances. Besides, the shaft deterioration increases maintenance and energy costs. ([16, 77, 114]).

Motivated by the benefits of improving this technology, numerous control approaches to reduce the loads by the wind variation in the wind turbine have been proposed in the literature ([66, 99]). Nevertheless, most of the research efforts are focused on the deterioration of individual components of the turbine and do not consider changes in the wind conditions and their interactions with the control system to analyze the drive-train deterioration and control.

It is expected that wind turbines are operated under a poorly adapted control strategy during significant periods, affecting the efficiency of the turbine. However, Chapter 3 demonstrated that the changes in the wind affect the deterioration, and the modification of the control gain can benefit or accelerate degradation.

In this chapter, the assumption that it is possible to find a control gain that allows managing degradation is considered by using an adequate control gain depending on the type of wind. The proposed control strategy allows for finding a trade-off between generated and dissipated energy using optimization to find suitable control gains.

## 4.2 Problem Statement

In a wind turbine, the control gain of the generator is usually adjusted without considering changes in the wind flow conditions. The MPPT control law for VS-FP wind turbines in Equation 2.8 shows that the generated torque depends on optimal control gain  $K_c^{opt}$  and rotor angular speed  $\omega_r$ . However,  $\omega_r$  varies depending on the wind and is not controllable. On the other hand,  $K_c^{opt}$  is fixed and defined based on the value of  $C_p^{max}$  to maximize energy extraction. The MPPT control law does not account for the type of wind or its variability, nor does it take into account the degradation of the system.

Nevertheless, in Chapter 3, it has been shown that when the control system ignores wind conditions, the efficiency and the degradation of the turbine are significantly affected. As stated in Chapter 3, the four following observations can be made:

- The dissipated energy increases when the wind conditions are of high turbulence;
- The chosen control gain impacts the degradation (is considered here the dissipated energy  $E_d$  to be an indicator of degradation level), for instance:

$$E_d = \begin{cases} \text{Increases when} & K_c > K_c^{opt} \\ \text{Decreases when} & K_c < K_c^{opt} \end{cases}$$

where  $K_c$  stands for the chosen control gain and  $K_c^{opt}$  is the theoretical optimal feedback control gain ;

- A control gain chosen higher than the optimal one leads to a greater energy production than a control gain smaller than the optimal one, i.e consider two possible control gain choices  $K_c^a$  and  $K_c^b$ , around the optimal one, such that

$$K_c^a < K_c^{opt} < K_c^b, \quad (4.1)$$

then, choosing  $K_c^b$  leads to higher energy production than choosing  $K_c^a$  ;

- However, even if the choice of a higher gain  $K_c^b$  leads to a higher energy production, in the case of high turbulent flow, this increase in energy production is not that significant.

Considering these observations, a trade-off can be found between the dissipated and the generated energy by a proper choice of a control gain, and the problem is thus to design a control strategy that allows the selection of a suitable control gain  $K_c^s$  according to the wind conditions. In this chapter, it is assumed that those wind conditions are identified, on-line, by a given algorithm that is outside the scope of this thesis.

### 4.3 Proposed Gain-Scheduling Control Strategy

This chapter proposes a gain-scheduling wind-turbine control strategy to manage the degradation and to optimize the lifetime of the mechanical transmission components while maintaining an acceptable efficiency of a wind turbine under varying weather conditions. In the next section, the proposed control architecture will be presented.

#### 4.3.1 Gain-Scheduling Control Architecture

On the proposed control strategy, we consider that it is necessary to make an adequate selection of the control gain  $K_c$ , and the value of this parameter should vary considering the level of dissipated energy and the type of wind.

The control parameter  $K_c$  is a degree of freedom for solving the problem: maximization of the generated power while respecting a suitable rate of deterioration. A solution could be a convex combination of optimal controllers associated with every class of wind. In this thesis, it is assumed that there are different classes of wind and an optimal control gain is available for each of them, e.g., for two classes we have:

$$K_c = \gamma K_c^1 + (1 - \gamma) K_c^2 \quad (4.2)$$

To reach this objective, we propose a gain-scheduling control strategy, which architecture is shown in Figure 4.1.

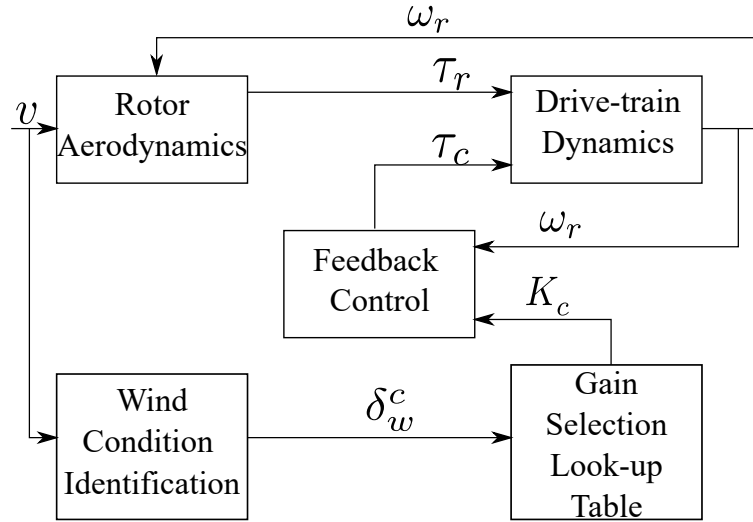


Figure 4.1: Architecture of the proposed gain-scheduling control strategy.

On the proposed strategy, it is possible to use the same simplified model presented on Equation 3.1 for simulate the dynamic on the drive-train. However, the MPPT control law have been modified to use a suitable control gain instead of fixed value of  $K_c^{opt}$

The straightforward way to select the adequate control gain is through the wind information, which can be utilized for identifying the wind speed conditions  $\delta_w^c$  (i.e. laminar or turbulent flow), as follows:

$$\delta_w^c = \begin{cases} 1 & \text{if } v \text{ corresponds to turbulent flow} \\ 0 & \text{if } v \text{ corresponds to laminar flow} \end{cases}$$

The index  $\delta_w^c$  can be considered as a gain-scheduling variable. Note that in this chapter, an example with two conditions will be utilized. However, the strategy can be applied to as many wind conditions as required.

On the other hand, the feedback gains  $K_c$ , are stored in a previously designed look-up table, and will be selected according to the wind conditions  $\delta_w^c$  as it is illustrated in Figure 4.2. The values of the control gain  $K_c$  can be obtained off-line by solving an optimization problem as is explained in the next section.

Remark that the system presented in Equation 3.1, the varying parameter (Equation 3.7) and the MPPT control law (Equation 2.8), can be rewritten as a Linear Parametric Varying (LPV) control system which is intrinsically stable for any positive feedback gain in (2.8). In particular, the stability guarantees of the proposed control architecture can be stated by using the available LPV and polytopic analysis tools, see for instance [4].

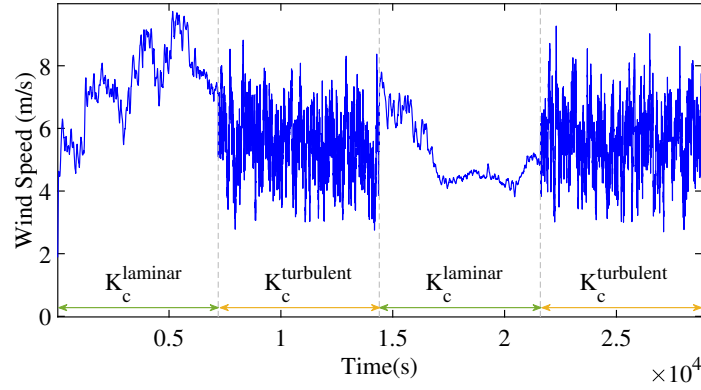


Figure 4.2: Example of gain-scheduling depending on two wind conditions.

### 4.3.2 Optimization for gain-scheduling control design

The interest of adopting a gain-scheduling control approach is the possibility of selecting suitable control gains  $K_c^s$  for each wind condition, which allows to reach a trade-off between dissipated and generated energy. Hence, those gains can be obtained as the solution of an optimization problem.

To obtain the value of the control gains, it is necessary to implement off-line simulations of the system as presented in Figure 4.3, for each type of wind (i.e.laminar or turbulent).

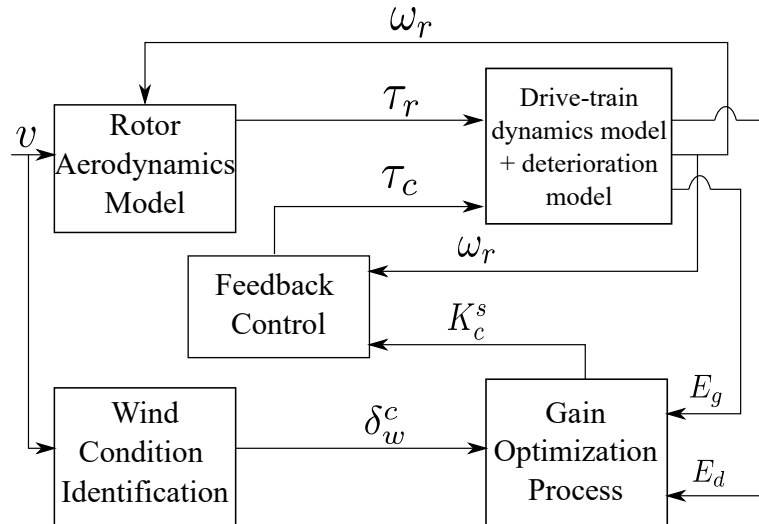


Figure 4.3: Scheme of the off-line optimization process for designing feedback control gains.

For each case (i.e.laminar or turbulent), the value of the gain is obtained as the one that minimizes the ratio of the dissipated energy  $E_d$  over the generated energy  $E_g$  under the considered wind conditions:

$$K_c^s = \arg \min_{K_c} \left( \frac{E_d(K_c, w_r)}{E_g(K_c, w_r)} \right) \quad (4.3)$$

All the gains obtained for each possible situation are stored in a look-up table. The control system will recover these gains, online, to implement the control loop.

#### 4.4 Evaluation of performance of proposed strategy

An experiment was conducted to evaluate the proposed gain-scheduling control strategy that considered different control gains depending on the wind conditions. In this work, we considered two scenarios of wind speed conditions (laminar and turbulent) to validate the proposed Gain-scheduling control strategy. Each case was evaluated separately, in order to obtain two possible suitable control gains, as shown below:

$$K_c^s = \begin{cases} K_c^{Turbulent} & \text{optimal } K_c \text{ for turbulent flow} \\ K_c^{Laminar} & \text{optimal } K_c \text{ for laminar flow} \end{cases}$$

The same scenario used in Chapter 3 was considered for performance evaluation, using a VS-FP turbine with a horizontal axis and fixed gearbox. The turbine has a rated power of 2 MW and a 100 m rotor diameter. The power coefficient curve,  $C_p$  versus  $\lambda$ , has a value of 0.4615 at  $\lambda_0$  equal to 6.4. Therefore, using Equation 2.9, the theoretical optimal feedback control gain is  $K_c^{opt} = 9.5065e5$ .

The dynamical system presented in Equation 3.1 was used to simulate the generated energy and dissipated energy (i.e., degradation) in the transmission shaft by considering the need to adapt the control gain depending on the variations in wind nature. The drive-train system is represented by two rigid masses connected by a flexible shaft.

To evaluate the proposed strategy effectively and determine the appropriate control gain, it is necessary to have a wind scenario with at least two different wind conditions. To create this scenario, real data of laminar flow and a simulated scenario of turbulent flow were used (the model presented in [77] was implemented throughout the simulations, as explained in Chapter 2 and 3). The utilized laminar flow case is presented in Figure 4.4a, and the turbulent flow in Figure 4.4b.

For each scenario, the strategy was implemented to find the optimal control gain, as presented in Table 4.1. Subsequently, a carefully designed scenario with both types of wind was created, as shown in Figure 4.5. In this figure, the green lines represent periods with laminar flow, while the yellow lines represent periods with turbulent flow.

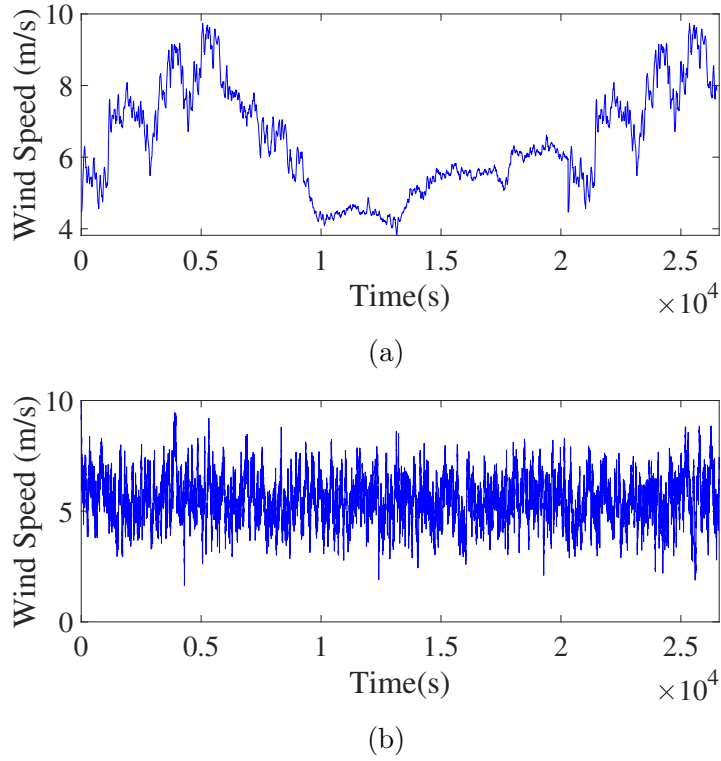


Figure 4.4: Considered wind speed conditions: (a) laminar and (b) turbulent

#### 4.4.1 Results & Discussions

The first step in designing the gain-scheduling control strategy is to find the optimal values for  $K_c^{Laminar}$  and  $K_c^{Turbulent}$ . The optimization process presented in Section 4.3.2 was simulated offline separately for the laminar and turbulent cases, using the wind data shown in Figure 4.4 as input.

The results presented that  $K_c^{Laminar}$  can take values until 11% above  $K_c^{opt}$  and  $K_c^{Turbulent}$  can take values until 15% below  $K_c^{opt}$ . To simplify the analysis, this thesis considered that  $K_c^{Laminar}$  and  $K_c^{Turbulent}$  take values around the ones presented in Table 4.1.

Table 4.1: Suitable control gains for laminar and turbulent wind conditions

$K_c^{Laminar}$	$K_c^{Turbulent}$
1.0552e6	1.4260e5

The wind scenario presented in Figure 4.5 was designed to consider variations between two different wind conditions: laminar and turbulent wind. The regions where laminar wind is implemented are indicated in green, while those with turbulent wind are marked in yellow. Dotted vertical lines were also included to indicate changes in wind conditions across all Figures.



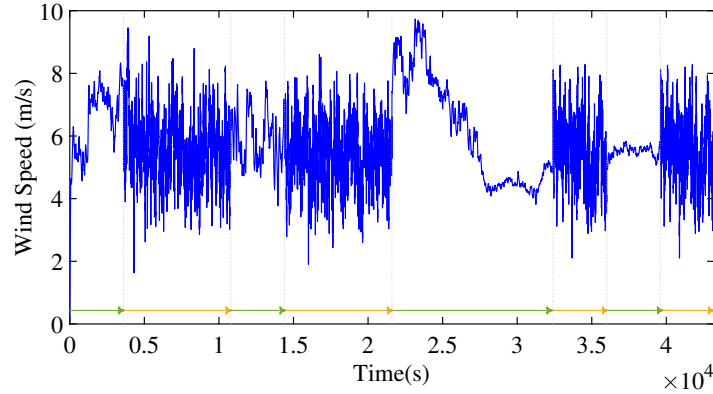


Figure 4.5: Simulated scenario of wind speed with different wind conditions.

For validation of the proposed gain-scheduling control strategy, the same changing wind condition scenario was used for testing and comparing four different choices of the control gain:

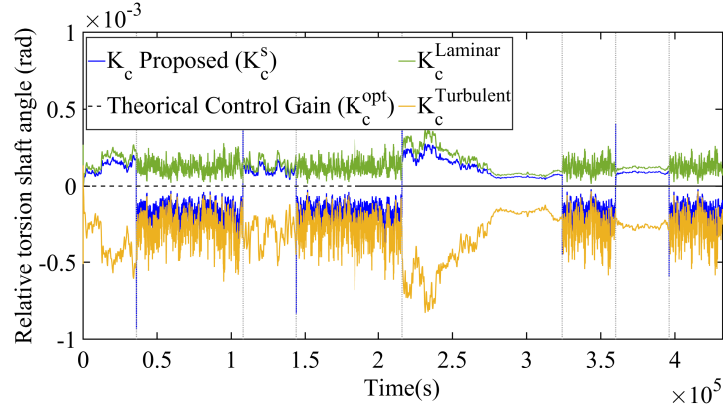
- Case with the Proposed  $K_c^s$  Switching Scheme: during all the simulation,  $K_c$  is switched between  $K_c^{Laminar}$  and  $K_c^{Turbulent}$  depending on the wind conditions;
- Case with the Theoretical Optimal Control Gain  $K_c^{opt}$ : during all the simulation,  $K_c$  is set at the constant value of  $9.5065e5$
- Case with  $K_c^{laminar}$ : during all the simulation,  $K_c$  is set at a constant value obtained as optimal under laminar conditions
- Case with  $K_c^{turbulent}$ : during all the simulation,  $K_c$  is set at a constant value obtained as optimal under turbulent conditions

To validate the gain-scheduling control strategy, the dynamical system presented in Equation 3.1 was utilized:

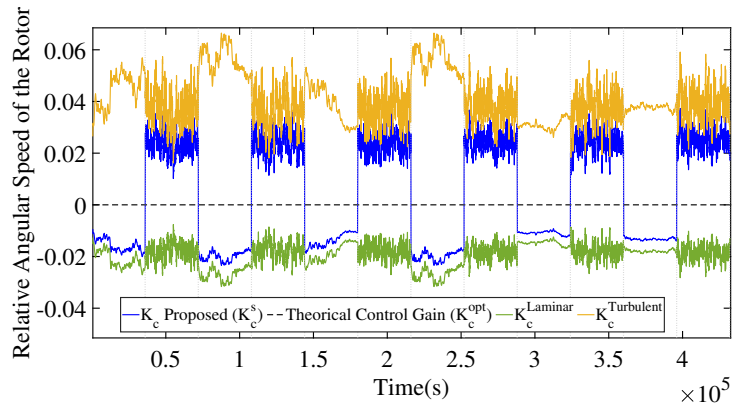
Regarding the torsion angle  $\theta_s$ , it has been observed that the angle varies depending on the switches made in  $K_c$  under different wind conditions. Figure 4.6a illustrates the comparison of  $\theta_s$  behavior to the optimal case: The results demonstrate that wind conditions have an impact on the variation of  $\theta_s$ , which can be minimized by adjusting the control gain appropriately. The case with  $K_c^{Laminar}$  resulted in more variation in  $\theta_s$  compared to the optimal case, while  $K_c^{Turbulent}$  consistently remained below the nominal case. However,  $K_c^s$  can be adjusted based on wind conditions and directly influences the variations in  $\theta_s$ , bringing it closer to the theoretically optimal case.

Concerning the relative angular speed of the rotor  $\omega_r$  with respect to the optimal case, the results show that  $K_c^{Laminar}$  leads to a minor rotation, in contrast to  $K_c^{Turbulent}$ , which leads to more significant values. Note that in the case where is implemented  $K_c^s$ ,

$\omega_r$  changes depending on the wind conditions but allows us to see that it is the closest approximation to the theoretical optimal case.



(a)



(b)

Figure 4.6: Comparison for different feedback gains: a) Relative torsion shaft angle  $\theta_s$ , and b) Relative angular speed  $\omega_r$

To compare the efficiency of the evaluated cases, the power coefficient can be analyzed in Figure 4.7, which shows the behavior of  $C_p$ . As expected, the highest  $C_p$  is obtained by using  $K_c^{opt}$ . However, it is worth noting that the difference between the other cases and the optimal case is not significant. The most noticeable difference is concerning the case using  $K_c^{Laminar}$  when the wind was turbulent.

Figure 4.8a shows the generated energy for different  $K_c$ : with  $K_c^{opt}$  it is possible to generate more energy, followed by the case where  $K_c^{Laminar}$  is used, because a greater  $K_c$  leads to a higher generation of energy. Nevertheless, the gain-scheduling control strategy allows for improving energy generation when the wind exhibits periods of turbulent conditions.

Besides, Figure 4.8b illustrates the dissipated energy for the period of evaluation. The case with  $K_c^{Laminar}$  dissipated a higher amount of energy. Moreover, in the case of

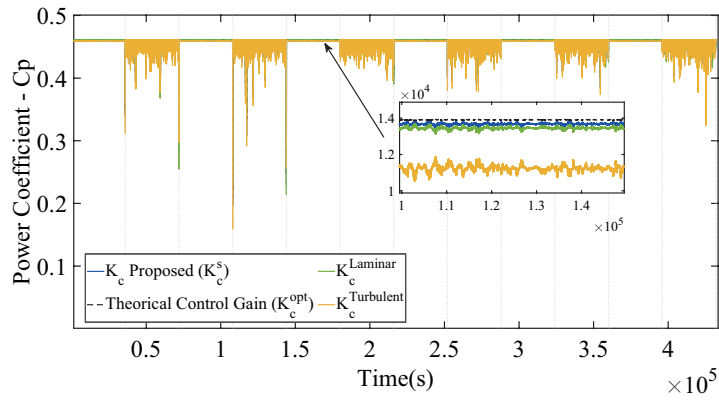
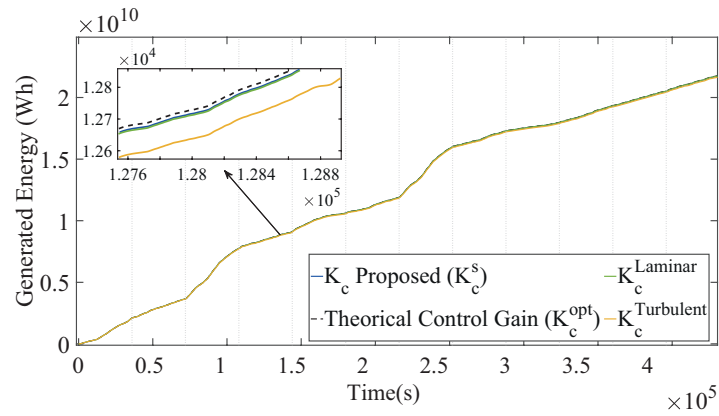
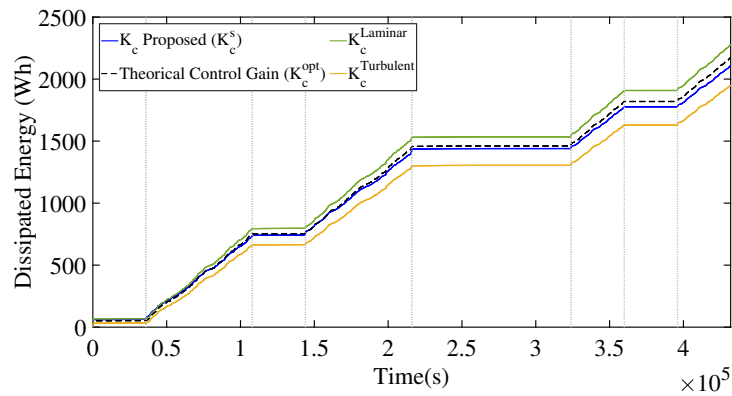


Figure 4.7: Comparison of the power coefficient  $C_p$  with respect to the theoretical optimal case.

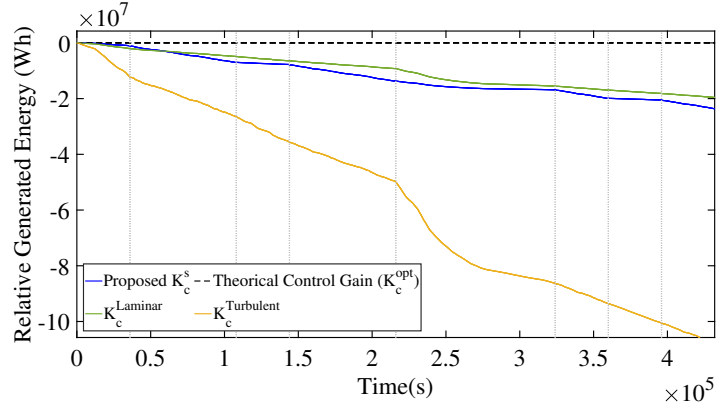


(a)

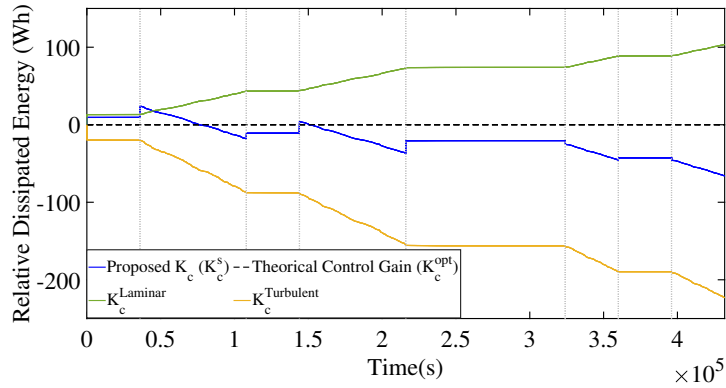


(b)

Figure 4.8: a) Generated energy for different feedback gains  $K_c$ , and b) Dissipated energy for different feedback gains  $K_c$



(a)



(b)

Figure 4.9: Comparison with respect to the optimal case from: a) Relative generated energy, and b) Relative dissipated energy

$K_c^{Turbulent}$ , a  $K_c$  lower than the optimal leads to minor degradation. Nevertheless, it can be seen that the gain-scheduling control strategy allows to follow the behavior of the case with  $K_c^{opt}$  in terms of energy dissipation.

To further discuss these results, let's consider the generated and dissipated energy and compare them with the  $K_c^{opt}$  scenario:

- Generated energy: The optimal case always leads to a significant amount of generated energy, and a greater  $K_c$  increases the energy generation. However, if the control gain is switched according to the wind conditions ( $K_c^s$ ), it is still possible to increase the generation of energy almost at the level reached under laminar ideal conditions, see Figure 4.9a.
- Dissipated energy: regarding the generated energy, a higher generation leads at the same time to a significant level of dissipated energy, and hence degradation. For this reason, the dissipated energy in the case with  $K_c^{laminar}$  is above the

optimal ones. However, the  $K_c^{Turbulent}$  is below the other cases with a significant difference, while the case with suitable control gain  $K_c^s$  allows to keep a low level of dissipated energy, dissipating less energy than in the cases with  $K_c^{Laminar}$  and even with  $K_c^{opt}$ , see Figure 4.9b.

We can thus conclude that the proposed control adaptation strategy allows to increase energy generation in turbulent cases and decreases dissipated energy in the drive-train system (when compared to situation where  $K_c$  is higher than optimal). As a consequence, the system can profit of both a higher generation of energy and a lower dissipated energy.

## 4.5 Conclusions

This chapter proposes a gain-scheduling control strategy to optimize the efficiency of a wind turbine under varying weather conditions, finding an optimal trade-off between the generated energy and degradation (due to dissipated energy) in the drive-train. The proposed strategy considers the variation of the wind conditions to alternate between different suitable control gains, maximizing the generated energy and decreasing the dissipated energy.

The proposed strategy was tested using different wind speed scenarios to consider a more complete panorama about the possible wind conditions affecting the turbine. Real data measurement was used to simulate the wind conditions for laminar flow, while for turbulent wind conditions, a stochastic model was used to simulate it.

The results show that it is possible to maximize the generated energy and decrease the dissipated energy by switching the control gains depending on wind flow conditions, decreasing the variations in the shaft angle, and getting closest to the theoretical optimal behavior.

Stability conditions of the proposed control scheme can be obtained by expressing the whole dynamical control system as a Linear Parametric Varying system and, by using suitable available tools in this area.



# Long-Term Estimation of Deterioration

---

## Contents

<b>5.1</b>	<b>Introduction</b>	<b>79</b>
<b>5.2</b>	<b>Methodology for Long-Term Estimation of Deterioration</b>	<b>80</b>
<b>5.3</b>	<b>Evaluation of Performance of the Proposed Methodology for Long-Term Estimation of Deterioration</b>	<b>83</b>
5.3.1	Implementation of Proposed Methodology by Steps	84
5.3.2	Results & Discussions	87
<b>5.4</b>	<b>Conclusions</b>	<b>91</b>

---

This chapter proposes a methodology to analyze the long-term degradation of a wind turbine drive-train on which a gain-scheduling control strategy is implemented and considering the variation in the wind conditions. The degradation in the transmission is modeled through a simplified dynamical system based on contact mechanics, employing the dissipated energy as an indicator of the degradation in the transmission system. In addition, the gain-scheduling control strategy presented in 4 is considered to assign a control gain according to the wind flow conditions. Numerical experiments were considered to illustrate the proposed approach, assuming a 2 MW variable speed-fixed pitch turbine with a horizontal axis and fixed gearbox.

The contributions presented in this chapter, have been published in the article entitled "Long-term degradation estimation of wind turbine drive-train under a gain-scheduling control strategy according to the weather conditions.", and presented in the 5th IFAC Workshop on Advanced Maintenance Engineering, Services, and Technology - AMEST 2022.

## 5.1 Introduction

The maintenance strategies have to be able to consider deterioration in the long term due to action in the short term. For this reason, multiple studies have investigated the prediction of the remaining useful lifetime (RUL) using data-based methods, which can require significant amounts of information and result in complex predictions that

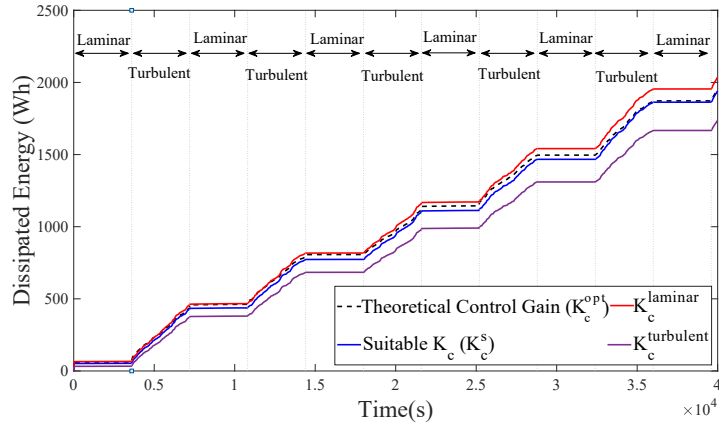


Figure 5.1: Dissipated Energy for different control feedback gains  $K_c$ .

can be difficult to implement computationally. Besides, do not consider the effect of changes in wind conditions for the predictions in the long term. ([11, 31, 66, 68, 139, 144]).

The degradation of a wind turbine is significantly affected when the control system is adjusted without considering the wind flow conditions. The analysis presented in Chapter 3 demonstrated an accelerated degradation when the control gain is different from the nominal gain ( $K_c^{opt}$ ). Besides, the changes in the wind flow nature (e.g. laminar and turbulent wind) lead to an increment of dissipated energy.

The results in Chapter 4, as illustrated in Figure 5.1, shows the behavior of  $E_d$  for the different cases of control gains. The figure demonstrates that turbulent wind leads to accelerated degradation. However, it is possible to observe that implementing a gain-scheduling control strategy can decrease the energy dissipated.

Note that the case with  $K_c^{Laminar}$  always leads to a degradation greater than with  $K_c^{Turbulent}$  due to a greater  $K_c$  always leads to a more significant amount of dissipated energy, as it is mentioned in Chapter 3. Nevertheless, using a suitable control gain, the behavior can be approximated to the theoretical optimal control case.

This chapter proposes a methodology to simulate deterioration in the mechanical components of the drive-train in a wind turbine for the extended term when subjected to a control strategy adapted to follow the variations in the wind conditions. The approach allows simulating degradation by learning an empirical relationship with random effect between Dissipated Energy and Time and then generating new information using the learned relation with the inferred probability law for the random variables.

Furthermore, the methodology is tested for different periods of the useful theoretical lifetime of a wind turbine, considering the variation in the wind conditions changing between laminar and turbulent flow, using a sequence generated by a Markov Chain.



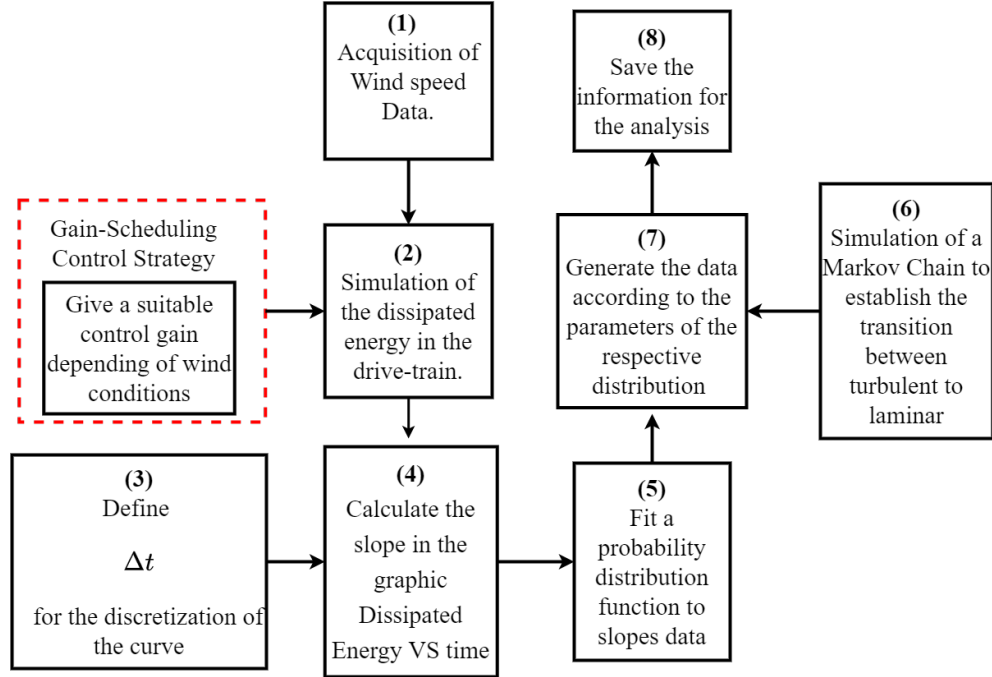


Figure 5.2: Diagram flow to represent the proposed methodology of long-term estimation of deterioration.

Finally, the results allow knowing the percentage of degradation that can be reduced if a gain-scheduling control approach is implemented, considering the wind conditions.

## 5.2 Methodology for Long-Term Estimation of Deterioration

This section presents an approach to evaluate the deterioration in the long-term of a drive-train in a wind turbine by learning the curve of Dissipated energy vs. Time for different wind conditions and using a Markov chain to estimate the transition between each case of wind conditions.

The rate of change of the dissipated energy (i.e., degradation) depends on the control gain  $K_c$  and the nature of the wind. This rate is also a random variable. If we denote the rate as  $\mathbf{s}$ , it can be said that  $\mathbf{s} \sim \varphi(K_c, \delta_w^c)$ , where  $\varphi$  represents a probabilistic law, and  $\delta_w^c$  describes the wind conditions.

The principle of long-term estimation is to learn the distribution of slopes as a function of wind nature and control gain. Once this distribution is learned, it is possible to simulate wind history (e.g. with a Markov Chain approach) and use the probabilistic model  $\varphi$  to generate the slopes  $\mathbf{s}$  and simulate the deterioration.

This probabilistic model  $\varphi$  can be seen as a surrogate probabilistic model for deterioration, allowing the problem of long-term simulations under a given control strategy to

be solved.

The process for simulating long-term deterioration is illustrated in the diagram presented in Figure 5.2, and comprises the following steps:

Steps (1) to (5) must be made for each wind condition separately. This work will consider two wind conditions (i.e., laminar and turbulent).

### Acquisition of Information

1. **Acquisition of Wind Speed Data:** Using historical or synthetic data to get the wind speed information, consider separating the information for each wind condition.
2. **Simulation of the dissipated energy in the drive-train implementing the gain-schedule control strategy:** Use the deterioration model presented in Chapter 3 for simulating the dissipated energy. Besides, following the process explained in Chapter 4, estimate a suitable control gain depending on the wind conditions (in this work,  $K_c^{laminar}$  and  $K_c^{turbulent}$ ).

### Learning Stage

3. **Define  $\Delta t$  for the discretization:** Define a constant or discrete interval  $\Delta t$  to analyze dissipated energy information with a one-second sampling period. Consider an example, where it will be use one day of simulation (86.400s), it is possible to use a discretization of 10 minutes ( $\Delta t = 600s$ ).
4. **Estimate the slope in the Dissipated Energy VS time curve:** Estimate the slope of the Dissipated Energy VS time curve for each  $\Delta t$  period. COnsidering the example used in the point before, for the case of  $\Delta t = 600s$  and one day of simulation (86.400s), this leads to 144 data of slopes.
5. **Fit a probability distribution function to slopes data:** Find an appropriate probability distribution and estimate the respective parameters that fit the data of the slopes in each case of interest.

### Simulating Stage

6. **Simulation of a Markov Chain to establish the transition between wind conditions:** To simulate long-term wind conditions, it is necessary to establish a sequence of changes between them; using a Markov chain allows modeling the transition probability between each wind regimen and the probability of sojourn in each flow regimen.
7. **Generate new slope data:** Considering a Markov Chain sequence, generate

new slope data using the fitted probability distribution function.

8. Save the information for the analysis.

The procedure can be done with as many repetitions as desired to improve the exactitude of the analysis, as well as different wind conditions (e.g., considering different turbulence levels).

### 5.3 Evaluation of Performance of the Proposed Methodology for Long-Term Estimation of Deterioration

For the evaluation of the proposed methodology, this chapter will utilize the information of a wind turbine with the same characteristics that the case used in Chapter 3 and 4:

A VS-FP wind turbine of 2 MW and 100 m of rotor diameter with horizontal-axis, with  $C_p^{max} = 0.4615$  at  $\lambda_0 = 6.4$  and considering the Equation 2.9,  $K_c^{opt} = 9.5065e^5$ .

The considered wind turbine drive-train degradation was simulated using the dynamic system presented in Equation 3.1. In addition, the variability in the wind between laminar and turbulent flow was taken into account to estimate the deterioration behavior under realistic conditions.

#### 5.3.1 Implementation of Proposed Methodology by Steps

Here, it is presented the process of implementing the proposed methodology by following the sequence of steps presented in Figure 5.2:

1. **Acquisition of Wind Speed Data:** To observe the changes in slopes between wind conditions, it was obtained laminar and turbulent with high-intensity wind data for evaluating performance.

Figure 5.3 presents the wind profile used during the simulations. For laminar wind conditions, it was used real measured data, and for turbulent flow, was implemented one level of the wind generation model presented in Ma et al. [77]. In both scenarios, it was assumed constant conditions for 5.5 hours (20,000 seconds).

2. **Simulation of the Dissipated Energy in the Drive-Train Implementing the Gain-Schedule Control Strategy:** Using the deterioration model presented in Chapter 3, it was simulated the dissipated energy for each case of wind condition (laminar and turbulent).

Furthermore, the results from evaluating the performance of the gain-scheduling control strategy proposed in Chapter 4 were implemented to determine a suitable control gain for each wind condition. The values of  $K_c^{Laminar}$  and  $K_c^{Turbulent}$  were:

- For laminar wind:  $K_c^{Laminar}$  can take values up to 11% above  $K_c^{opt}$ .

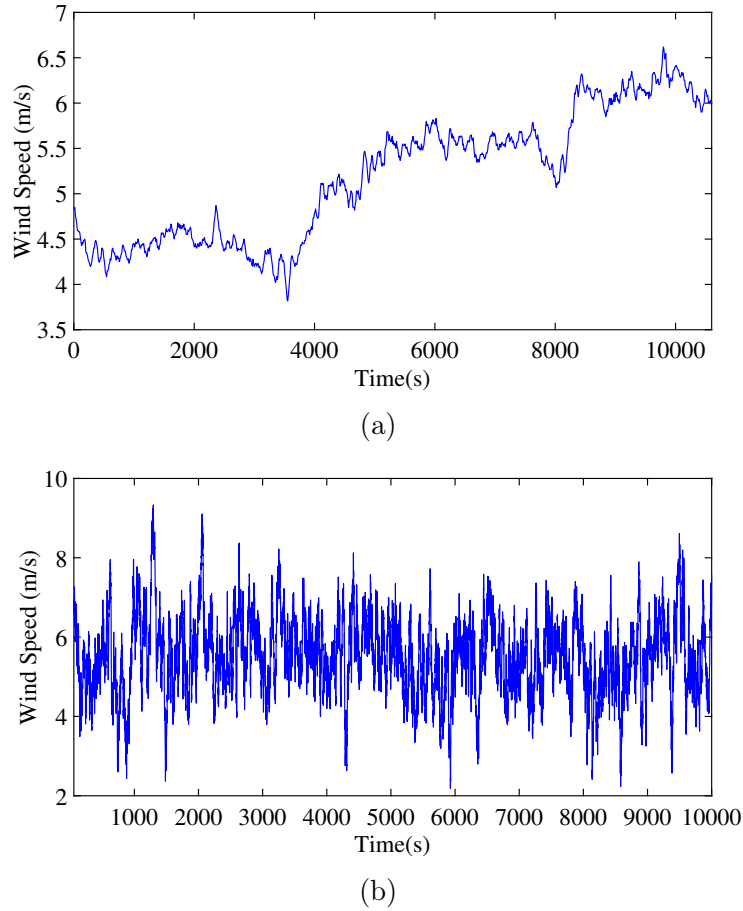
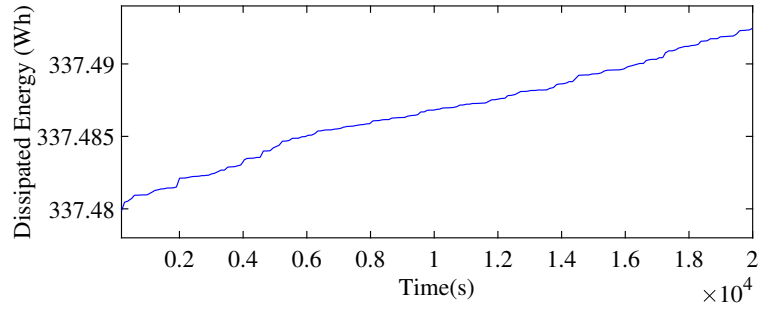


Figure 5.3: Considered wind speed conditions: (a) Laminar and (b) Turbulent

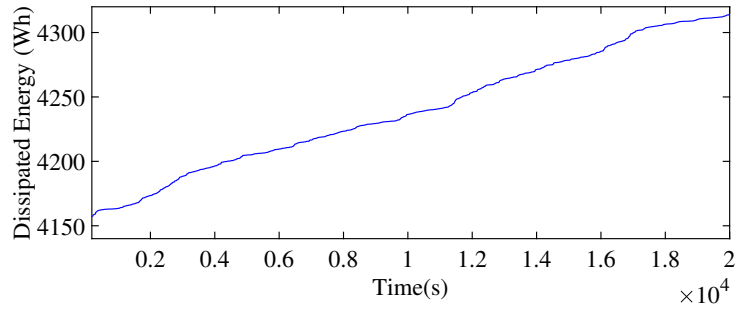
- For turbulent wind:  $K_c^{Turbulent}$  can take values down to 15% below  $K_c^{opt}$ .

After simulating the deterioration of the system considering the suitable control gains depending on the wind conditions, the cases of interest are illustrated in Figure 5.4a for laminar case, and Figure 5.4b for turbulent case. Also was implemented a reference case for laminar and turbulent wind conditions dissipated energy. These simulations will be denominated as "nominal" cases and were obtained using the same wind as input but with a constant control gain at  $K_c^{opt}$ . The dissipated energy for the laminar and turbulent conditions is presented in Figure 5.4c and 5.4d respectively.

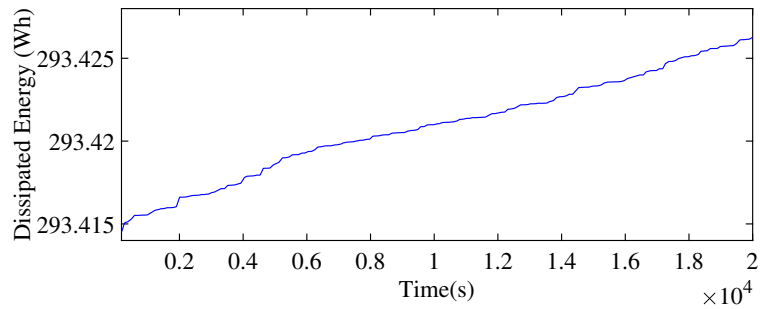
3. **Define  $\Delta t$  for the discretization:** In this work, the curve Dissipated Energy vs. Time was discretized assuming that  $\Delta t = 600s$ , due to the fact the transition between wind conditions is not instantaneous and the record time in some systems is usually 10 minutes (e.g., SCADA).
4. **Estimation of the slope in the Dissipated Energy VS time:** The slopes



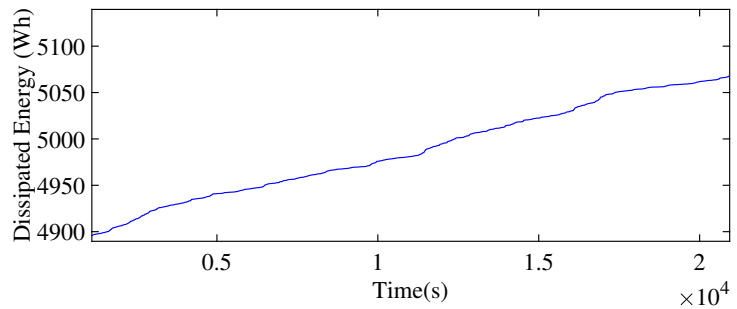
(a) Dissipated Energy with:Laminar wind with  $K_c^{Laminar}$



(b) Dissipated Energy with:Turbulent wind with  $K_c^{Turbulent}$



(c) Dissipated Energy with:Laminar wind with  $K_c^{nom}$



(d) Dissipated Energy with:Turbulent wind with  $K_c^{nom}$

Figure 5.4: Dissipated Energy with: (a)Laminar wind with  $K_c^{nom}$  and (b) Turbulent wind with  $K_c^{nom}$

were estimated considering the equation of the slope or gradient of a line, e.g., for the case between two points  $x_1$  and  $x_2$ , the slope of the curve of dissipated energy will be:

$$s = \frac{E_d(2) - E_d(1)}{\Delta t}$$

5. **Fit probability distribution to slope data:** Due to the variability in wind levels under the same wind regime, the slopes of the "Dissipated Energy vs Time" relationship can be considered as realizations of a random variable. In the proposed methodology, the learning steps can involve understanding the distribution of slopes under different wind regimes. This, in turn, will enable the prediction of the long-term deterioration and the characterization of the associated uncertainty. Such information can be useful for tasks like RUL prediction.

Probability distribution functions were fitted of slopes data in each case using the Distribution Fitter app (Matlab Software). The results show that the better fit for each case is:

- Slopes data from dissipated energy curve in laminar case: Beta distribution
  - Slopes data from dissipated energy curve in turbulent case: Gamma distribution
6. **Simulation of a Markov Chain to establish the transition between wind conditions:** A Markov Chain with a transition matrix  $T$  was established to simulate the transition between laminar and turbulent flow. In this work, the transition probability matrix controlling the change between turbulent and laminar is given as follows:

$$T = \begin{pmatrix} 0.7 & 0.3 \\ 0.3 & 0.7 \end{pmatrix} \quad (5.1)$$

It means that at each time step of 600 s, there is a 70 % chance of staying in turbulent flow and a 30 % chance of changing from turbulent to laminar flow.

7. **Generate new slope data:** Simulate synthetic slope data using the parameters of the probability functions. This data will allow you to estimate the dissipated energy between two points every  $\Delta t$  moment. Select the appropriate probability function based on the wind conditions.
8. **Replicate:** To obtain an image of the degradation during the useful lifetime of the wind turbine, perform the analysis for different periods. This work considered using 100 replicates in each case to comprehensively understand the varied sequences of changes between laminar and turbulent flow.

### 5.3.2 Results & Discussions

To analyze the dissipated energy in each scenario, we can refer to Figure 5.4. These graphs support the conclusions outlined in Chapter 4. Specifically, it is possible to observe that the energy dissipation is lower during the analysis period when using laminar flow and  $K_c^{opt}$  (Figure 5.4c) compared to using  $K_c^{Laminar}$  (Figure 5.4a). However, in the turbulent scenario, we observe more significant degradation with  $K_c^{opt}$  (Figure 5.4d) than with the suitable control gain  $K_c^{Turbulent}$ .

For learning the behavior of the curve, the slopes were estimated every 10 minutes ( $\Delta t = 600s$ ), and each set of data was fit with a probability distribution function as follows:

- Laminar Flow: The data in the case of  $K_c^{opt}$  and  $K_c^{Turbulent}$  was fit with a Beta distribution. Figure 5.6a shows the graphic of the density function for the data set of slopes calculated from the curve of Dissipated Energy vs. Time with Laminar flow and  $K_c^{Laminar}$ . Similar results were obtained for the nominal case (Figure 5.6b).
- Turbulent Flow: In the case of the turbulent flow, the Gamma distribution shows a better fitting to the data of slopes calculated from the curve of Dissipated Energy vs. Time with turbulent flow and  $K_c^{Turbulent}$  (Figure 5.7).

With fitted probability laws, it is possible to generate new slope data. Nevertheless, this work aims to reproduce wind alternating between the laminar and turbulent flow. The sequences of changes between both flow regimes were selected through a Markov chain. They were implemented using the transition matrix in Equation 5.1, considering using the suitable control gain depending on the wind condition. Also, the case was simulated using  $K_c^{opt}$  to be used as a reference.

To obtain an image of the degradation during the useful lifetime of the wind turbine, the analysis was performed for different periods with 100 replicates in each case. This provided a big picture under varied sequences of changes between laminar and turbulent flow. The process was carried out for different periods of 1 (Figure 5.5), 5 (Figure 5.8a), 10 (Figure 5.8b), 15 (Figure 5.8c), and 20 years (Figure 5.8d).

For example, let's take the case of 1 year shown in Figure 5.5. The figure shows the dissipated energy after one simulation year with 100 replicates. It is possible to observe that the amount of energy dissipated by the case with the suitable control gain is always smaller than that of the case with generated energy.

Table 5.1 summarizes the average energy dissipated for the case with  $K_c^{opt}$  and the suitable control gain  $K_c^s$ . It also shows the percentage difference between the optimized and nominal cases after the evaluation period and the average simulation time required to obtain the results.

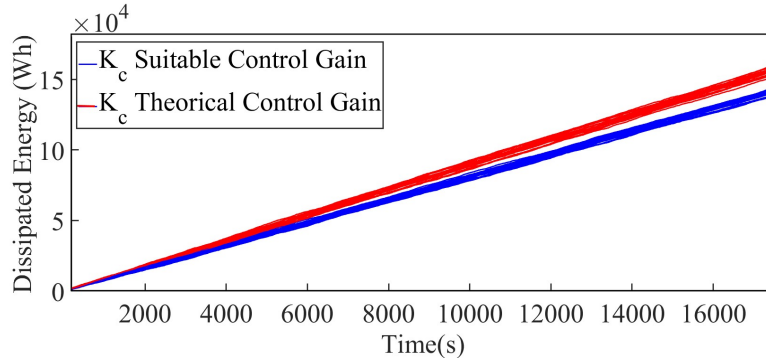


Figure 5.5: Dissipated Energy in one year of simulation using a suitable control gain and theoretical control gain for a period of: 1 Year

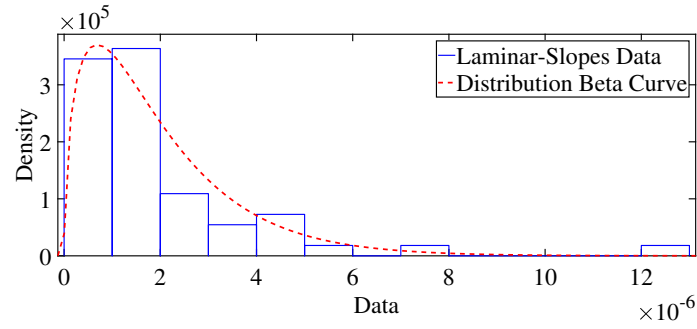
The results indicate a significantly greater energy dissipation when the  $K_c$  is not switched when necessary and suitable to the wind conditions; in all the periods under evaluation, the difference is more than 9%, which indicates a significant increase in the deterioration when no suitable mechanism of the control gain is implemented. Besides, table 5.1 shows the average time for running the simulation during the different periods, demonstrating the short time necessary to obtain an image of deterioration for long-term periods.

Table 5.1: Comparison of dissipated energy in different periods

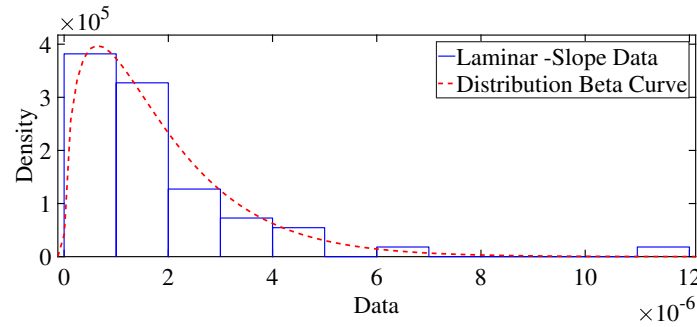
Number of years	Dissipated Energy $K_c^s$ (Wh)	Dissipated Energy $K_c^{opt}$ (Wh)	Difference (%)	Average time (sec)
1	1.446e5	1.570e5	9.307	8.271
5	7.152e5	7.906e5	9.535	8.816
10	1.419e6	1.572e6	9.694	9.913
15	2.139e6	2.369e6	9.702	11.216
20	2.843e6	3.150e6	9.743	11.956

A t-test was performed to ensure the variability in the samples; in all the cases, the test rejected the hypothesis that the means of the replicate-wise dissipated energy are equal for both simulated scenarios (static vs suitable gain), and the  $p - value \approx 0$  indicates there is robust evidence in favor of the alternative hypothesis.



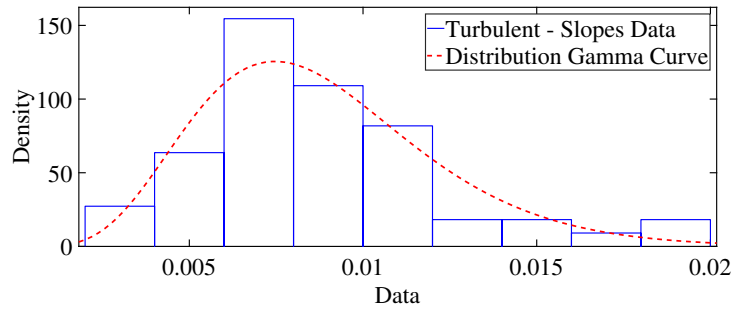


(a)

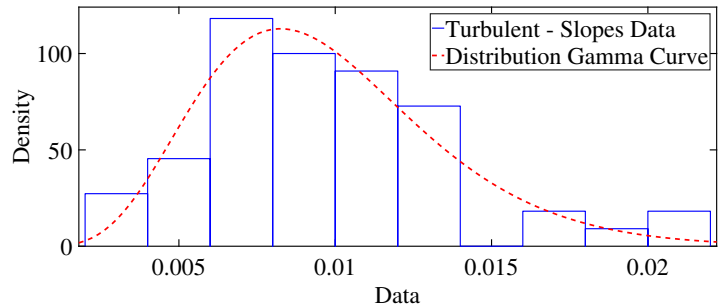


(b)

Figure 5.6: Density function of a Beta distribution using a data-set of slopes in a curve Dissipated Energy VS Time. Case: a) Using the suitable  $K_c^{Laminar}$ , and b) Using the  $K_c^{opt}$ .

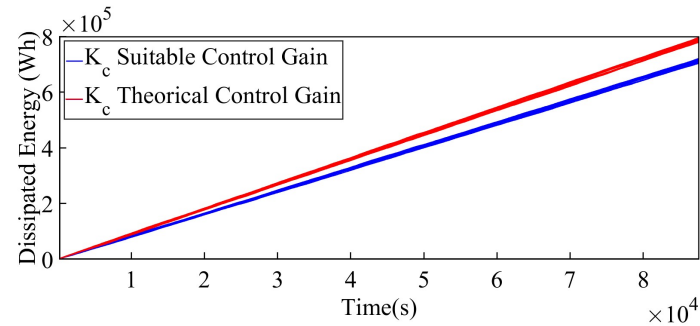


(a)

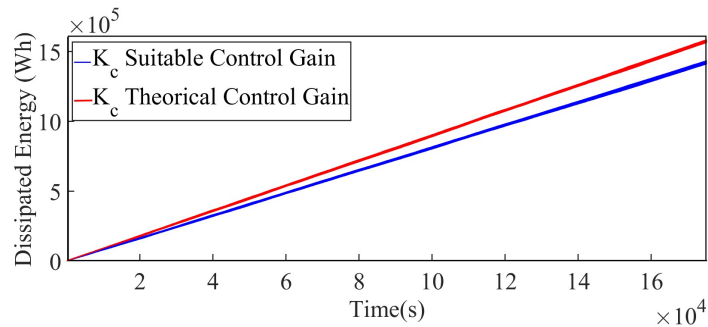


(b)

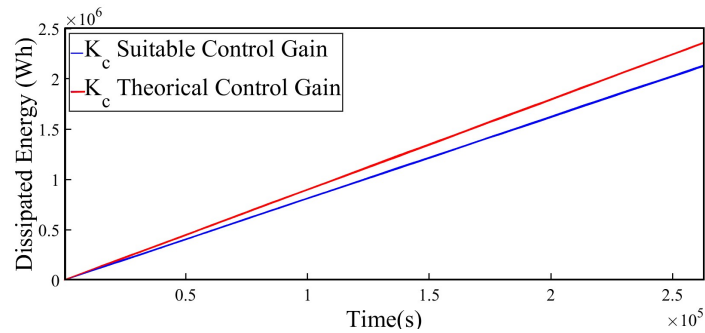
Figure 5.7: Density function of a Gamma distribution using a data-set of slopes in a curve Dissipated Energy VS Time. Case: a) Using the suitable  $K_c^{Turbulent}$ , and b) Using the nominal  $K_c^{opt}$ .



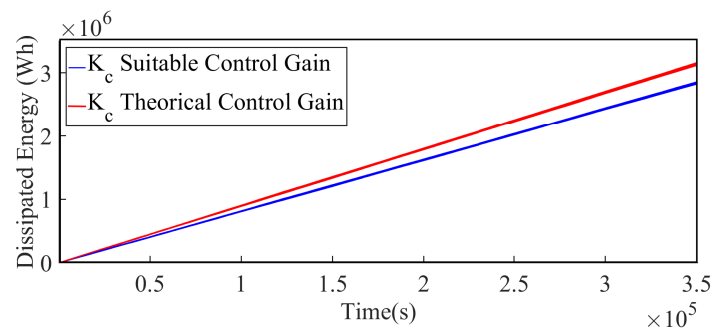
(a)



(b)



(c)



(d)

Figure 5.8: Simulated Dissipated Energy using a suitable control gain and theoretical control gain for the periods of: a) 5 years, b) 10 years, c) 15 years, and d) 20 years

## 5.4 Conclusions

This chapter proposed a methodology to analyze the long-term degradation of a drive-train wind turbine using a gain-scheduling control strategy and considering the variation in the wind conditions.

Real measurements of laminar wind were implemented; the turbulent flow was simulated using a stochastic model based on a Markov chain. Moreover, the dissipated energy was estimated employing a dynamic model based on contact mechanics for the case of laminar and turbulent flow, considering the theoretical control gain and an optimized control gain depending on the win conditions.

The dissipated energy rate for turbulent flow is more accelerated than in the laminar case. As a result, the slope is more pronounced in the Dissipated Energy VS. Time curve. It is possible to learn the slope of the curve to use this behavior in extrapolation and keep the effect of the wind in a second-wise simulation.

Different probabilistic distribution functions were employed to generate new slope data using the function parameters, and a Markov Chain was simulated to know the sequences of the transitions between the laminar and turbulent flow.

The proposed methodology was illustrated under different periods to know the degradation behavior during the useful life of the wind turbine with an extrapolation of the Dissipated Energy vs. Time curve. The results show that using the gain-scheduling control strategy, it is possible to reduce by more than 9% the energy dissipation in the drive-train compared with the nominal theoretical case.



# Control of the Rate of Deterioration

---

## Contents

<b>6.1</b>	<b>Introduction</b>	<b>93</b>
<b>6.2</b>	<b>Problem Statement</b>	<b>94</b>
<b>6.3</b>	<b>Proposed Deterioration Control Strategy</b>	<b>95</b>
6.3.1	Design of Deterioration Controller	97
<b>6.4</b>	<b>Performance Evaluation: Numerical Scenario &amp; Results</b>	<b>99</b>
6.4.1	Design of Deterioration Controller	100
6.4.2	Evaluation of the performance of degradation control strategy	100
<b>6.5</b>	<b>Conclusions</b>	<b>108</b>

---

This section presents an intelligent control strategy to minimize the degradation rate of a drive-train wind turbine when a change in the wind or set point occurs. The proposed method enables the turbine to adapt under different conditions while maintaining as much as possible energy generation without accelerating too much the degradation process. To achieve this objective, the proposed strategy consists of adjusting the maximum power point tracking control gain using a robust H-infinity control strategy considering a drive-train modeled through a simplified dynamical system based on contact mechanics, employing the dissipated energy as an indicator of the degradation in the shaft. This strategy guarantees the system's stability in the presence of uncertainties and external disturbances, such as changes in wind conditions.

The contributions presented in this chapter, have been submitted in the Journal "Engineering Applications of Artificial Intelligence", under the article entitled Intelligent robust control for the degradation rate of a wind turbine drive-train,

## 6.1 Introduction

The degradation of transmission in a VS-FP wind turbine was analyzed in Chapter 3 using the MPPT control law, finding that the performance of this type of system is adversely affected when the control system is not adjusted according to the wind flow conditions. Furthermore, the research establishes that a change in the control gain from nominal conditions has an impact on energy dissipation, highlighting the necessity of an adaptive control strategy that considers changes in the wind. However,

in Chapter 4 a gain-scheduling control strategy was proposed, this strategy aims to adapt the adaptation of the control gain depending on the wind conditions to optimize the efficiency of mechanical transmission components, even when wind flow varies. This approach can help reduce the cost of wind energy by improving reliability and reducing the maintenance costs associated with wind turbine transmission systems.

Considering the importance of predicting and addressing long-term deterioration while also considering short-term wind changes, in Chapter 5 was presented a methodology that simulates the degradation of the transmission in a long-term under varying wind conditions by learning an empirical relationship with random effect between Dissipated Energy and Time. The results of this study show when is adapted the proposed gain scheduling strategy, was obtained a decrease in degradation of more than 9% in all cases evaluated and the possibility of obtaining a fast prediction of long-term degradation.

The present chapter is based on the preliminary work presented in the chapters before (3, 4, and 5) and aims to develop a novel intelligent control strategy that minimizes the degradation of a wind turbine drive-train when occurs wind or set point changes. The proposed method enables the turbine to operate under different conditions while maintaining as much as possible the energy generation without accelerating the degradation process. To achieve this objective, a robust H-infinity control strategy is implemented to adapt the theoretical control gain to an intelligent control gain that guarantees the stability of the system and finds the optimal balance between degradation (dissipated energy) and performance (generated energy) in the presence of uncertainties and external disturbances, such as changes in wind conditions.

## 6.2 Problem Statement

As it was mentioned, dissipated energy can be used as a measure of degradation. Therefore, it is possible to use the instantaneous loss power or dissipated power  $P_d$  as an instantaneous degradation measure and refer to this parameter as  $\beta$ .

$$\dot{D} = P_d = \beta \quad (6.1)$$

Considering the definition of  $P_d$  presented on Equation 3.8,  $\beta$  can be written as:

$$\beta = B_s(\omega_g - \omega_r)^2 \quad (6.2)$$

The dynamics of wind energy are described using a simplified model based on Equation 3.1. This model incorporates torsional loads and resonance modes in the drive-train, allowing for the definition of a torsional parameter  $\vartheta$ , as:

$$\vartheta = \omega_g - \omega_r \quad (6.3)$$

Therefore,  $\beta$  can be rewritten using Equation 6.3 as follows:

$$\beta^{1/2} = \sqrt{B_s} \vartheta \quad (6.4)$$

On the other hand, as it has been demonstrated in Chapter 3 changes in the control around may lead to accelerated degradation if the wind conditions are not considered. Therefore, adjusting the control gain around  $K_c^{opt}$  considering the wind nature can minimize the degradation when there is a change in either wind speed ( $v$ ) or the set-point. The amount of adjustment required is defined as  $\Delta k_c$ .

$$K_c = K_c^{opt} + \Delta k_c \quad (6.5)$$

Thus, the generated torque can be re-expressed as follows:

$$\tau_c = (K_c^{opt} + \Delta k_c)(\omega_r)^2 \quad (6.6)$$

Besides, the dynamics in a drive-train of a VS-FP wind turbine can be described by using the system presented in Equation 3.1 :

$$\begin{pmatrix} \dot{\theta}_s \\ \dot{\omega}_r \\ \dot{\omega}_g \end{pmatrix} = \begin{pmatrix} 0 & 1 & -1 \\ -\frac{K_s}{I_r} & -\frac{B_s}{I_r} & \frac{B_s}{I_r} \\ \frac{K_s}{I_g} & \frac{B_s}{I_g} & -\frac{B_s}{I_g} \end{pmatrix} \begin{pmatrix} \theta_s \\ \omega_r \\ \omega_g \end{pmatrix} + \begin{pmatrix} 0 & 0 \\ \frac{1}{I_r} & 0 \\ 0 & -\frac{1}{I_g} \end{pmatrix} \begin{pmatrix} \tau_r \\ \tau_c \end{pmatrix}$$

A modification of the system presented in Equation 3.1 can be made by considering Equation 6.6 for introducing the  $\Delta k_c$  in the dynamic model of the drive-train. If the system is evaluated around a specific region of operation as a reference, it is possible to define a value of  $\omega_r$  for this point, and recalling that  $B_s$  can be estimated considering the Equation 3.6. The new system is defined as:

$$\begin{pmatrix} \dot{\theta}_s \\ \dot{\omega}_r \\ \dot{\omega}_g \end{pmatrix} = \begin{pmatrix} 0 & 1 & -1 \\ -\frac{K_s}{I_r} & -\frac{B_s}{I_r} & \frac{B_s}{I_r} \\ \frac{K_s}{I_g} & \frac{B_s - K_c^{opt} \bar{\omega}_r^2}{I_g} & -\frac{B_s}{I_g} \end{pmatrix} \begin{pmatrix} \theta_s \\ \omega_r \\ \omega_g \end{pmatrix} + \begin{pmatrix} 0 & 0 \\ \frac{1}{I_r} & 0 \\ 0 & -\frac{\bar{\omega}_r^2}{I_g} \end{pmatrix} \begin{pmatrix} \tau_r \\ \Delta k_c \end{pmatrix} \quad (6.7)$$

The system outlined in equation 6.7 enables the utilization of  $\Delta k_c$  to produce changes in the indicator of deterioration  $\beta$ , across the states of torsion angle  $\theta_s$ , rotor angular speed  $w_r$ , and generator angular speed  $w_g$ .

### 6.3 Proposed Deterioration Control Strategy

This section presents a control strategy that allows the turbine to operate under variable conditions while maintaining energy generation and preventing accelerated degradation.

A degradation control strategy is proposed to address the problem of minimizing the degradation of a wind turbine's drive-train when there are changes in wind or set point. By minimizing the error ( $e$ ) that is produced by changes in an indicator of deterioration-rate ( $\beta$ ) with respect to a reference deterioration-rate ( $\beta^r$ ), that is  $e = \beta - \beta^r$ . Besides, the control action can be made by an intelligent modification to the control gain ( $\Delta k_c$ ), considering that any change on the  $K_c$  will impact the generation of energy. The general architecture of the control strategy is illustrated in Figure 6.1.

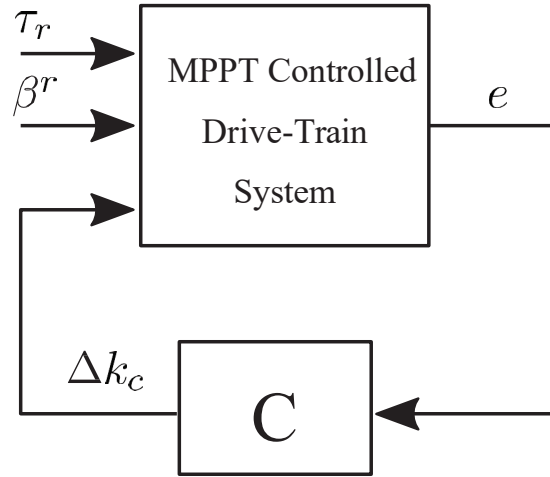


Figure 6.1: Proposed control strategy for deterioration rate considering an intelligent modification of the control gain  $\Delta k_c$

One of the goals of this strategy is to maximize energy generation. To achieve this, it is crucial to apply the MPPT control law outlined in Equation 6.6. Nonetheless, it is also important to consider a trade-off between generation and degradation. Therefore, a two-level composed control loop is considered the most straightforward way to incorporate a degradation control strategy.

Figure 6.2 illustrated the proposed Intelligent Robust Control Strategy to achieve the trade-off between generated energy and deterioration. The scheme presented in Figure 6.2 is a detailed version of Figure 6.1 where it is possible to appreciate the role of the MPPT controller, and the role of the Deterioration controller as an additional input to this MPPT system. Note that the variable  $\beta$ , is estimated by using the measurement of the states: the torsion angle  $\theta_s$ , rotor angular speed  $\omega_r$ , and generator angular speed  $\omega_g$ , as stated in Equation (6.2).

The dynamics of the drive-train system can be simulated using Equation 3.1. This equation estimates the torsion angle  $\theta_s$ , rotor angular speed  $\omega_r$ , and generator angular speed  $\omega_g$  using the rotor torque  $\tau_r$  and generator torque  $\tau_g$  as inputs. The wind variability can be considered using Equation 2.4, which uses wind speed as input. On the other hand,  $\tau_g$  is estimated using Equation 6.6, which presents a modification of the MPPT control law.



Finally, the deterioration controller consists of a robust controller designed using  $H_\infty$  theory, which guarantees system stability despite uncertainties and external disturbances.

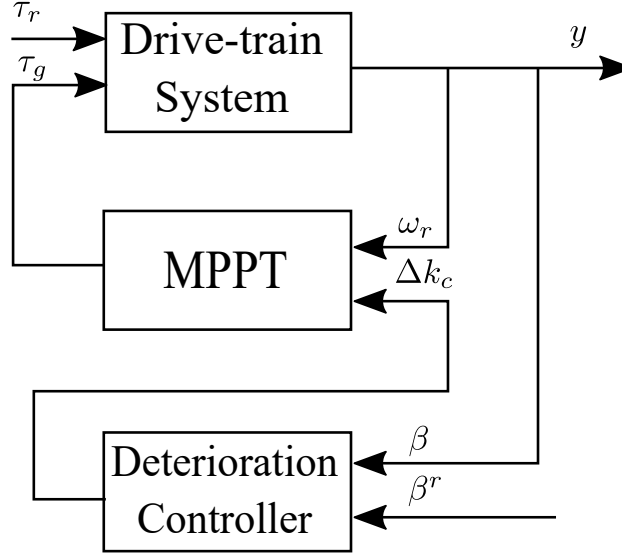


Figure 6.2: Proposed Intelligent Robust Control Strategy implementing a  $H_\infty$  method

### 6.3.1 Design of Deterioration Controller

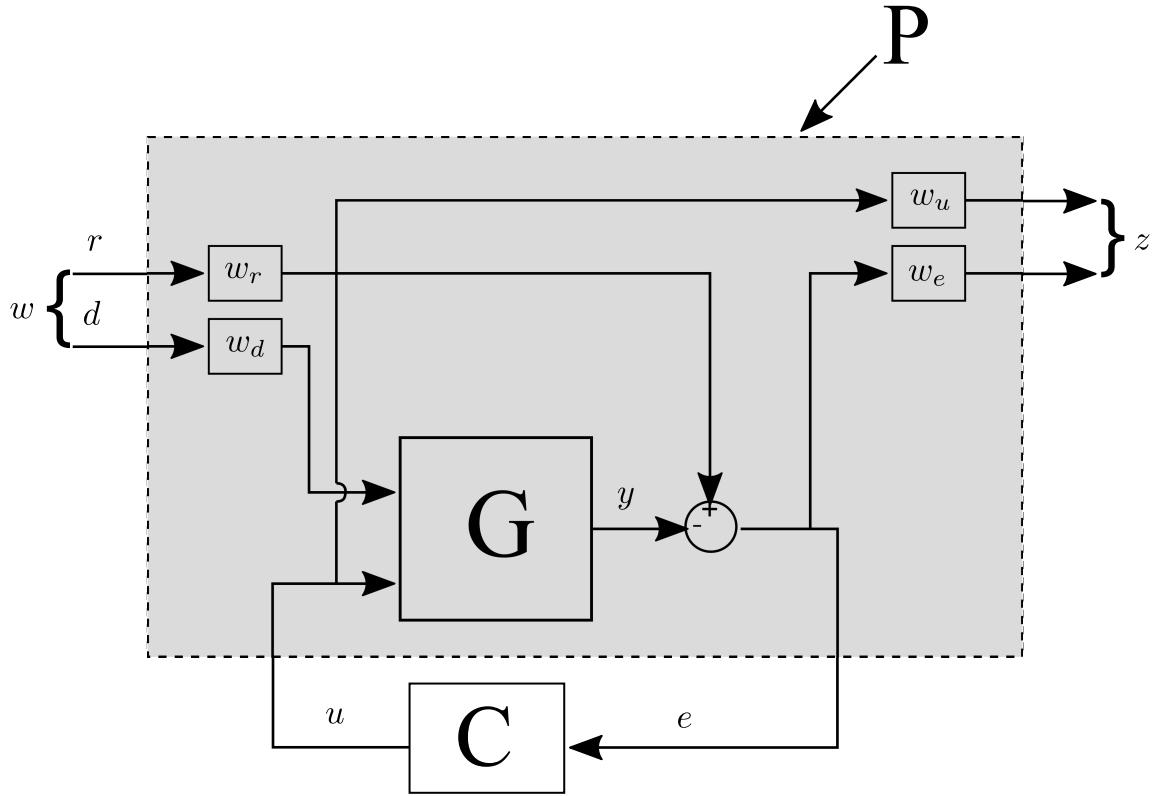
The purpose of this section is present the theory and guidelines necessary to design a deterioration controller for drive-train wind turbines using  $H_\infty$  method. The  $H_\infty$  theory allows to obtain an optimal stable controller even when changes in wind conditions are presented.

The general  $H_\infty$  theory considers the system presented in Figure 6.3, where the objective of this strategy is to find a controller ( $C$ ) for a plant ( $P$ ) that generates a control signal ( $u$ ) based on the measured output ( $y$ ). This signal must counteract the influence of inputs ( $w$ ) (disturbances ( $d$ ) and the reference signal ( $r$ )) on the controller outputs ( $z$ ), thereby minimizing the  $H_\infty$  norm of the closed-loop transfer function ( $G_{zw}$ ) from  $w$  to  $z$  [34, 120, 127], as follow:

$$C_{opt} = \operatorname{argmin}_{C \in D} \| G_{zw}(P, C) \|_\infty \quad (6.8)$$

where  $C$  is the optimized controller, and  $D$  is a group of controller that stabilizes  $P$ .

In the traditional  $H_\infty$  controller synthesis, it is common to consider a sensitivity function  $S$  for managing performance and a complementary sensitivity function  $T$  for managing stability. Each sensitivity function has an associated weighted function that acts as a low-pass and high-pass filter [14, 120]. Commonly,  $w_e$  is the weight function asso-

Figure 6.3: Standard scheme for  $H_\infty$  control synthesis

ciated with the performance (measure) in the controller synthesis, penalizes the lower frequencies of the error, and is defined in Equation 6.9.

$$\frac{1}{w_e(s)} = \frac{s + w_b\epsilon}{s/M_s + w_b} \quad (6.9)$$

With  $\epsilon \approx 0$ ,  $M_s < 2$  (6 dB), and  $w_b$  influencing closed-loop bandwidth (higher  $w_b$  leading to faster disturbance rejection, faster closed-loop tracking response, and better robustness).

On the other hand, the  $w_u$  is the robustness weight function (stability constraint) in the controller synthesis, amplifies the higher frequencies of the control actions, which can be estimated as:

$$\frac{1}{w_u(s)} = \frac{\epsilon_1(s) + w_{bc}}{s + M_u w_{bc}} \quad (6.10)$$

$M_u$  is chosen based on the low-frequency behavior of the process.  $w_{bc}$  influences the closed-loop bandwidth. Lower  $w_{bc}$  values provide better noise limitation and roll-off starting from  $w_{bc}$  to reduce the effects of modeling errors.

Based on the information presented before, the design of a deterioration controller for a drive-train in a VS-FP wind turbine requires defining the system  $G$ , which takes the

form described below:

$$G = \begin{cases} \dot{x} = Ax + Bu \\ y = Cx \end{cases}$$

Here,  $\dot{x} = Ax + Bu$  can be defined using the system presented in Equation 6.7, with the disturbance  $\tau_r$  and the controlled variable  $\Delta k_c$  as inputs, and  $\beta$  as the output.

To define  $P$ , consider it as the transfer function matrix from  $[w \ u]^T$  to  $[z \ y]^T$ , where  $w$ ,  $z$ ,  $y$ , and  $u$  are defined as:

$$w = \begin{cases} d = \tau_r \\ r = \beta^r \end{cases} \quad u = \Delta k_c \quad y = \beta$$

$$z = \begin{cases} z_1 \\ z_2 \end{cases} \quad z_1 = w_e e \quad z_2 = w_u \Delta k_c$$

In addition, weighting functions can also be used to attenuate disturbances and references. In this strategy, we consider implementing a weight function of disturbance ( $w_d$ ) and another for the reference ( $w_{st}$ ):

$$\tau_r^* = w_d \tau_r \quad (6.11)$$

and,

$$\beta^{r*} = w_{st} \beta^r \quad (6.12)$$

Considering the error ( $e$ ) as the difference between  $y$  and  $r$ , it can be defined as:

$$e = \beta - \beta^{ref} \quad (6.13)$$

## 6.4 Performance Evaluation: Numerical Scenario & Results

This section presents the evaluation of the performance of the proposed degradation-aware control strategy using the simulation framework that was utilized in the preceding chapters, which is considered a simplified model for representing the transmission system of a VS-FP wind turbine. This model considers the entire transmission system as a combination of two rigid bodies connected by a flexible shaft ( See Figure. 3.1).

For the evaluation of the proposed strategy, recall that the wind turbine in consideration have a 2 MW capacity and a rotor diameter of 100 m. The turbine operates on a horizontal axis with a fixed gear. For this turbine,  $C_{p_{max}}$  takes a value of 0.4615 at  $\lambda_0 = 6.4$ . Therefore, the theoretical optimal feedback control gain will be  $K_c^{opt} = 9.5065e5$ .

The evaluation of the performance of the controller considered different scenarios:

- Changes in the set-point ( $\beta^{ref}$ ): To analyze the controller performance to changes in the set-point, steps were induced in the set-point and replicated in different wind scenarios with low turbulence around a wind with a constant mean.
- Variations in the disturbance ( $\tau_r$ ): To evaluate the controller performance when changes in wind speed occur, a series of steps were induced in addition to variations in turbulence, and as a consequence, the magnitude of  $\tau_r$  varied.

#### 6.4.1 Design of Deterioration Controller

To design a robust deterioration controller using  $H_\infty$  method, some steps must be taken to implement it:

- Definition of process  $G$ : The system presented in Equation 6.7, requires defining an operation area to obtain the value  $\bar{\theta}_s$ ,  $\bar{\omega}_r$ , and  $\bar{\omega}_g$ . Therefore, the dynamic of the drive-train can be simulated, implementing the deterioration model, considering a case with  $K_c^{opt}$  and a variable wind speed of around 8 m/s. The obtained mean values of the states of the system for the range of operation selected are:

Table 6.1: Parameters for the estimation of system  $G$

$\bar{\theta}_s$	$\bar{\omega}_r$	$\bar{\omega}_g$
$2.8e^{-2} \text{ rad}$	$1.57 \text{ rad/s}$	$1.6 \text{ rad/s}$

- Definition of the augmented plant  $P$ : The augmented plant is defined by considering the process  $G$ , and estimating the weight functions, which were used to analyze the behavior of disturbances in the control system and design a robust controller to handle these disturbances while maintaining stability. Table 6.2 shows the parameters considered for this analysis.

Table 6.2: Parameters of the Sensitivity functions

$M_s$	$\omega_b$	$\epsilon$	$M_u$	$\omega_{bc}$	$\epsilon_1$
2	1	$1e^{-3}$	1	20	$1e^{-3}$

- Synthesis of the controller: The controller has been designed by using the available function **hinfsyn** from the Robust control toolbox (Matlab). By considering the proposed augmented plant, the function provides the parameters of controller gain, closed-loop transfer function, and  $H_\infty$  norm for synthesizing the controller for the target performance level considering the architecture presented in Figure 6.3.

#### 6.4.2 Evaluation of the performance of degradation control strategy

It is essential to analyze how the control system behaves under variations in disturbances and set point to evaluate the proposed degradation control strategy's performance. In order to obtain a complete analysis, the performance will be compared

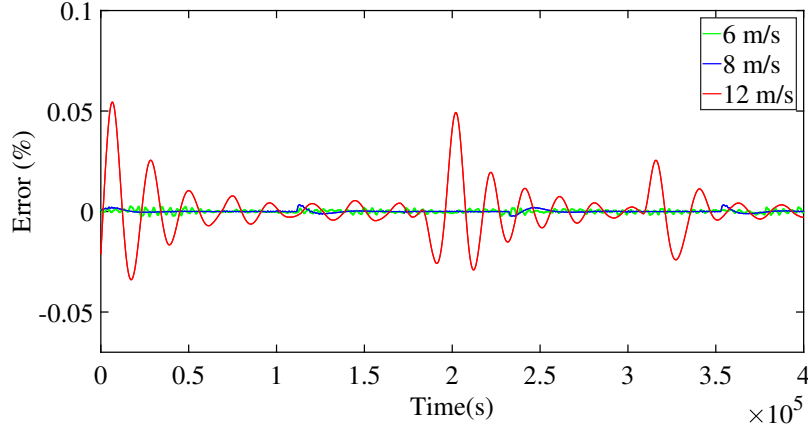


Figure 6.4: Estimated error of estimation of the controller

between two scenarios: one with theoretically optimal control characteristics and a constant gain of  $K_c^{opt}$ , and the other with the proposed controller implementation. This comparison will determine the effectiveness of the controller compared to a theoretically optimal control strategy that uses a constant gain and does not consider the optimization of the system's degradation.

#### 6.4.2.1 Evaluation of performance: Changes on reference $\beta^r$

The response of the controller to changes in the set point was evaluated considering that the value of  $\beta$  can vary in a wide range between  $2e^6$  and  $11e^8$  due to the constraints considered for controller synthesis. To analyze the controller's response to abrupt changes in  $\beta^r$ , steps were added as shown in Figure 6.5, where the dotted vertical lines indicate when a step occurs.

Figure 6.5 presents the controller's response when variations of the reference are made abruptly for three different wind speeds: a) 6m/s (Figure 6.5a), b) 8 m/s (Figure 6.5b), and c) 12 m/s (Figure 6.5c). In all the cases, it is noted that the controller closely follows the set point, even when the steps occur. However, it is noted in Figure 6.5c some variations in  $\beta$  that can be attributed to the effect of the variations in the wind caused by turbulence.

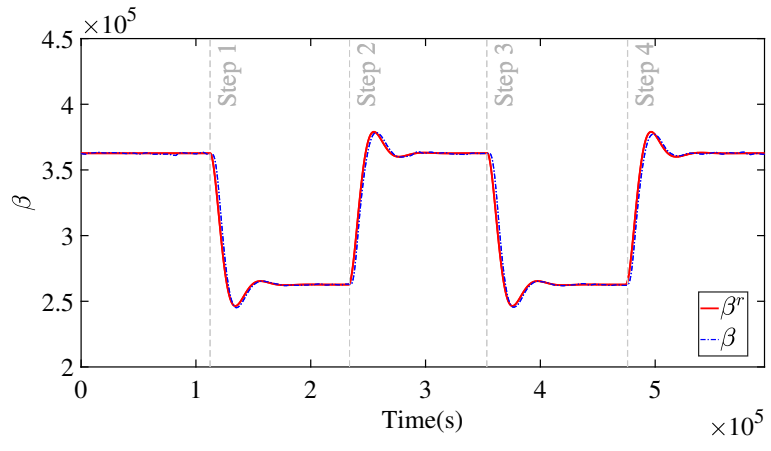
The robustness of the controller and good response to changes in the reference are observed from the comparison between  $\beta$  and  $\beta^r$ . The variations on the error during the process are shown in Figure 6.4, where the estimation errors of  $\beta$  with respect to  $\beta^{ref}$  takes values of  $6.4409 \times 10^{-5}\%$ ,  $6.7225 \times 10^{-7}\%$ , and  $4.66 \times 10^{-3}\%$  for the cases with mean wind speeds of 6 m/s, 8 m/s, and 12 m/s, respectively.

The degradation of the drive-train system can be analyzed by examining Figure 6.6. The analysis of the energy dissipated for the three scenarios is presented with a comparison with respect to a case where the controller is not implemented in Figure 6.6a

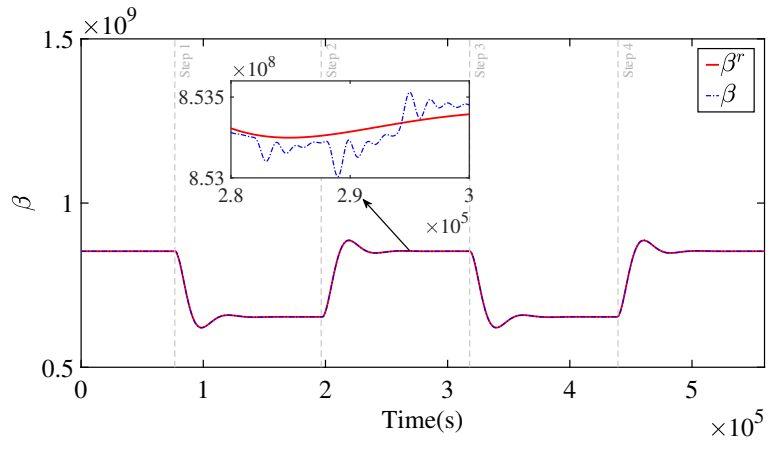
for 6 m/s, Figure 6.6b for 8 m/s , and 12 m/s on Figure 6.6c.

In all three scenarios, the total energy dissipated is significantly lower than in the reference case. The differences are as follows: a) 178.42% lower, b) 0.0619% lower, and c) 18.3988% lower. This demonstrates that implementing the controller leads to a decrease in the total dissipation of energy.

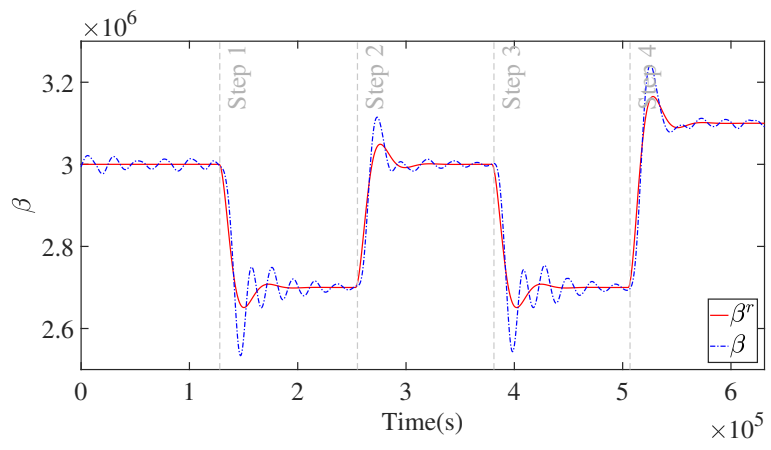
Regarding the generated energy, Figure 6.7 illustrates the difference in generated energy between the two cases analyzed. For the three scenarios of interest (6 m/s, 8 m/s, and 12 m/s), the scenario using the controller produced less energy, with differences of 19.227%, 0.897%, and 0.9913%. Furthermore, in Figure 6.7a, it is possible to see that the slope of the curve noticeably fluctuates each time a step in  $\beta^{ref}$  occurs, and the energy generation difference remains constant before the first step. Therefore, the divergence in energy generation results from the changes in  $\beta^r$ .



(a)

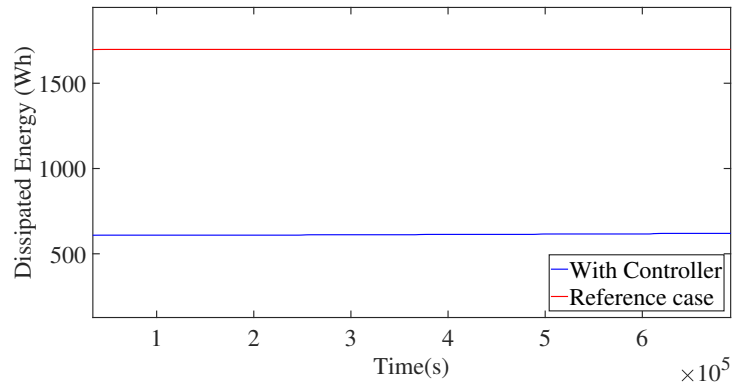


(b)

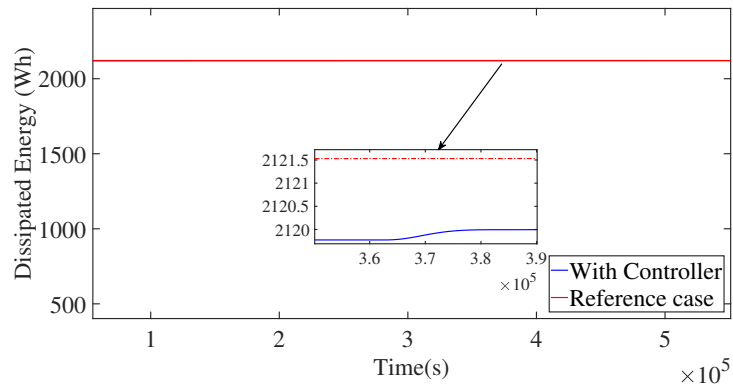


(c)

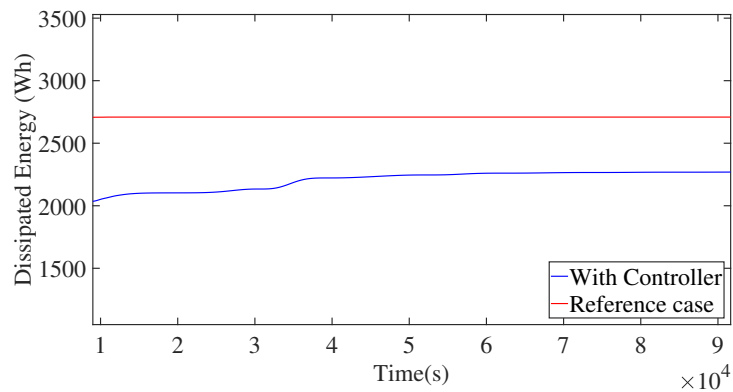
Figure 6.5: Comparison in the deterioration rate between a case with  $\beta$  and  $\beta^{ref}$



(a)



(b)



(c)

Figure 6.6: Comparison of Dissipated Energy between a scenario with controller and reference scenario for wind of: a) 6m/s, b) 8 m/s, and c) 12 m/s



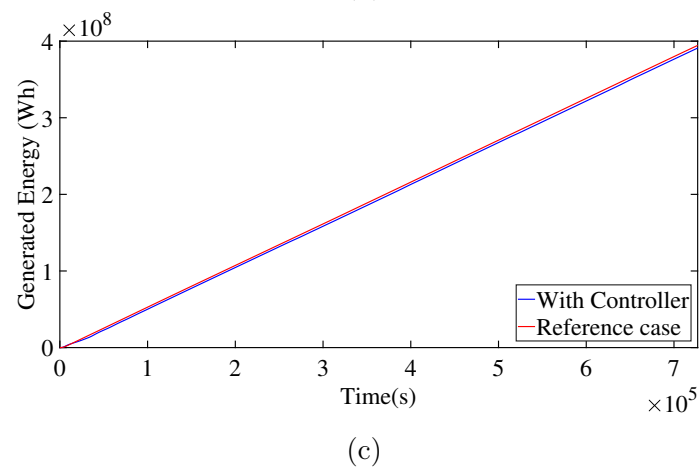
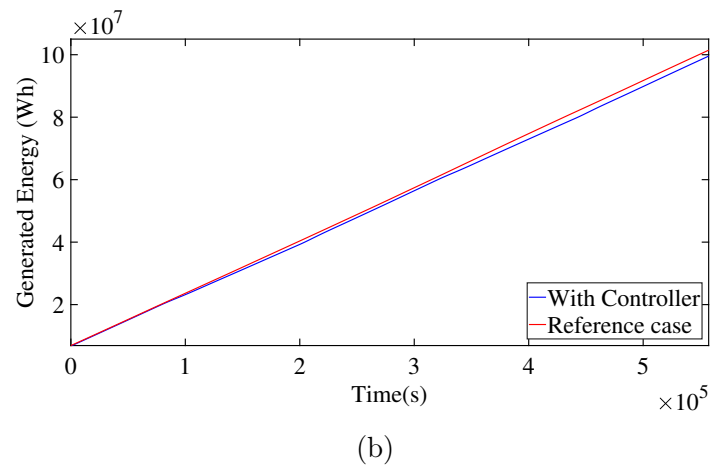
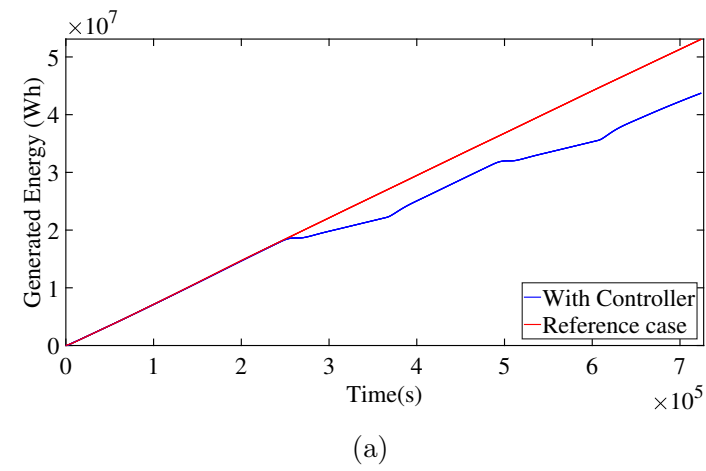


Figure 6.7: Comparison of Generated Energy between a scenario with controller and reference scenario for wind of: a) 6m/s, b) 8 m/s, and c) 12 m/s

### 6.4.2.2 Evaluation of performance: Disturbances

A wind scenario was created to assess the controller's ability to maintain stability while handling disturbances due to changes in the wind. The scenario considers a low turbulence wind with a mean of 8 m/s and induced steps to change the mean of the wind (See Figure 6.8). In this section, it is considered a low turbulence wind designed to avoid abrupt variations that can induce additional noise, allowing for analysis of the effects of controlled variations in the disturbances through the steps.

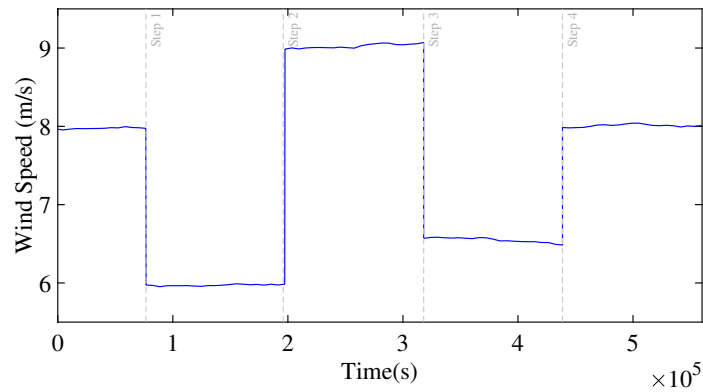


Figure 6.8: Wind Speed Case considered for the evaluation of performance to disturbances.

In Figure 6.9, it can be seen that the controller effectively followed the set point even during significant disturbances, managing perturbations while maintaining system stability with a mean error of 0.96%. The controller shows a peak when Step 2 occurs due to the significant variation in wind speed. However, after a short period, the controller reaches stability and continues following the reference.

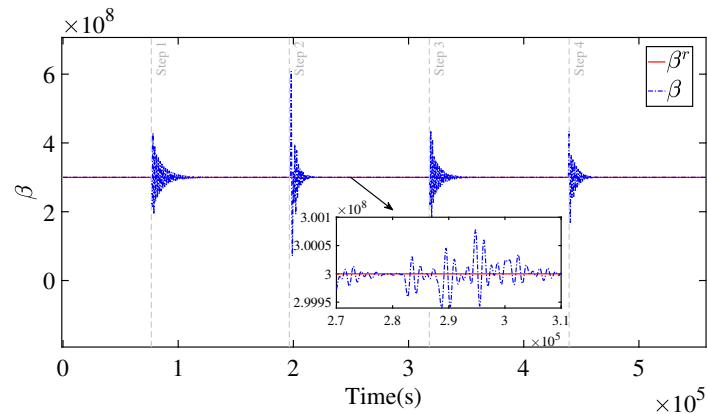


Figure 6.9: Comparison of  $\beta$  and  $\beta^{ref}$  under disturbances

On the other hand, to evaluate the performance of the controller, as in the previous section, the case of interest was compared with a case where the controller was not implemented, and the control gain was kept at a constant value of  $K_c^{opt}$ .

Figure 6.10 illustrates that implementing the controller resulted in a variation in the rate of system deterioration. Although the dissipation of energy from the case with the controller was initially higher in a short period, the controller subsequently reduced the rate of deterioration and maintained it below the rate of the case without the controller.

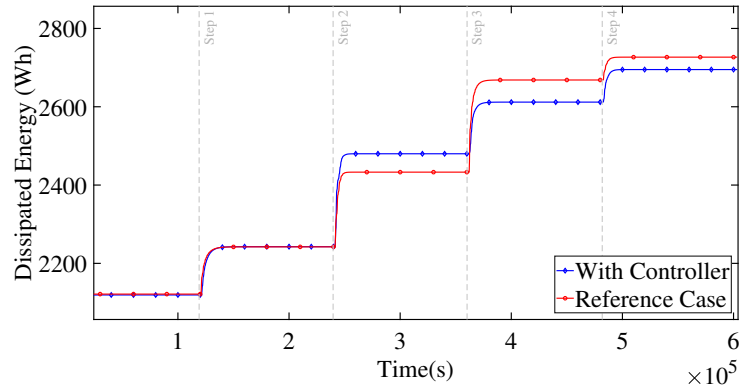


Figure 6.10: Evaluation of performance of controller under disturbances in dissipated energy

Furthermore, Figure 6.11 shows the difference in dissipated power ( $P_d$ ) between the reference scenario and the case with the controller. The peaks in  $P_d$  caused by the introduced steps in the simulation can be identified, allowing the analysis of the effect of each step on the dissipated energy. The controller decreases the effect of the disturbance, reducing the value of  $P_d$  compared to the case without controller implementation.

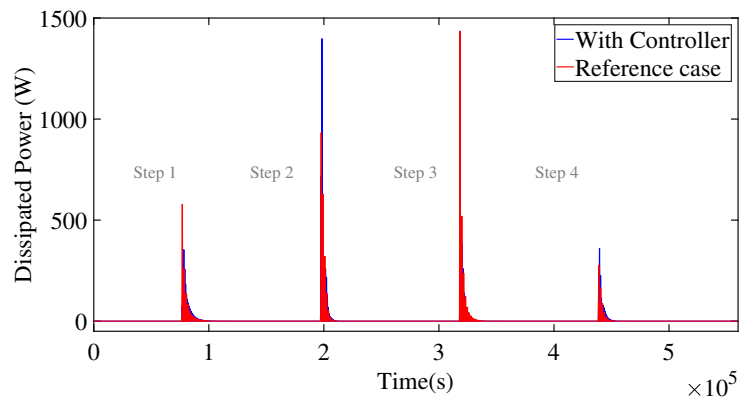


Figure 6.11: Evaluation of performance of controller under disturbances in dissipated power

Finally, in Figure 6.12, the behavior of the energy generation curve is affected by changes in the set-point ( $\beta^r$ ). As a result, the slope of the curve changes each time a step occurs. However, the changes in slope observed with the  $H_\infty$  controller compared to the theoretically optimal control gain are smoother, resulting in a lower energy generation rate of -16.275%. The reduction in generated energy is a result of the controller's objective to strike a balance between degradation and performance

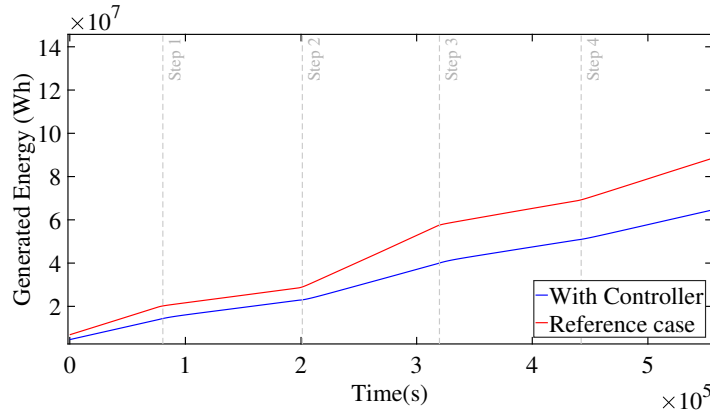


Figure 6.12: Evaluation of performance of controller under disturbances in: Generated Energy

## 6.5 Conclusions

A novel control strategy for minimizing the degradation rate of a wind turbine's drivetrain while maintaining energy generation under varying conditions was presented in this section. The proposed approach consists of an intelligent control strategy of the common MPPT control law used in VS-FP wind turbines, complemented by a robust  $H_\infty$  controller designed and implemented to ensure stability in the presence of uncertainties and external disturbances, such as changes in wind conditions.

The simulation used a deterioration model that considers contact mechanics to estimate the deterioration of the shaft and a simulated low-turbulent wind to obtain different scenarios. The wind was generated using stochastic equations that generated different classes of wind speeds by incorporating a drift and diffusion term. The low-level turbulence used in the simulation replicated the wind study at speeds of 6 m/s, 8 m/s, and 12 m/s, for evaluating the performance of the proposed control strategy under different wind scenarios.

The strategy developed utilizes the  $H_\infty$  controller design methodology, which is suitable for addressing uncertainties and disturbances in the system, considering an index of deterioration and the necessary adjustment to find the trade-off between dissipated energy and generated energy as a variable of control.

The proposed control strategy's effectiveness was evaluated by analyzing the results under two scenarios: disturbance variations and set-point changes. The comparison with a theoretically optimal control strategy that uses a constant gain and does not consider the optimization of the system's degradation demonstrated that implementing the proposed controller resulted in a significant decrease in the rate of system deterioration, reducing the dissipated energy between 0.0619% and 178.42%.

In conclusion, the designed controller proved to be effective for managing degradation in variable-speed wind turbines with fixed-pitch transmission. The simulation results

---

showed significant improvements in energy dissipation and generation, and the controller was shown to maintain system stability. The results also indicate that the controller can handle disturbances and changes in the reference while maintaining system stability. Overall, these results suggest that the designed controller can be a valuable tool for managing degradation in variable-speed wind turbines with fixed-pitch transmission in industrial applications.

Future research should aim to implement the proposed control strategy in an experimental system to demonstrate its effectiveness in real-world applications. Additionally, it may be beneficial to integrate the proposed strategy with a remaining useful lifetime control method, considering the previously made advancements in long-term degradation estimation for wind turbine drive-trains.



# Conclusions & Perspectives

This thesis focuses on modeling and controlling the degradation rate on the drive-train on variable speed and fixed pitch wind turbines with a horizontal axis. The research shows that changes in wind conditions and the use of non-optimized control can accelerate the degradation of the system and affect efficiency. The thesis brings a novel method for modeling deterioration in the wind turbine by using the dissipated energy as an indicator. Besides, it proposes different approaches to minimize the system's degradation by implementing a control adequate to the wind conditions and a methodology to estimate the deterioration of the system in the long term:

Chapter 2 provided an overview of wind turbines, including their functioning, deterioration, and control strategies. The importance of precise control systems and accurate wind modeling was emphasized in achieving maximum wind turbine performance. The chapter also highlighted various methods for assessing the level of degradation, including mixed methods, which are often implemented in wind turbine degradation studies. Lastly, deterioration-aware control was introduced to manage wind turbine behavior and health. Overall, the chapter provides insights into the theory and practice of wind turbines and emphasizes the importance of effective control strategies in achieving optimized performance and reliability.

Chapter 3 proposed a model for drive train degradation based on dissipated energy, which was tested using real and simulated data. The simulation results provided a comprehensive analysis of the possible scenarios that can affect the degradation of the wind turbine. One of the significant observations is the impact of wind speed variances on the torsion angle and the resulting amount of dissipated energy, which can lead to accelerated degradation of the system. Moreover, the results highlighted the possibility of obtaining a trade-off between generated energy and turbine degradation under sub-optimal control conditions. The proposed model allows us to estimate the dissipated energy at the drive train for different wind conditions and control gains, providing a view of the possible situations affecting turbine degradation.

Chapter 4 proposes a gain-scheduling control strategy for wind turbines, which aims to optimize the efficiency of the wind turbine under varying wind conditions. The approach considers the variation of the wind conditions to alternate between different suitable control gains estimated using an optimization. The simulation was developed to test the strategy using different wind speed scenarios and constant and variable control gains. The proposed gain-scheduling control strategy is a promising approach to optimize the efficiency of wind turbines, considering the variation of wind conditions. By maximizing the generated energy and decreasing the dissipated energy, the proposed strategy allows for a more sustainable and efficient use of wind energy.

In Chapter 5, a methodology was proposed to analyze the long-term degradation of

a wind turbine's drive train using a gain-scheduling control strategy and considering variations in wind conditions. The dissipated energy rate for turbulent flow is more accelerated than in the laminar case. As a result, the slope is more pronounced in the Dissipated Energy VS. Time curve. It is possible to learn the slope of the curve to use this behavior in extrapolation and keep the effect of the wind in a second-wise simulation. The degradation in the drive train was simulated using a dynamic system, and the variability in the wind between laminar and turbulent flow was considered to understand the deterioration behavior under realistic conditions. Different probabilistic distribution functions were employed to generate new slope data using the function parameters, and a Markov Chain was simulated to know the sequences of the transitions between the laminar and turbulent flow. The proposed methodology was tested under different periods to know the degradation behavior during the useful life of the wind turbine with an extrapolation of the Dissipated Energy vs. Time curve. The results show that it is possible to reduce energy dissipation in the drive train by more than 9% by using the gain-scheduling control strategy compared with the nominal theoretical case.

In chapter 6, a control strategy was proposed for minimizing the degradation rate of a wind turbine's drive-train while maintaining energy generation under varying conditions. The strategy consists of an intelligent control approach for the common MPPT control law used in VS-FP wind turbines and implementing a robust  $H_\infty$  controller designed to ensure system stability in the presence of uncertainties and external disturbances, such as wind conditions. The approach's effectiveness was evaluated by analyzing the results under two scenarios: disturbance variations and set-point changes. The comparison with a theoretically optimal control strategy that uses a constant gain and does not consider the optimization of the system's degradation demonstrated that implementing the proposed controller resulted in a significant decrease in the rate of system deterioration, reducing the dissipated energy until -178.42%. The results suggest the proposed control strategy can be valuable for managing degradation in variable-speed wind turbines with fixed-pitch transmission in industrial applications.

This thesis has defined a solid foundation for further investigation into the optimization of wind turbine efficiency and reliability. The perspectives for future research, building on the contributions of this work, include:

- **Stability and Adaptability:** Enhancing the stability of the gain scheduling control scheme through the use of Linear Parametric Varying (LPV) tools.
- **RUL Estimation Integration:** The methodology proposed for long-term estimation of deterioration provides a versatile framework that can be further refined to improve the accuracy of Remaining Useful Life (RUL) estimations for wind turbines. This advancement is crucial for optimizing predictive maintenance strategies, and potentially improving the way wind turbines are managed and maintained.



- 
- **Energy Generation Prognosis:** There is significant potential for the development of an energy generation prognosis system, leveraging the long-term estimation methodology introduced in this thesis.
  - **Pitch Angle Control:** Future research could explore incorporating the pitch angle as a second degree of freedom in control strategies. This inclusion could enhance the dynamic response of wind turbines to environmental changes, further optimizing energy capture and reducing mechanical stress.
  - **Industrial Application:** The degradation rate controller outlined in this thesis shows promising potential for industrial applications, particularly in wind turbine management. Its practical implementation could lead to significant advancements in turbine efficiency, reliability, and lifespan, marking a substantial contribution to renewable energy technology.



# Bibliography

- [1] M.A. Abdullah et al. “A review of maximum power point tracking algorithms for wind energy systems.” In: *Renewable and Sustainable Energy Reviews* 16 (5 June 2012), pp. 3220–3227 (cit. on pp. 22, 24, 26).
- [2] Hamed H.H. Aly. “An intelligent hybrid model of neuro Wavelet, time series and Recurrent Kalman Filter for wind speed forecasting.” In: *Sustainable Energy Technologies and Assessments* 41 (Oct. 2020), p. 100802 (cit. on p. 28).
- [3] Mohammed Alzubaidi, Kazi N. Hasan, and Lasantha Meegahapola. “Impact of Probabilistic Modelling of Wind Speed on Power System Voltage Profile and Voltage Stability Analysis.” In: *Electric Power Systems Research* 206 (May 2022), p. 107807 (cit. on p. 28).
- [4] P. Apkarian, P. Gahinet, and G. Becker. “Self-scheduled  $H_\infty$  control of linear parameter-varying systems: a design example.” In: *Automatica* 31.9 (1995), pp. 1251–1261 (cit. on p. 68).
- [5] Juan Arenas and Mohamed Badaoui. “Stochastic modelling of wind speeds based on turbulence intensity.” In: *Renewable Energy* 155 (Aug. 2020), pp. 10–22 (cit. on p. 28).
- [6] Meysam Asadi and Kazem Pourhossein. “Wind farm site selection considering turbulence intensity.” In: *Energy* 236 (2021), p. 121480 (cit. on p. 11).
- [7] Davide Astolfi et al. “Data-Driven Assessment of Wind Turbine Performance Decline with Age and Interpretation Based on Comparative Test Case Analysis.” In: *Sensors* 22 (9 Apr. 2022), p. 3180 (cit. on p. 30).
- [8] R. Ata and Y. Kocyigit. “An adaptive neuro-fuzzy inference system approach for prediction of tip speed ratio in wind turbines.” In: *Expert Systems with Applications* 37 (7 July 2010), pp. 5454–5460 (cit. on p. 10).
- [9] Ahmed Samir Badawi et al. “Power prediction mode technique for Hill Climbing Search algorithm to reach the maximum power point tracking.” In: IEEE, Nov. 2020, pp. 1–7 (cit. on p. 26).
- [10] Hao Bai et al. “Design of an Active Damping System for Vibration Control of Wind Turbine Towers.” In: *Infrastructures 2021, Vol. 6, Page 162* 6 (11 July 2021), p. 162 (cit. on p. 12).
- [11] Marcia Baptista et al. “Remaining useful life estimation in aeronautics: Combining data-driven and Kalman filtering.” In: *Reliability Engineering and System Safety* 184 (Apr. 2019), pp. 228–239 (cit. on p. 79).
- [12] J.J. Barradas-Berglind, Bayu Jayawardhana, and Rafael Wisniewski. “Wind turbine control with active damage reduction through energy dissipation.” In: IEEE, July 2016, pp. 5897–5902 (cit. on p. 35).
- [13] Jose Barradas-Berglind, Rafael Wisniewski, and Mohsen Soltani. “Fatigue damage estimation and data-based control for wind turbines.” In: *IET Control Theory and Applications* 9 (7 Apr. 2015), pp. 1042–1050 (cit. on p. 34).
- [14] R.W. Beaven, M.T. Wright, and D.R. Seaward. “Weighting function selection in the H infinity design process.” In: *Control Engineering Practice* 4 (5 May 1996), pp. 625–633 (cit. on p. 97).

- [15] F.D. Bianchi, R.J. Mantz, and C.F. Christiansen. “Gain scheduling control of variable-speed wind energy conversion systems using quasi-LPV models.” In: *Control Engineering Practice* 13 (2 Feb. 2005), pp. 247–255 (cit. on pp. 9, 10, 13, 44).
- [16] Fernando D Bianchi, Ricardo J Mantz, and Hernán De Battista. *Wind Turbine Control Systems*. Springer, 2007 (cit. on pp. 8, 10, 11, 13, 14, 21, 23, 24, 27, 43, 65).
- [17] Khoury Boutrous, Fatiha Nejjari, and Vicenç Puig. “Health-aware LPV Model Predictive Control of Wind Turbines.” In: *IFAC-PapersOnLine* 53 (2 2020), pp. 826–831 (cit. on p. 36).
- [18] Khoury Boutrous, Vicenç Puig, and Fatiha Nejjari. “A Two-Level Economic Health-Aware LPV MPC of a Wind Turbine.” In: IEEE, June 2023, pp. 1–6 (cit. on p. 34).
- [19] Raymond Byrne et al. “A Study of Wind Turbine Performance Decline with Age through Operation Data Analysis.” In: *Energies* 13 (8 Apr. 2020), p. 2086 (cit. on pp. 11, 12, 29, 30).
- [20] Rudy Calif. “PDF models and synthetic model for the wind speed fluctuations based on the resolution of Langevin equation.” In: *Applied Energy* 99 (Nov. 2012) (cit. on p. 47).
- [21] Rudy Calif and Richard Emilion. “Characterization and Stochastic Modeling of Wind Speed Sequences.” In: *Progress in Turbulence and Wind Energy IV*. Ed. by Martin Oberlack et al. Springer, 2012, pp. 235–238 (cit. on p. 47).
- [22] Giacomo Capizzi et al. “Performance Monitoring of Wind Turbines Gearbox Utilising Artificial Neural Networks and Steps toward Successful Implementation of Predictive Maintenance Strategy.” In: *Processes* 2023, Vol. 11, Page 269 11 (1 Jan. 2023), p. 269 (cit. on p. 12).
- [23] Palmer Carlin. “Analytic Expressions for Maximum Wind Turbine Average Power in a Rayleigh Wind Regime.” In: *National Renewable Energy Laboratory -NREL* (Jan. 1997) (cit. on p. 21).
- [24] A Cetrini et al. “On-line fatigue alleviation for wind turbines by a robust control approach.” In: *International Journal of Electrical Power and Energy Systems* 109 (2019), pp. 384–394 (cit. on p. 44).
- [25] Hao Chen et al. “Assessing probabilistic modelling for wind speed from numerical weather prediction model and observation in the Arctic.” In: *Scientific Reports* 11 (1 Apr. 2021), p. 7613 (cit. on p. 27).
- [26] International Electrotechnical Commission et al. “Wind turbines-part 1: design requirements.” In: *IEC61400-1* (2005) (cit. on p. 11).
- [27] Rallou Dadioti. “Numerical wind resource assessment in urban environments.” In: (2017) (cit. on p. 11).
- [28] Juchuan Dai et al. “Ageing assessment of a wind turbine over time by interpreting wind farm SCADA data.” In: *Renewable Energy* 116 (Feb. 2018), pp. 199–208 (cit. on p. 31).
- [29] Juchuan Dai et al. “Research on power coefficient of wind turbines based on SCADA data.” In: *Renewable Energy* 86 (Feb. 2016), pp. 206–215 (cit. on p. 22).
- [30] Paula J. Dempsey and Shuangwen Sheng. “Investigation of data fusion applied to health monitoring of wind turbine drivetrain components.” In: *Wind Energy* 16 (4 May 2013), pp. 479–489 (cit. on p. 31).

- [31] Yifei Ding et al. “Remaining useful life estimation using deep metric transfer learning for kernel regression.” In: *Reliability Engineering and System Safety* 212 (Aug. 2021) (cit. on p. 79).
- [32] M. Hung Do and Dirk Söffker. “State-of-the-art in integrated prognostics and health management control for utility-scale wind turbines.” In: *Renewable and Sustainable Energy Reviews* 145 (July 2021), p. 111102 (cit. on pp. 33–36).
- [33] M. Hung Do and Dirk Söffker. “Wind Turbine Lifetime Control Using Structural Health Monitoring and Prognosis.” In: *IFAC-PapersOnLine* 53 (2 2020), pp. 12669–12674 (cit. on pp. 36, 37).
- [34] M. Hung Do and Dirk Söffker. “Wind turbine robust disturbance accommodating control using non-smooth H-infinity optimization.” In: *Wind Energy* 25 (1 Jan. 2022), pp. 107–124 (cit. on pp. 27, 97).
- [35] Zuo Dong et al. “Improving the accuracy of wind speed statistical analysis and wind energy utilization in the Ningxia Autonomous Region, China.” In: *Applied Energy* 320 (Aug. 2022), p. 119256 (cit. on p. 28).
- [36] Guglielmo D’Amico, Filippo Petroni, and Flavio Praticco. “First and second order semi-Markov chains for wind speed modeling.” In: *Physica A: Statistical Mechanics and its Applications* 392 (5 Mar. 2013), pp. 1194–1201 (cit. on p. 28).
- [37] Tobiloba Elusakin and Mahmood Shafiee. “Fault diagnosis of offshore wind turbine gearboxes using a dynamic Bayesian network.” In: *International Journal of Sustainable Energy* 41 (11 Dec. 2022), pp. 1849–1867 (cit. on p. 12).
- [38] Ergin Erdem and Jing Shi. “ARMA based approaches for forecasting the tuple of wind speed and direction.” In: *Applied Energy* 88 (4 Apr. 2011), pp. 1405–1414 (cit. on p. 28).
- [39] Monica Spinola Felix et al. “Degradation analysis in a controlled flexible drive train subject to torsional phenomena under different wind speed conditions.” In: IEEE, Nov. 2022, pp. 90–95 (cit. on p. 33).
- [40] Susan A. Frost, Kai Goebel, and Léo Obrecht. “Integrating Structural Health Management with Contingency Control for Wind Turbines.” In: *International Journal of Prognostics and Health Management* 4 (3 Nov. 2013) (cit. on p. 35).
- [41] Tania García-Sánchez et al. “Modelling Types 1 and 2 Wind Turbines Based on IEC 61400-27-1: Transient Response under Voltage Dips.” In: *Energies* 13 (16 Aug. 2020), p. 4078 (cit. on p. 10).
- [42] Sonja Germer and Axel Kleidon. “Have wind turbines in Germany generated electricity as would be expected from the prevailing wind conditions in 2000-2014?” In: *PLOS ONE* 14 (2 Feb. 2019), e0211028 (cit. on p. 29).
- [43] Houda Ghamlouch, Mitra Fouladirad, and Antoine Grall. “The use of real option in condition-based maintenance scheduling for wind turbines with production and deterioration uncertainties.” In: *Reliability Engineering System Safety* 188 (2019), pp. 614–623 (cit. on p. 32).
- [44] Nima Gorjian et al. *A review on degradation models in reliability analysis*. Springer London, 2010, pp. 369–384 (cit. on pp. 13, 29).
- [45] Aleš Gosar and Marko Nagode. “Dissipated energy-based fatigue lifetime calculation under multiaxial plastic thermo-mechanical loading.” In: *International Journal of Damage Mechanics* 24 (1 Jan. 2015), pp. 41–58 (cit. on p. 33).

- [46] Qinkai Han et al. “Non-parametric hybrid models for wind speed forecasting.” In: *Energy Conversion and Management* 148 (Sept. 2017), pp. 554–568 (cit. on p. 28).
- [47] Rui He et al. “Condition-based maintenance optimization for multi-component systems considering prognostic information and degraded working efficiency.” In: *Reliability Engineering and System Safety* 234 (June 2023), p. 109167 (cit. on p. 31).
- [48] Weifei Hu. *Advanced Wind Turbine Technology*. Springer International Publishing, May 2018, pp. 1–349 (cit. on pp. 8, 10).
- [49] Yang Hu et al. “Prognostics and health management: A review from the perspectives of design, development and decision.” In: *Reliability Engineering and System Safety* 217 (Jan. 2022), p. 108063 (cit. on p. 34).
- [50] Kenneth Hunt and Erskine Crossley. “Coefficient of restitution interpreted as damping in vibroimpact.” In: *Journal of Applied Mechanics* 42 (2 1975) (cit. on pp. 45, 49).
- [51] Sung ho Hur. “Short-term wind speed prediction using Extended Kalman filter and machine learning.” In: *Energy Reports* 7 (Nov. 2021), pp. 1046–1054 (cit. on p. 28).
- [52] Mark Hutchinson and Feng Zhao. *Global Wind Report 2023*. Global Wind Energy Council, Mar. 2023 (cit. on pp. 7, 8).
- [53] Michael Hölling, Joachim Peinke, and Stefan Ivanell. *Wind Energy - Impact of Turbulence*. Ed. by Michael Hölling, Joachim Peinke, and Stefan Ivanell. Vol. 2. Springer Berlin Heidelberg, 2014 (cit. on p. 11).
- [54] Tushar Jain and Joseph Yamé. “Health-aware fault-tolerant receding horizon control of wind turbines.” In: *Control Engineering Practice* 95 (Feb. 2020), p. 104236 (cit. on p. 35).
- [55] Nyam Jargalsaikhan et al. “A control algorithm to increase the efficient operation of wind energy conversion systems under extreme wind conditions.” In: *Energy Reports* 8 (Nov. 2022), pp. 11429–11439 (cit. on p. 26).
- [56] Kathryn Johnson et al. “Control of variable-speed wind turbines: Standard and adaptive techniques for maximizing energy capture.” In: *IEEE Control Systems Magazine* 26 (3 July 2006), pp. 70–81 (cit. on pp. 9, 10, 13, 21).
- [57] Paul Johnson, Sydney Howell, and Peter Duck. “Partial differential equation methods for stochastic dynamic optimization: an application to wind power generation with energy storage.” In: *Philosophical Transactions of the Royal Society A: Mathematical, Physical and Engineering Sciences* 375 (2100 Aug. 2017), p. 20160301 (cit. on p. 28).
- [58] Sangkyun Kang et al. “Comparison of different statistical methods used to estimate Weibull parameters for wind speed contribution in nearby an offshore site, Republic of Korea.” In: *Energy Reports* 7 (2021), pp. 7358–7373 (cit. on p. 28).
- [59] Despina Karamichailidou, Vasiliki Kaloutsas, and Alex Alexandridis. “Wind turbine power curve modeling using radial basis function neural networks and tabu search.” In: *Renewable Energy* 163 (Jan. 2021), pp. 2137–2152 (cit. on p. 22).
- [60] Fatemeh Karimi Pour et al. “Health-aware control design based on remaining useful life estimation for autonomous racing vehicle.” In: *ISA Transactions* 113 (2021), pp. 196–209 (cit. on p. 28).
- [61] Syed Muhammad Raza Kazmi et al. “A Novel Algorithm for Fast and Efficient Speed-Sensorless Maximum Power Point Tracking in Wind Energy Conversion Systems.” In: *IEEE Transactions on Industrial Electronics* 58 (1 Jan. 2011), pp. 29–36 (cit. on p. 26).

- [62] Edwin Kipchirchir et al. “Prognostics-based adaptive control strategy for lifetime control of wind turbines.” In: *Wind Energy Science* 8 (4 Apr. 2023), pp. 575–588 (cit. on p. 36).
- [63] Bryant Le and John Andrews. “Modelling wind turbine degradation and maintenance.” In: *Wind Energy* 19 (4 Apr. 2016), pp. 571–591 (cit. on pp. 12, 13).
- [64] He Li et al. “Failure Rate Assessment for Onshore and Floating Offshore Wind Turbines.” In: *Journal of Marine Science and Engineering* 10 (12 Dec. 2022), p. 1965 (cit. on p. 12).
- [65] Jianlan Li et al. “Reliability assessment of wind turbine bearing based on the degradation-Hidden-Markov model.” In: *Renewable Energy* 132 (Mar. 2019), pp. 1076–1087 (cit. on pp. 13, 30).
- [66] Yao Li et al. “Fatigue Reliability Analysis of Wind Turbine Drivetrain Considering Strength Degradation and Load Sharing Using Survival Signature and FTA.” In: *Energies* 13 (8 Apr. 2020) (cit. on pp. 65, 79).
- [67] Davi Ribeiro Lins et al. “Comparison of the performance of different wind speed distribution models applied to onshore and offshore wind speed data in the Northeast Brazil.” In: *Energy* 278 (Sept. 2023), p. 127787 (cit. on p. 28).
- [68] Hui Liu et al. “A new hybrid ensemble deep reinforcement learning model for wind speed short term forecasting.” In: *Energy* 202 (July 2020) (cit. on pp. 12, 28, 79).
- [69] Xiaoxu Liu, Zhiwei Gao, and Michael Z. Q. Chen. “Takagi–Sugeno Fuzzy Model Based Fault Estimation and Signal Compensation With Application to Wind Turbines.” In: *IEEE Transactions on Industrial Electronics* 64 (7 July 2017), pp. 5678–5689 (cit. on p. 35).
- [70] Xiran Liu, Dan Zhao, and Nay Lin Oo. “Numerical prediction of the power coefficient improvements of three laterally aligned Savonius wind turbines above a forward facing step.” In: *Journal of Wind Engineering and Industrial Aerodynamics* 228 (Sept. 2022), p. 105112 (cit. on p. 10).
- [71] Yanhua Liu, Ron J. Patton, and Shuo Shi. “Actuator fault tolerant offshore wind turbine load mitigation control.” In: *Renewable Energy* 205 (Mar. 2023), pp. 432–446 (cit. on p. 35).
- [72] S Loew, D Obradovic, and C L Bottasso. “Model predictive control of wind turbine fatigue via online rainflow-counting on stress history and prediction.” In: *Journal of Physics: Conference Series* 1618 (2 Sept. 2020), p. 022041 (cit. on p. 34).
- [73] Angeliki Loukatou et al. “Stochastic wind speed modelling for estimation of expected wind power output.” In: *Applied Energy* 228 (2018), pp. 1328–1340 (cit. on pp. 27, 28).
- [74] Y. Lu, J. Tang, and H. Luo. “Wind Turbine Gearbox Fault Detection Using Multiple Sensors With Features Level Data Fusion.” In: *Journal of Engineering for Gas Turbines and Power* 134 (4 Apr. 2012) (cit. on p. 31).
- [75] Ningsu Luo and Yolanda Vidal. *Wind Turbine Control and Monitoring*. Ed. by Ningsu Luo, Yolanda Vidal, and Leonardo Acho. Springer International Publishing, 2014 (cit. on p. 14).
- [76] Jinrui Ma. “Prognosis and Maintenance Modelling for Wind Turbines.” Theses. Université de Technologie de Troyes, June 2019 (cit. on pp. 28, 29).

- [77] Jinrui Ma, Mitra Fouladirad, and Antoine Grall. “Flexible wind speed generation model: Markov chain with an embedded diffusion process.” In: *Energy* 164 (Dec. 2018), pp. 316–328 (cit. on pp. 11, 28, 29, 47, 65, 70, 84).
- [78] J F Manwell, J G McGowan, and A L Rogers. *Wind Energy Explained*. John Wiley and Sons, Ltd, 2009 (cit. on p. 28).
- [79] Enzo Marino, Alessandro Giusti, and Lance Manuel. “Offshore wind turbine fatigue loads: The influence of alternative wave modeling for different turbulent and mean winds.” In: *Renewable Energy* 102 (2017), pp. 157–169 (cit. on p. 11).
- [80] Manuel S Mathew, Surya Teja Kandukuri, and Christian W Omlin. “Estimation of Wind Turbine Performance Degradation with Deep Neural Networks.” In: *PHM Society European Conference* 7 (1 June 2022), pp. 351–359 (cit. on pp. 29, 30).
- [81] Eduardo J.N. Menezes and Alex Maurício Araújo. “Wind turbine structural control using H-infinity methods.” In: *Engineering Structures* 286 (July 2023), p. 116095 (cit. on p. 27).
- [82] Eduardo José Novaes Menezes, Alex Maurício Araújo, and Nadège Sophie Bouchonneau da Silva. “A review on wind turbine control and its associated methods.” In: *Journal of Cleaner Production* 174 (Feb. 2018), pp. 945–953 (cit. on p. 26).
- [83] Tobias Meyer, Thorben Kaul, and Walter Sextro. “Advantages of reliability-adaptive system operation for maintenance planning.” In: *IFAC-PapersOnLine* 48.21 (2015), pp. 940–945 (cit. on p. 44).
- [84] Farid K. Moghadam et al. “Power train degradation modelling for multi-objective active power control of wind farms.” In: *Forschung im Ingenieurwesen* 87 (1 Mar. 2023), pp. 13–30 (cit. on p. 34).
- [85] Hossam H.H. Mousa, Abdel-Raheem Youssef, and Essam E.M. Mohamed. “State of the art perturb and observe MPPT algorithms based wind energy conversion systems: A technology review.” In: *International Journal of Electrical Power and Energy Systems* 126 (2021), p. 106598 (cit. on p. 25).
- [86] Alessandro Murgia et al. “Data-driven characterization of performance trends in ageing wind turbines.” In: *Journal of Physics: Conference Series* 2507 (1 May 2023), p. 012019 (cit. on pp. 30, 31).
- [87] S. M. Muyeen et al. “Fault Analysis of Wind Turbine Generator System Considering Six-Mass Drive Train Model.” In: IEEE, Dec. 2006, pp. 205–208 (cit. on p. 42).
- [88] S.M. Muyeen et al. “Comparative study on transient stability analysis of wind turbine generator system using different drive train models.” In: *IET Renewable Power Generation* 1 (2 2007), p. 131 (cit. on p. 42).
- [89] Bunlung Neammanee, Somporn Sirisumrannukul, and Somchai Chatratana. *Control Strategies for Variable-speed Fixed-pitch Wind Turbines*. Ed. by SM Muyeen. Wind Power. 2010, pp. 210–232 (cit. on p. 26).
- [90] Amir Rasekhi Nejad, Zhen Gao, and Torgeir Moan. “Fatigue Reliability-based Inspection and Maintenance Planning of Gearbox Components in Wind Turbine Drivetrains.” In: *Energy Procedia* 53 (2014), pp. 248–257 (cit. on p. 12).
- [91] Jackson G. Njiri et al. “Consideration of lifetime and fatigue load in wind turbine control.” In: *Renewable Energy* 131 (2019), pp. 818–828 (cit. on p. 33).



- [92] Diego RODRIGUEZ OBANDO. “From Deterioration Modeling to Remaining Useful Life Control: a comprehensive framework for post-prognosis decision-making applied to friction drive systems.” 2016 (cit. on p. 44).
- [93] Peter F. Odgaard, Chris Damgaard, and Rasmus Nielsen. “On-Line Estimation of Wind Turbine Power Coefficients Using Unknown Input Observers.” In: *IFAC Proceedings Volumes* 41 (2 2008), pp. 10646–10651 (cit. on pp. 10, 13, 22).
- [94] Jon Olauson, Per Edström, and Jesper Rydén. “Wind turbine performance decline in Sweden.” In: *Wind Energy* 20 (12 Dec. 2017), pp. 2049–2053 (cit. on pp. 12, 29, 30).
- [95] Chinedu I. Ossai, Brian Boswell, and Ian J. Davies. “A Markovian approach for modelling the effects of maintenance on downtime and failure risk of wind turbine components.” In: *Renewable Energy* 96 (Oct. 2016), pp. 775–783 (cit. on p. 30).
- [96] Kumarasamy Palanimuthu and Young Hoon Joo. “Reliability improvement of the large-scale wind turbines with actuator faults using a robust fault-tolerant synergetic pitch control.” In: *Renewable Energy* (Aug. 2023), p. 119164 (cit. on p. 35).
- [97] Ching-Tsai Pan and Yu-Ling Juan. “A Novel Sensorless MPPT Controller for a High-Efficiency Microscale Wind Power Generation System.” In: *IEEE Transactions on Energy Conversion* 25 (1 Mar. 2010), pp. 207–216 (cit. on p. 26).
- [98] Yubin Pan et al. “Performance degradation assessment of a wind turbine gearbox based on multi-sensor data fusion.” In: *Mechanism and Machine Theory* 137 (July 2019), pp. 509–526 (cit. on p. 31).
- [99] Yubin Pan et al. “Performance degradation assessment of wind turbine gearbox based on maximum mean discrepancy and multi-sensor transfer learning.” In: *Structural Health Monitoring* 20 (1 Jan. 2021) (cit. on pp. 31, 65).
- [100] Jayshree Pande et al. “A Review of Maximum Power Point Tracking Algorithms for Wind Energy Conversion Systems.” In: *Journal of Marine Science and Engineering* 9 (11 Oct. 2021), p. 1187 (cit. on p. 22).
- [101] Han Peng et al. “A Review of Research on Wind Turbine Bearings and Failure Analysis and Fault Diagnosis.” In: *Lubricants* 2023, Vol. 11, Page 14 11 (1 July 2022), p. 14 (cit. on p. 12).
- [102] Tahere Pourseif et al. “Design of H-infinity Controller for Wind Turbine in the Cold Weather Conditions.” In: IEEE, Sept. 2018, pp. 1–6 (cit. on p. 27).
- [103] Wenxin Qiao et al. “New degradation feature extraction method of planetary gearbox based on alpha stable distribution.” In: *Journal of Mechanical Science and Technology* 35 (1 Jan. 2021), pp. 1–19 (cit. on p. 31).
- [104] Yi Qin et al. “A new supervised multi-head self-attention autoencoder for health indicator construction and similarity-based machinery RUL prediction.” In: *Advanced Engineering Informatics* 56 (Apr. 2023), p. 101973 (cit. on p. 32).
- [105] Mohsen Rahimi. “Drive train dynamics assessment and speed controller design in variable speed wind turbines.” In: *Renewable energy* 89 (2016), pp. 716–729 (cit. on p. 44).
- [106] S. Rajakumar and D. Ravindran. “Optimization of Wind Turbine Power Coefficient Parameters using Hybrid Technique.” In: *Journal of The Institution of Engineers (India): Series C* 93 (2 June 2012), pp. 141–149 (cit. on p. 22).
- [107] Marvin Rausand, Anne Barros, and Arnljot Hoyland. *System Reliability Theory*. 3rd ed. Wiley, Oct. 2020 (cit. on pp. 30, 31).

- [108] Guorui Ren et al. “The analysis of turbulence intensity based on wind speed data in onshore wind farms.” In: *Renewable Energy* 123 (2018), pp. 756–766 (cit. on p. 11).
- [109] Niklas Requate and Tobias Meyer. “Active Control of the Reliability of Wind Turbines.” In: *IFAC-PapersOnLine* 53 (2 2020), pp. 12789–12796 (cit. on p. 36).
- [110] Osborne Reynolds. “On the dynamical theory of incompressible viscous fluids and the determination of the criterion.” In: *Philosophical Transactions of the Royal Society of London. (A.)* 186 (Dec. 1895) (cit. on p. 47).
- [111] Diego Rodriguez-Obando. “From Deterioration Modeling to Remaining Useful Life Control : a comprehensive framework for post-prognosis decision-making applied to friction drive systems.” Université Grenoble Alpes, Nov. 2018 (cit. on pp. 29, 44).
- [112] Diego Rodriguez-Obando, John J. Martinez, and Christophe Berenguer. “Set-invariance analysis for deterioration prediction on a roller-on-tire actuator.” In: IEEE, Sept. 2016, pp. 87–92 (cit. on pp. 32, 43, 44).
- [113] Diego Jair Rodriguez Obando, John Jairo Martinez Molina, and Christophe Bérenguer. “Set-invariance analysis for deterioration prediction on a roller-on-tire actuator.” In: *SysTol 2016 - 3rd International Conference on Control and Fault-Tolerant Systems*. Ed. by V. Puig et al. Proceedings of the 2016 3rd Conference on Control and Fault-Tolerant Systems (SysTol), Barcelona, Spain, Sept. 7-9, 2016. Barcelone, Spain: IEEE, Sept. 2016, pp. 87–92 (cit. on pp. 43, 44).
- [114] Elena E Romero, John J Martinez, and Christophe Bérenguer. “Degradation of a wind-turbine drive-train under turbulent conditions: Effect of the control law.” In: *Conference on Control and Fault-Tolerant Systems, SysTol 2021-September* (July 2021), pp. 335–340 (cit. on p. 65).
- [115] Lotfi Saidi, Arij Nasfia Hayder, and Majdi Saidi. “Remaining useful life prognosis for wind turbine using a neural network with a long-term prediction.” In: *Wind Engineering* (Apr. 2022), p. 0309524X2210851 (cit. on p. 32).
- [116] Yves-Marie Saint-Drenan et al. “A parametric model for wind turbine power curves incorporating environmental conditions.” In: *Renewable Energy* 157 (Sept. 2020), pp. 754–768 (cit. on p. 22).
- [117] Hector Eloy Sanchez, Teresa Escobet, and Vicenç Puig. “Health-aware Model Predictive Control of Wind Turbines using Stiffness Degradation Approach.” In: *IFAC-PapersOnLine* 53 (2 2020), pp. 10348–10353 (cit. on p. 34).
- [118] Hector Eloy Sanchez et al. “Health-aware model predictive control of wind turbines using fatigue prognosis.” In: *International Journal of Adaptive Control and Signal Processing* 32 (4 Apr. 2018), pp. 614–627 (cit. on p. 33).
- [119] Scopus. *Analysis of research trends on Wind Turbine Deterioration or Degradation*. July 2023 (cit. on p. 29).
- [120] Olivier Sename and Soheib Fergani. “Robustness and  $H_\infty$  control of MIMO systems.” In: *IVSS 2017 - Intelligent Vehicles International Summer School*. Compiègne, France, July 2017 (cit. on p. 97).
- [121] Ameneh Forouzandeh Shahraki. “A Review on Degradation Modelling and Its Engineering Applications.” In: *International Journal of Performability Engineering* (2017) (cit. on p. 30).

- [122] Jie Shan et al. “A parallel compact firefly algorithm for the control of variable pitch wind turbine.” In: *Engineering Applications of Artificial Intelligence* 111 (July 2022), p. 104787 (cit. on p. 13).
- [123] Wei Shi et al. “Dynamic modeling and analysis of a wind turbine drivetrain using the torsional dynamic model.” In: *International Journal of Precision Engineering and Manufacturing* 14 (1 Jan. 2013), pp. 153–159 (cit. on p. 43).
- [124] J. Enrique Sierra-Garcia, Matilde Santos, and Ravi Pandit. “Wind turbine pitch reinforcement learning control improved by PID regulator and learning observer.” In: *Engineering Applications of Artificial Intelligence* 111 (May 2022), p. 104769 (cit. on p. 13).
- [125] Silvio Simani. “Application of a Data-Driven Fuzzy Control Design to a Wind Turbine Benchmark Model.” In: *Advances in Fuzzy Systems* 2012 (2012), pp. 1–12 (cit. on p. 26).
- [126] Silvio Simani. “Data-driven design of a PI fuzzy controller for a wind turbine simulated model.” In: *IFAC Conference on Advances in PID Control* (13 Mar. 2012) (cit. on p. 26).
- [127] Sigurd Skogestad and Ian Postlethwaite. *Multivariable Feedback Control: Analysis and Design*. John Wiley and Sons, Inc., 2005 (cit. on p. 97).
- [128] Sakiru Adebola Solarin and Mufutau Opeyemi Bello. “Wind energy and sustainable electricity generation: evidence from Germany.” In: *Environment, Development and Sustainability* 24 (7 July 2022), pp. 9185–9198 (cit. on p. 8).
- [129] Yuan Song et al. “Design and Validation of Pitch H-Infinity Controller for a Large Wind Turbine.” In: *Energies* 15 (22 Nov. 2022), p. 8763 (cit. on p. 27).
- [130] Iain Staffell and Richard Green. “How does wind farm performance decline with age?” In: *Renewable Energy* 66 (June 2014), pp. 775–786 (cit. on p. 29).
- [131] Bernhard Stoevesandt et al. *Handbook of Wind Energy Aerodynamics*. Ed. by Bernhard Stoevesandt et al. Springer International Publishing, 2022 (cit. on p. 11).
- [132] Hongsheng Su, Xuping Duan, and Dantong Wang. “Optimization of periodic maintenance for wind turbines based on stochastic degradation model.” In: *Archives of Electrical Engineering* (July 2021) (cit. on p. 32).
- [133] Hongsheng Su, Dantong Wang, and Xuping Duan. “Condition Maintenance Decision of Wind Turbine Gearbox Based on Stochastic Differential Equation.” In: *Energies* 13 (17 Aug. 2020), p. 4480 (cit. on p. 32).
- [134] Hongsheng Su, Yifan Zhao, and Xueqian Wang. “Analysis of a State Degradation Model and Preventive Maintenance Strategies for Wind Turbine Generators Based on Stochastic Differential Equations.” In: *Mathematics* 11 (12 June 2023), p. 2608 (cit. on p. 32).
- [135] Wei Sun, Xiang Li, and Jing Wei. “An Approximate Solution Method of Dynamic Reliability for Wind Turbine Gear Transmission with Parameters of Uncertain Distribution Type.” In: *International Journal of Precision Engineering and Manufacturing* 19 (6 June 2018), pp. 849–857 (cit. on p. 31).
- [136] Jie Tang, Alexandre Brouste, and Kwok Leung Tsui. “Some improvements of wind speed Markov chain modeling.” In: *Renewable Energy* 81 (Sept. 2015), pp. 52–56 (cit. on p. 28).
- [137] D.S. Tchankov and K.V. Vesselinov. “Fatigue life prediction under random loading using total hysteresis energy.” In: *International Journal of Pressure Vessels and Piping* 75 (13 Nov. 1998), pp. 955–960 (cit. on p. 32).

- [138] Marvin Trisakti, Levin Halim, and Bagus Made Arthaya. “Power Coefficient Analysis of Savionus Wind Turbine Using CFD Analysis.” In: *IEEE*, Dec. 2019, pp. 24–29 (cit. on p. 22).
- [139] Biao Wang et al. “A Hybrid Prognostics Approach for Estimating Remaining Useful Life of Rolling Element Bearings.” In: *IEEE Transactions on Reliability* 69 (1 July 2020), pp. 401–412 (cit. on p. 79).
- [140] Thomas Michael Welte et al. “Integration of Degradation Processes in a Strategic Off-shore Wind Farm Oandamp;M Simulation Model.” In: *Energies* 10 (7 July 2017), p. 925 (cit. on p. 30).
- [141] WindEurope. *Wind energy today*. 2023 (cit. on p. 8).
- [142] Ziyang Xu et al. “A state-of-the-art review of the vibration and noise of wind turbine drivetrains.” In: *Sustainable Energy Technologies and Assessments* 48 (Dec. 2021), p. 101629 (cit. on p. 12).
- [143] Yangyang Yan. “Load characteristic analysis and fatigue reliability prediction of wind turbine gear transmission system.” In: *International Journal of Fatigue* 130 (Jan. 2020), p. 105259 (cit. on p. 12).
- [144] Boyuan Yang, Ruonan Liu, and Enrico Zio. “Remaining useful life prediction based on a double-convolutional neural network architecture.” In: *IEEE Transactions on Industrial Electronics* 66 (12 Dec. 2019), pp. 9521–9530 (cit. on p. 79).
- [145] Jianxiang Yang, Anle Mu, and Nailu Li. “Dynamical Analysis and Stabilization of Wind Turbine Drivetrain via Adaptive Fixed-Time Terminal Sliding Mode Controller.” In: *Mathematical Problems in Engineering* 2019 (July 2019), pp. 1–14 (cit. on p. 33).
- [146] Xiuxing Yin et al. “Reliability aware multi-objective predictive control for wind farm based on machine learning and heuristic optimizations.” In: *Energy* 202 (July 2020), p. 117739 (cit. on p. 36).
- [147] Abdel-Raheem Youssef, Hossam H.H. Mousa, and Essam E.M. Mohamed. “Development of self-adaptive P and O MPPT algorithm for wind generation systems with concentrated search area.” In: *Renewable Energy* 154 (2020), pp. 875–893 (cit. on p. 25).
- [148] Zhe Zhang et al. “Analysis of urban turbulence intensity observed by Beijing 325-m tower and comparison with the IEC turbulence model for small wind turbines.” In: *Journal of Wind Engineering and Industrial Aerodynamics* 241 (2023), p. 105511 (cit. on p. 11).
- [149] Carlos D. Zuluaga, Mauricio A. Álvarez, and Eduardo Giraldo. “Short-term wind speed prediction based on robust Kalman filtering: An experimental comparison.” In: *Applied Energy* 156 (Oct. 2015), pp. 321–330 (cit. on p. 28).
- [150] Chengming Zuo et al. “Investigation of Data Pre-Processing Algorithms for Power Curve Modeling of Wind Turbines Based on ECC.” In: *Energies* 16 (6 Mar. 2023), p. 2679 (cit. on p. 22).